Atkins, Nigel Philip (2005) *Microfluidic PCR devices with electrochemical detection of DNA.* PhD thesis.

http://theses.gla.ac.uk/4880/

Copyright and moral rights for this thesis are retained by the author

A copy can be downloaded for personal non-commercial research or study, without prior permission or charge

This thesis cannot be reproduced or quoted extensively from without first obtaining permission in writing from the Author

The content must not be changed in any way or sold commercially in any format or medium without the formal permission of the Author

When referring to this work, full bibliographic details including the author, title, awarding institution and date of the thesis must be given

Glasgow Theses Service
http://theses.gla.ac.uk/
theses@gla.ac.uk

Microfluidic PCR Devices With Electrochemical Detection of DNA

Thesis submitted to the

Department of Electronics and Electrical Engineering

University of Glasgow

for the degree of Doctor of Philosophy

Nigel Philip Atkins

August 2005

© Nigel Atkins 2005

This work is dedicated to my parents and grandparents.

Abstract

This research undertaken involved designing, fabricating and testing of a microfluidic PCR microdevice with real-time electrochemical detection. The aim was to provide an analytical device which could lower the cost and the time taken for running DNA amplification. The later addition of automated sample handling and detection would thereby reduce the time taken and consequently the overall cost.

The real-time electrochemical detection utilised an electrochemical assay for the detection of DNA invented by Molecular Sensing Ltd. It used a single strand ferrocenylated probe DNA molecule which could be detected with an electrochemical cell. The integration of an electrochemical cell was a key feature of this work, along with the immobilisation of the *Taq* polymerase at its working temperature.

Taq polymerase enzyme and T7 polymerase enzyme were immobilised on to microspheres. *Taq* polymerase was immobilised in four ways and T7 polymerase was immobilised in only one method. After immobilisation the enzymes were unable to amplify DNA within PCR experiments.

Microfluidic PCR devices, which incorporate the above two features, were designed and fabricated. 3 basic ideas of devices were investigated, flow-through, straight line and cyclic triangle device. All the devices had fundamental problems which inhibited there ability to successfully amplify DNA.

An electrochemical assay was used within a microfluidic device with internal electrochemical detection, which utilised a filter to bring about sequence specific DNA detection. Using biotinylated complementary probe DNA attached to streptavidin coated beads to hybridise to the sample DNA. This device incorporated a solid phase extraction and clean up step as well as producing sequence specific DNA detection.

Acknowledgements

I would first like to acknowledge and thank Prof. Jon Cooper for allowing me to undertake this Ph.D. Secondly I would like to thank Molecular Sensing Ltd (now part of Osmetech, Roswell, GA, USA) for the additional funding and support, especially Russ Keay and John Clarkson. Also thank you to the EPSRC for funding the research.

As well as saying thank you to the people that fund me, I would like to thank all the people in Bioelectronics. Both post-docs (special thanks to Dave) and other students (special thanks to Mairi) who have helped in any shape or form. Of course a big thank you to the bioelectronics technicians for help across the board during my 4 years here.

I would like to single out Paul Monaghan for all the advice about fabrication and generally for his ideas, and for being very patient in the writing of this thesis. Also, as a drinking partner and for getting me to pick up my saxophone again after many years.

Outside of the department I would like to say thank you to all at GUBC, who for some unknown reason actually listen to me and let me forget all about my Ph.D for a little while each week. Also thanks to Bodie and Jess for letting me call them or email them whenever I needed, even though it must really annoy them, and for letting me stay at their flats when in London.

Lastly I have to thank my family. My brother, Derek, for letting me stay at his abode every time I go to Nottingham and also for never asking how the Ph.D was going, as he soon worked out I didn't want to talk about it. Also thank you to Mum and Dad because they didn't complain when I said I was not going to work but to do a Ph.D, maybe next time they should!, and for supporting me through all my years.

Contents

1 Introduction **1**

1.1 Research Aim 1

1.2 Polymerase Chain Reaction 2

1.2.1 Components of a PCR 2

1.2.2 Workings of PCR 3

1.2.3 Uses of PCR 5

1.3 Microdevices 5

1.3.1 Benefits of Miniaturisation 5

1.3.2 History of Miniature Devices 6

1.3.2.1 Capillary Electrophoresis Devices 7

1.3.2.2 Other Electrokinetically Pumped Devices . . 8

1.3.2.3 Mixing Within Microsystems and Mixing Devices 9

1.3.2.4 Biological Samples Within Microdevices . . . 10

1.4 PCR Microdevices 15

1.4.1 PCR Devices with Reaction Chambers 16

1.4.2 Flow-Through PCR Devices 19

1.4.3 Other PCR Devices 23

1.5 Electrochemical Detection of DNA 26
1.5.1 Introduction of Electrochemical Cells and Potentiostat 26
1.5.2 History of Electrochemical DNA Detection 28
1.5.3 On-Chip Electrochemical Detection 31
1.5.4 Electrochemical DNA Detection Devices 34
1.6 Conclusion 37

2 Device Fabrication **38**
2.1 An Introduction to Fabrication 38
2.1.1 Moulding Methods 38
2.1.2 Etching Methods 39
2.1.3 Additive Methods 40
2.1.4 General Microfabrication Processes 41
2.1.5 Theory of Photolithography 42
2.1.6 Introduction to Photolithography 42
2.1.7 Why Use Photolithography? 43
2.2 Materials 44
2.2.1 Photoresist 44
2.2.1.1 Chemical Bases and Effect of UV 45
2.2.2 Silicon 46
2.2.3 Glass 46
2.2.4 PDMS 46
2.2.4.1 Advantages of PDMS 47
2.2.4.2 Structure and Curing of PDMS 48
2.2.4.3 Oxidisation of PDMS Surface 49
2.2.5 RTV PDMS 50

2.3 Procedures Used in this Thesis 51
  2.3.1 Order of Fabrication 51
  2.3.2 Mask Design and Fabrication 53
    2.3.2.1 Electron Beam Designs 54
    2.3.2.2 Acetate Designs 54
  2.3.3 Substrate Preparation 55
  2.3.4 Spin Coating Thin Films of Photoresist 55
  2.3.5 Exposure 57
  2.3.6 Development 58
  2.3.7 Silicon Etching 58
  2.3.8 Metal Deposition 59
  2.3.9 Lift Off 60
  2.3.10 Moulding 61
    2.3.10.1 Moulding of PDMS 61
    2.3.10.2 Moulding of RTV PDMS 62
  2.3.11 Bonding 62
    2.3.11.1 Silicon to Glass 62
    2.3.11.2 PDMS Plasma Bonding 62
  2.3.12 External Fluid Interfacing 63
    2.3.12.1 Thin Layers of PDMS 63
    2.3.12.2 Thick Layers of PDMS 64
    2.3.12.3 Glass 64
    2.3.12.4 RTV PDMS 65
  2.3.13 Electrical Connections 66
  2.3.14 Electrochemical Cell 67

2.4 External Instrumentation 67
  2.4.1 Pumps 67
  2.4.2 Tubing and Pump Fittings 68
  2.4.3 Potentiostat 68

3 Immobilisation of Polymerase Enzymes 69

3.1 Introduction 69
  3.1.1 Structural and Mechanistic Discussion of *Taq* Polymerase 70
    3.1.1.1 History of *Taq* polymerase 70
    3.1.1.2 Basic Structure of *Taq* Enzyme 70
    3.1.1.3 Conformational Change With and Without DNA 71
    3.1.1.4 Translation of DNA Through Polymerases . . 72
  3.1.2 Methods of Immobilisation 73
    3.1.2.1 Biotin-Streptavidin 73
    3.1.2.2 Carbodiimide 75
    3.1.2.3 Glutaraldehyde 78
    3.1.2.4 Passive Adsorption 79
  3.1.3 Estimating the Amount of Enzyme Per Bead 80
3.2 Materials 80
  3.2.1 Buffers 82
3.3 Methods 82
  3.3.1 Immobilisation of *Taq* Polymerase 82
    3.3.1.1 Biotin-Streptavidin Immobilisation 82
    3.3.1.2 Carbodiimide Reaction 84
    3.3.1.3 Glutaraldehyde Reaction 85

3.3.1.4 Passive Absorption Method 85
3.3.2 PCR Reaction with *Taq* on Microspheres 87
3.3.3 Gel Electrophoresis of PCR Products 88
3.3.4 Immobilisation of T7 DNA Polymerase 88
3.3.5 Assessment of Enzyme Immobilisation 89
3.3.5.1 Protein Staining to Determine Thermal Loss . 89
3.3.5.2 Immobilisation of HRP to Investigate Immobilisation Procedures 90
3.4 Results of PCR Using Immobilised Enzyme and Discussion . . 91
3.4.1 Results of PCR Amplification Using Immobilised *Taq* Polymerase 91
3.4.1.1 Biotin-Streptavidin Immobilisation 91
3.4.1.2 Glutaraldehyde 94
3.4.1.3 Carbodiimide 95
3.4.1.4 Passive Adsorption 96
3.4.2 Results of PCR Amplification Using Immobilised T7 DNA Polymerase 100
3.4.3 Discussion of Immobilisation of Polymerases 101
3.5 Control Experiments for the Assessment of Immobilisation . . 105
3.5.1 Assessing Enzyme Activity Post-Immobilisation 105
3.5.1.1 Biotin-Streptavidin 105
3.5.1.2 Carbodiimide 106
3.5.1.3 Glutaraldehyde 107
3.5.1.4 Passive Adsorption 108
3.5.1.5 Discussion of HRP Immobilisation 109
3.5.2 Assessment of Attachment of Polymerases by Passive Adsorption 110

3.5.2.1 MES Immobilisation of *Taq* Polymerase . . . 110
3.5.2.2 Tris-HCl Buffer Immobilisation of *Taq* Polymerase . . . 111
3.5.2.3 T7 Polymerase Immobilisation . . . 112
3.5.2.4 Discussion of Heating Passively Absorbed Polymerases . . . 113
3.6 Conclusion . . . 114

4 Microfluidic PCR devices **115**
4.1 Introduction . . . 115
4.2 Research Outline . . . 115
4.2.1 Requirements of PCR Microfluidic Device . . . 115
4.2.2 Real-Time Ferrocene Assay . . . 116
4.2.3 Considerations in the Designing of PCR Microfluidic Devices . . . 118
4.3 Designing of Device . . . 118
4.3.1 Fulfilling Basic Requirements . . . 118
4.3.2 Flow-Through Device . . . 119
4.3.2.1 Physical Dimensions . . . 120
4.3.3 Linear Device . . . 124
4.3.4 Cyclic Triangle Device . . . 127
4.4 Fabrication of PCR Devices . . . 129
4.4.1 Flow Through Device . . . 129
4.4.1.1 Silicon and PDMS . . . 130
4.4.1.2 Glass and RTV PDMS . . . 130
4.4.1.3 Silicon and Glass . . . 131

4.4.1.4 Surface Passivation 132

4.4.2 Linear Device 132

4.4.2.1 Glass and RTV PDMS 132

4.4.2.2 Silicon and PDMS 133

4.4.2.3 Silicon and Glass 134

4.4.2.4 Silicon and Glass with Low Pressure Exit . . 135

4.4.3 Cyclic Triangle Device 136

4.4.4 Heaters 138

4.5 Results and Discussion 141

4.5.1 Flow-Through Device 141

4.5.1.1 Etched Silicon with PDMS Cover 141

4.5.1.2 RTV PDMS Moulded Over Photoresist 142

4.5.1.3 Etched Silicon with Glass Cover 143

4.5.2 Linear Device 144

4.5.2.1 RTV PDMS Device 145

4.5.2.2 Etched Silicon with PDMS 145

4.5.2.3 Etched Silicon with Glass Cover Device . . . 146

4.5.2.4 Etched Silicon with Glass Cover and Low Pressure Outlet 146

4.5.2.5 Overall Performance of the Straight Line Device 146

4.5.3 Cyclic Triangle Device 147

4.6 Conclusion 148

4.7 Future Work 149

5 DNA Sequence Specific Detection using an Electrochemical Cell Within a Microfluidic Device 152

5.1 Introduction 152

  5.1.1 Sequence Specific Detection of DNA Assay 152

  5.1.2 Microelectrodes vs Macroelectrodes 154

5.2 Materials 155

5.3 Design and Fabrication 156

  5.3.1 Device Design 156

    5.3.1.1 Electrode Design 156

    5.3.1.2 Filter Design 158

  5.3.2 Fabrication of Device 159

    5.3.2.1 Electrode Fabrication 159

    5.3.2.2 Microchannel and Filter Fabrication 160

    5.3.2.3 Device Integration 161

5.4 Experimental Procedure 162

  5.4.1 Macroelectrodes 162

  5.4.2 Microelectrodes 163

    5.4.2.1 Cyclic Voltammetry of Single Stranded Ferrocenylated DNA 163

    5.4.2.2 Detection of Sequence Specific Ferrocenylated Oligonucleotide 163

5.5 Results and Discussion 165

  5.5.1 Macroelectrodes 165

  5.5.2 Microelectrodes 167

    5.5.2.1 Cyclic Voltammetry 167

    5.5.2.2 Sequence Specific Ferrocenylated Oligonucleotide 168

5.6 Conclusion 171
5.7 Future Work 172

6 Conclusion and Future Work **173**

6.1 Conclusions Drawn From Research 173
    6.1.1 Immobilisation of Polymerase Enzymes 173
    6.1.2 Microfluidic PCR Devices 174
    6.1.3 Sequence Specific Detection of DNA 174
6.2 Future Work 174
    6.2.1 Immobilisation of Polymerase Enzymes 174
    6.2.2 Microfluidic PCR Devices 175
    6.2.3 Sequence Specific Detection of DNA 175

Bibliography **177**

List of Figures

1.1 Schematic of one PCR cycle: (a) the dsDNA template is melted at 95°C to form two ssDNA; (b) primers attach to the 3' end of the single strand template DNA at 60°C; (c) enzyme attaches to the 3' end of the primer; (d) the enzyme extends the primer at 72°C by addition of the complementary dNTP from the solution; (e) the enzyme extends the primer until it reaches the end of the strand or until the temperature is raised to form 2 exact copies of the template dsDNA; (f) the end of the cycle is reached and the number of template strands is doubled for the next cycle. 4

1.2 Illustration of the mechanism for the sample injection devised by Harrison *et. al.*[8]: (a) the sample is moved by electrokinetic fluid flow through the sample channel crossing the separation channel. The potential moving the sample was switched off leaving a plug within the separation channel; (b) a separating potential is applied along the separation channel and the sample plug moves along the channel and is separated. 8

1.3 Picture of yeast cells being moved through a microfluidic channel by electroosmotic flow within a device fabricated by Li *et. al.*[18] 100V was applied across the length of the channel with the cells moving from the high voltage towards the ground. . . 9

1.4 Micromixer fabricated by Bessoth *et. al.*[22] showing the diffusion of fluorescein and rhodamine B across streamlines formed within a laminar flow regime. At this flow rate, 50μl/min, the time scale of this picture was ~9ms. 10

1.5 a) Schematic of the channel structures used by Jacobson *et. al*[23] for the digestion of DNA by restriction enzyme and sizing of the products along the separation channel (labelled waste 2). b),c) and d) Show the generation of a plug of reaction mixture for separation and sizing. All fluid movement is by electroosmotic flow, so a precise volume of digested enzyme can be separated each time the reaction process is run. 11

1.6 Schematic of the double T-junction used by Schilling *et. al.*[27] to lyse cells, extract β-galatosidase and react the enzyme with a fluorogenic substrate. The cells were chemically lysed in the channel at the interface, working within a laminar flow regime, between the cell flow and lysing agent flow. At the T-junction the two streamlines split because of the laminar flow regime, the extracted proteins flow towards the enzyme substrate. The resorufin was released from the substrate at the interface of the two streamlines and was detected within the second flow channel. 13

1.7 Schematic and image of the micromixer used by Burke *et. al.*[28] to find the reaction constants of enzyme reactions with fluorescein substrates. The network of microfluidic channels at the junction between the channels decreases the diffusion distance and therefore the time for the reaction to happen enabling fast reaction analysis. 14

1.8 Basic procedure, used by Pease *et. al.*,[30] for building up an array of oligonucleotides using photolithography.
15

1.9 Illustration of a silicon chamber fabricated by Daniel *et. al.*[35] which was thermally isolated from the rest of the wafer to produce rapid thermocycling. 17

1.10 Illustration of the device layout used by Waters *et. al.*[46] to cycle 4 PCR experiments at once and then individually separate the products all within the same device. 18

1.11 Illustration of the device fabricated by Lagally *et. al.*[49] 8 separate chambers and CE channels are shown with integrated heaters and pneumatic valves for automatic fluid control. . . . 19

1.12 Illustration of the flow-through device fabricated by Kopp *et. al.*[57] in which the one channel crosses three separate temperature zones to thermally cycle the PCR. In order for the reactants to extend the time within the extension zone a convoluted channel is used within that region. To ensure all the template was melted the first melt stage is extended by the same method. 20

1.13 Schematic of the device fabricated out of ceramic layers by Chou *et. al.*[58]. A view of the layout is shown above and a side view of the device showing air gaps and the channel width within the separate temperature zones. The air gaps are to help maintain the correct temperatures across the device. . . . 21

1.14 A schematic of the device fabricated by Obied *et. al.*[59] The device contains separate inlets for the PCR and RT PCR and the outlets for cycling the reaction through the different number of cycles. With the different temperatures being the various steps a) melting, b) extension, c) annealing and d) for the transcriptase enzyme to preform the RNA copying. 22

1.15 Illustration of the rotary PCR device fabricated by Liu *et. al.*[62] The microfluidic channel is shown along with the position of the heaters dividing the loop into different temperature zones. Electrodes are used for electrokinetic pumping of the fluid within the microfluidic channel. 24

1.16 Device used by Giordano *et. al.*[65] for PCR using IR mediated thermocycling. The reaction chamber were made from polyimide with a volume of 1.7μl. 25

1.17 Circuit diagram of a potentiostat. 27

1.18 Illustration of the triple helix formed, by Ihara *et. al.*,[90] to detect dsDNA by ferrocenylated oligonucleotide. 30

1.19 Martin *et. al.*[101] fabricated a device for CE-EC. A layout of the device is shown along with a picture of the electrodes demonstrating their placement compared to the separation channel. Multiple working electrodes were used to increase the sensitivity of the detection. 32

1.20 Illustration of the end of the separation channel and the electrodes of the device fabricated by Balwin *et. al.*[102]. The position of the electrodes under the "shelf" was used to decouple the separation voltage from the electrochemical cell, while stopping broadening of the bands, by using the detection reservoir to disperse the separation voltage. 33

1.21 Pictures of a) heart cell in microfabricated well with microelectrodes and b) the heart cell be contracted by applied voltage from Cai *et. al.*[110] 34

1.22 Device fabricated by Woolley *et. al.*[100] A schematic of the layout of the electrodes with the end of the separation channel and a scanning electron microscope image of the working electrode at the exit of the separation channel. 35

1.23 Picture of the microelectrode array for the detection of DNA fabricated by Liu *et. al.*[55] within an incubation chamber for alkaline phosphatase, for increasing the sensitivity of the system, in a microfluidic device. 36

1.24 Illustration of the sandwich capture probe system used by Liu *et. al.*[55] Capture of target ssDNA using immobilised ssDNA, followed by the hybridisation of the a ferrocenylated oligonucleotide. Detection of the ferrocene was achieved by using a "molecular wires" within the self assembled monolayer. 37

2.1 Illustration of the etch profiles gained using different techniques: a) glass etched isotropically by HF acid. The shape gained is due to the glass having been removed equally as quick side ways as vertically; b) silicon etched anisotropically by KOH, the silicon has been etched along a crystal lattice edge to gain the well defined shape; c) silicon etched anisotropically using an Surface Technologies System inductively coupled plasma (STS ICP), high selective etching giving a high aspect ratio etch. 40

2.2 Flow diagram to show the general process of device fabrication 41

2.3 A schematic of photolithography with positive photoresist: (a) substrate is cleaned; (b) photoresist is spun on to surface; (c) the photoresist is exposed with light through a mask; (d) exposed photoresist has been chemically modified by the light; (e) the pattern is developed, removing the exposed resist which is soluble in basic developer solution. 43

2.4 Reaction scheme of the reaction undergone by orthonaphthoquinonediazide (a) with UV light[117], through reactive intermediates of firstly a carbene (b), and then rearranging in to a ketene (c). The ketene reacts immediately with water in the atmosphere to form the soluble indenecarboxylic acid (d). . . . 45

2.5 Structure of polydimethylsiloxane as a monomer unit. 47

2.6 The hydrosilyation crosslinking reaction of polydimethylsiloxane (a) via terminal vinyl groups, with hydrosilane groups of methylsiloxanes, (b). Where R is the rest of the PDMS molecule, R1 is either a hydrogen atom or a methyl group. . . 49

2.7 The condensation reaction of oximosilane end groups with water to crosslink siloxane polymers during the curing of RTV PDMS. Where R1 and R2 are the rest of the PDMS polymer. 51

2.8 Flow diagram showing the general procedure of microfluidic device fabrication. 52

2.9 (a) a light field mask and (b) a dark field mask, of a "generalised" structure. 53

2.10 Organic solvent cleaning procedure. Samples are sonicated for 3min in each solvent and then rinsed throughly in flowing 18MΩ/cm deionised water and dried under nitrogen. 55

2.11 A stylised representation of the overhang produced by chlorobenzene in photoresist after exposure and development of the photoresist. The profile of resist after exposure and development: (a) without chlorobenzene soak; (b) with chlorobenzene soak. . 57

2.12 A schematic of the process to gain structured metal patterns on the substrate: (a) the substrate already had a layer patterned layer of photoresist on the surface; (b) metal is evaporated on to the whole of the surface, forming a uniformly thick layer; (c) photoresist is removed from the surface by organic solvent, lift off, leaving only the metal that was in contact with the surface of the substrate. 60

2.13 Illustration of PDMS moulding using a master (a). PDMS was poured on to the mould (b) and PDMS once cured after 1hr at 60°C was peeled off the mould and adhered to a flat substrate (c). 61

2.14 Illustration of using a syringe needle to interface with PDMS: (a) PDMS is cored using a modified gauge 21 syringe needle; (b) insertion of a blunted gauge 23 syringe needle to attach tubing to a PDMS device. 64

2.15 Illustration of the capillary interface into a RTV PDMS moulded channel: (a) RTV PDMS covering the resist filled channel; (b) RTV PDMS cut away and resist removed with ethanol; (c) capillary inserted in to widened channel. 66

3.1 Schematic of the structure of *Taq* polymerase. The right hand is described because of structures being called the fingers (red) and thumb (blue) around the palm (yellow). The palm is where the active site is situated. The hand makes up the polymerase activity domain of the enzyme. 5' nuclease activity domain (orange) is loosely attached to the inactive 3'-5' exonuclease activity domain (green). 71

3.2 Schematic of the change of position of the 5' nuclease (orange) domain when bound to DNA within the closed conformation. The 5' nuclease is now situated behind the palm (yellow), fingers (red) and the thumb (blue) but is still attached to the inactive 3'-5' exonuclease domain (green). 72

3.3 Flowchart to show the way in which enzymes are attached to beads using the biotin/streptavidin couple. 74

3.4 Mechanism of the free amine (b), in protein, to hydrolyse on n-hydroxysuccinimide ester (a) to form amide bond in final product (c). Where R is the spacer and biotin molecule. . . . 75

3.5 Illustration of carbodiimide reaction used in the immobilisation of polymerase. 75

3.6 Mechanism by which carbodiimide (EDAC), (a), react with carboxylic acids (-COOH), (b), from the protein, and amine groups (-NH_2), (c), on the beads. The reaction passes through a carbocation intermediate, *O*-acylisourea intermediate (d). Amide bond formation occurs by the nucleophilic attack on the intermediate by the amine group on the bead to from the final desired product (e). R1 and R2 represent the rest of the EDAC molecule not involved in the mechanism. 77

3.7 The α,β-unsaturated aldehyde (a) reacts with the free amine (-NH_2) of lysine groups within the protein by means of a Micheal type addition. R1 corresponds to the rest of the glutaraldehyde polymer including another α,β-unsaturated aldehyde group which reacts to an amine group, with the same mechanism, on the bead surface to couple the protein. R2 represents the non functionalized part the glutaraldehyde polymer. 79

3.8 Structures of NHS biotin molecules used in the immobilisation of *Taq* polymerase: a) biotin N-hydroxysuccinimide ester, denoted as -, with no spacer; b) biotinamidohexanoic acid N-hydroxysuccinimide ester, denoted as -X-, which contains a 6 atom spacer arm; c) biotinamidohexanoyl-6-aminohexanoic acid N-hydroxysuccinimide ester, denoted as -XX-, which contains a 14 atom spacer arm. 81

3.9 Illustration of how a shorter spacer arms (a) is more sterically hindered compared to a longer spacer arm (b). It can be seen that longer the spacer the more degrees of freedom of movement for the enzyme. 84

3.10 Image of gel after separation of products from a PCR. Lane: 0, 100bp ladder, 1, +ve control, 2, biotin-X-*Taq*, 3, biotin-XX-*Taq*, 4, unrelated experiment, 5, bead-biotin-X-*Taq*, 6, bead-biotin-XX-*Taq*. 92

3.11 Image of gel after separation of products from a PCR. Lane: 0, 100bp ladder, 1, -ve control, 2, +ve control, 3, biotin-*Taq*, 4, biotin-XX-*Taq*, 5, bead-biotin-*Taq*, 6, bead-biotin-XX-*Taq*. . 93

3.12 Image of a electrophoresis gel showing separation of PCR products from PCR using glutaraldehyde immobilised *Taq* polymerase. Lane: 0, 100bp ladder, 1, +ve control, 2 and 3 reactions using immobilised enzyme. 94

3.13 Image of gel after separation of PCR products by electrophoresis. Lane: 0, 100bp ladder, 1, +ve control, 2-4, unrelated experiment, 5-7, bead-*Taq* using carbodiimide coupling reaction, 8, +ve control. 95

3.14 Colour enhanced visualization of products of passive absorption of *Taq* polymerase on 1μm silica beads using 50mM Tris-HCl pH 7.2 buffer. Lane: 0, 100bp ladder, 1, +ve control, 2 and 3, bead-*Taq*. 96

3.15 Gel of products from physically adsorbed *Taq* polymerase on to 1μm silica beads using *Taq* in storage buffer at 5units/μl. Lane: 0, 100bp ladder, 1, +ve control, 2-5, bead-*Taq*, 6-8, unrelated experiment. 97

3.16 Colour inverted, to make viewing clearer, electrophoresis gel of products from the adsorption of *Taq* polymerase on to silica and polystyrene beads at pH 6. Lane: 0, 100bp ladder, 1, +ve control, 2 and 3, silica bead-*Taq*, 4 and 5, polystyrene bead-*Taq*, 6, empty lane, 7, +ve control. 98

3.17 Electrophoresis gel of comparison between PCR experiments with beads that have undergone a preheat step and beads with *Taq* that were used directly. lane: 0, 100bp ladder, 1, +ve control, 2 and 3, no preheating of beads, 4 and 5, preheated of beads. 100

3.18 Inverted colour image of the gel gained from products of T7 DNA polymerase physical adsorbed on to 1μm polystyrene beads. Lane: 0, 100bp ladder, 1, Control for amount of template DNA, 2, +ve control with free enzyme, 3 and 4, T7 enzyme adsorbed at room temperature, 5 and 6, T7 enzyme adsorbed at 4°C. 101

3.19 UV/Vis spectra of reaction between ABTS and HRP immobilised on beads by biotin-streptavidin couple. The blue trace shows the negative control whilst the red trace shows immobilised HRP by biotin with -xx- spacer. The green trace shows immobilised HRP by biotin with no spacer, whilst the black trace shows the positive control. 106

3.20 UV Vis spectra of ABTS radical cation after reaction with HRP immobilised to microspheres by carbodiimide method. The blue trace shows the negative control with the red and green traces show immobilised HRP using the carbodiimide reaction. The black trace shows the positive control. 107

3.21 UV Vis spectra of reaction mixture from glutaraldehyde immobilised HRP on to amine coated beads. The blue traces shows the negative control control, whilst the red and green traces show the immobilised HRP, using the glutaraldehyde method. The black trace shows the positive control. 108

3.22 UV Vis spectrums of reaction mixtures of ABTS after reaction with physically adsorbed HRP on to polystyrene beads. The blue trace shows the negative control with the red and green traces showing the immobilised HRP, whilst the black trace shows the positive control. 109

3.23 UV/Vis spectra of amido black in PCR buffer before (black) heating and after 10min at 95°C (red and green). Immobilisation of *Taq* polymerase was by physical adsorption using MES pH 6.0 as the buffer. 111

3.24 UV/Vis spectra of amido black in PCR buffer before (black) heating and after 10min at 95°C (red and green). Immobilisation was by physical adsorption carried out in Tris-HCl buffer, pH=8.0 at 25°C, of *Taq* polymerase. 112

3.25 UV/Vis spectra of amido black in PCR buffer before (black) heating and after 10min at 95°C (red and green). Immobilisation was by physical adsorption carried out in the Tris-HCl buffer, pH=8.0 at 25°C, of T7 polymerase. 113

4.1 Diagram shows two ferrocene moieties (Fc) attached to a oligonucleotide. 117

4.2 Schematic of the ferrocene electrochemical assay for the real-time monitoring of PCR: (a) primer and detection probe ss-DNA are annealed to the template during the annealing stage (60°C) of the PCR; (b) enzyme extends the primer and digests the probe strand by polymerase activity; (c) the complete PCR cycle results in amplified template being formed along with free ferrocene. This ferrocene can then be interrogated electrochemically and a measurement of the amount of amplification can be undertaken. 117

4.3 A stylized representation of the basic design for the flow through PCR device. This diagram shows a single channel crossing the three temperature zones to form the cycles. Direction of flow is shown by the arrows. 120

4.4 Results of simulation a 50μm deep channel, in silicon covered in PDMS, filled with water in Femlab (Comsol Ltd, London, UK) using chemical: convection and conduction and incompressible Navier-Strokes packages. The model was drawn as a 2.2mm long channel (only the first 0.35mm are shown here, with water flowing from left to right, direction of the arrow, at 1μl/min entering at a temperature of 300K). At the dotted line, marked C, the bottom edge of the channel was held at 360K within the model, to represent the device sitting on top of a heater. The physical parameters used for water were ρ 1, Cp 4.2 J/g K, K 0.6W/K m, η 0.001Pa s. 122

4.5 A diagram showing the layout of the flow-through device from the design software L-Edit (Tanner EDA). Inserts show the parallel channels 50μm wide and 50μm apart and the turns used within the channel. 124

4.6 A illustration of how a cycle is completed within the linear PCR device: (a) melt stage, the reaction plug lies within the first zone; (b) the plug is moved to the annealing stage passing through the 72°C zone; (c) plug moved back into the extension temperature zone; (d) and finally the cycle is completed by moving the reaction plug in to the melt zone. 125

4.7 Schematic of the linear design PCR microfluidic device. The array of channels crossing the three temperature zones enables a plug of reaction mixture to be flowed backwards and forwards to cycle the reaction. 126

4.8 An illustration of how a plug of PCR mixture was moved within the triangle device: (a) the plug in one side of triangle starts the cycle, and was moved onto the next side by applying pressure at inlet 1 (with outlet 6 opened to atmosphere); (b) the plug within the second temperature zone was moved onto next stage by pressure being applied along inlet 3 (with outlet 2 opened); (c) to finish the cycle, the plug was flowed back to its starting position by applying pressure to inlet 5 (outlet 4 opened). 128

4.9 The design and actual size of triangle device showing the radiator like channels to increase the channel length and therefore the plug volume within the device. Inlets and outlets have enlarged channels to allow the insertion of fused silica capillaries in to the etched silicon without tearing the PDMS cover.

129

4.10 A photograph of the flow through PCR device fabricated using an etched silicon wafer with a 500μm thick layer of PDMS. The PDMS was irreversibly bonded using oxygen plasma and the fused silica capillary inserted into the channel. 130

4.11 A Photograph of a flow-through device fabricated on a silicon wafer. The channel was etched in silicon, and a glass top layer, which was anodically bonded. The inlet and outlet were formed from fused silica capillaries and graphite ferrules. . . . 131

4.12 Photograph of the complete linear device fabricated by moulding RTV PDMS on patterned 30μm thick photoresist. 133

4.13 A photograph of the channel array moulded in RTV PDMS by photoresist. The uneven nature of the photoresist can be seen by the change in colours in the channel surface. The uneven nature of the photoresist is due to spinning of the photoresist on top of photoresist, so the surface is considerably less smooth and flat than normal. 133

4.14 Photographs of the linear device etched in silicon, showing the precise etching gained using the STS ICP. This device was covered with a PDMS layer, bonded after O_2 plasma activation. 134

4.15 A photograph of the complete linear device fabricated with an etched silicon wafer and PDMS cover. 134

4.16 A photograph of the straight line device fabricated by anodically bonding Pyrex glass to etched silicon wafer. The inlet and outlet are formed by drilling holes in the glass, before bonding, and using fused silica capillaries to connect the syringe pump. 135

4.17 Photograph of the straight line device fabricated with a cut micropipette tip to form a reservoir at the outlet to lower the pressure at the outlet. 136

4.18 Photograph of the cyclic triangle device which was fabricated from etched silicon and oxygen plasma bonded PDMS top layer. Inlets and outlets formed by insertion of fused silica capillaries and glued in place by RTV PDMS. 137

4.19 Graph to show the variation of the viscosity of glycerol and water solutions.[162] Showing the difference between undiluted glycerol and 1:1 glycerol : water solutions. 138

4.20 Illustration of the positioning of the thermistor in relation to the Peltier effect heat pump and the PCR device. 139

4.21 Photograph of the cartridge heaters and heat sink setup. . . . 140

4.22 Photograph of a flow through device fabricated by moulding RTV PDMS on a photoresist mould. The channel did not clear of photoresist in some parts, whilst has been cleared in others depending on the amount the photoresist that had pooled together. 143

4.23 Illustration of a possible design to evenly distribute the water plug into all the channels. 150

5.1 Illustration of the sequence specific detection assay: (a) streptavidin attached to a surface with 4 binding sites available for coupling with biotin; (b) biotinylated probe DNA is coupled to the streptavidin; (c) capture of the ferrocenylated target DNA from the sample solution by hybridisation to the probe DNA also cleaning the sample before the detection; (d) heating of the surface to 90°C releases the target DNA allow downstream detection by an electrochemical cell. 153

5.2 The biotin and TEG spacer used to attach the biotin to the ssDNA. The TEG spacer gives a 16 atom spacer to help the binding of the biotin to the streptavidin with limited steric hindrance. An advantage in using TEG as a spacer is that the oxygen atoms within the spacer produce a straighter backbone than other spacers, which can aid in hybridization.

155

5.3 The design of electrodes for the electrochemical detection of ferrocene oligonucleotide within a microfluidic channel. The insert shows the electrodes with widths of 15μm, 10μm and 5μm for the counter, reference and working electrode respectively with 10μm spacing between each of the electrodes. . . . 158

5.4 Illustration of the microfilter capturing microspheres within a flow channel. 159

5.5 Photograph of microelectrodes within microfluidic channel. The channel edge can be seen as it was placed over the 2mm long electrodes to ease the alignment of the channel (the slight out of focus is due to the PDMS substrate and the empty channel above the electrodes). The Ag/AgCl reference electrode is darker and not reflective like the Ag counter electrode due to the addition of chlorine to make the salt surface. 160

5.6 Scanning electron microscope picture of (a) the etched silicon mould showing the unetched channel with etched holes, which form raised pillars in the moulded PDMS and (b) structured PDMS showing the raised pillars, which make the filter, within the microchannel. 161

5.7 The voltammogram of the cyclic voltammetry investigation of ferrocenylated ssDNA within a macrosystem: (A) indicates the oxidation of the ferrocene; (B) shows the electrolysis of the background electrolyte; (C) indicates that the reaction was non-reversible as no reduction reaction is taking place; (D) shows the system has a small reduciton reaction so was quasi-reversible.[163] 166

5.8 The cyclic voltammogram of the ferrocene oligonucleotide using the microelectrodes within the microfluidic device. (A) Start of the oxidation sweep upwards with the electrochemical system stabilised after connection of the cell; (B) unidentified oxidation peak of unknown within the electrochemical cell; (C) the oxidation of the ferrocenylated oligonucleotide. (D) lack of a peak here shows the irreversible nature of the reaction within this system; (E) is a small reduction peak of the ferrocene making for a quasi-irreversible reaction. 167

5.9 Baseline corrected voltammogram of the detection of a specific DNA sequence using the biotinylated oligonucleotide assay. The device was heated from 150s and the flow through the device was started at 350s. The peak current is observed at 350s. Data starts at 150s due to the first 150s allowing the stabilisation of the electrochemical cell. 168

5.10 Background current generated by the heating of the device by the Peltier effect heat pump in the electrochemical cell within the microfluidic channel. The current rises as the electrodes were heated and after the flow starts, at 350s, the electrodes are again in solution and the temperature stops increasing. The first 150s are not displayed as these were to allow the electrochemical cell to stabilize. 170

List of Tables

2.1 A table to show the minimum possible feature size resolvable by each different type of mask process. 54

2.2 Table to show the spin speeds used for the different photoresists and different desired thickness. 56

2.3 Table to show the exposure times for the different photoresists used and at different thicknesses used. Power of the lamp used was 100W. 57

2.4 Developer type and time for the different photoresists used. . . 58

2.5 Table of the settings used in etching silicon wafers within the STS ICP 58

2.6 Table showing the settings used within the STS ICP for the oxidisation of PDMS 63

3.1 Table to show the final concentrations of reactants in the PCR experiments. 87

List of Abbreviations

A	Adenine
ABTS	2,2'-azino-bis(3-ethylbenzthiazoline-6-sulfonic acid)
Asp	Aspartic acid
BSA	Bovine serum albumin
C	Cytosine
CAD	Computer aided design
CE	Capillary electrophoresis
DMF	Dimethylformamide
DNA	Deoxyribonucleic acid
dNTPs	Deoxynucleoside triphosphates
dsDNA	Double stranded deoxyribonucleic acid
dTTP	Deoxythymidine triphosphate
EC	Electrochemical
EC-CE	Electrochemical detection with capillary electrophoresis separation
E.coli	*Escherichia Coli*
EDAC	*n*-(3-Dimethylaminopropyl)- *n*' -ethylcarbodiimide
EDTA	Ethylene diaminetetraacetic acid disodium salt
EOF	Electroosmotic flow

EtBr	Ethidium brominde
G	Guanine
Glu	Glutamic acid
HRP	Horse radish peroxidase
IR	Infra red radiation
ITO	Indium tin oxide
MES	2-(N-Morpholino)ethanesulfonic acid
NaAc	Sodium acetate
NHS	*n*-hydroxysuccinimide ester
PBS	Phosphate buffered saline solution
PCR	Polymerase chain reaction
PDMS	Poly(dimethylsiloxane)
pI	Isoelectric point
PMMA	Polymethylmetacrylate
PTFE	Polytetrafluoroethylene
RNA	Ribonucleic acid
RT PCR	Reverse transcriptase polymerase chain reaction
RTV	Room temperature vulcanisation poly(dimethylsiloxane)
sccm	Standard cubic centimeters per minute
ssDNA	Single stranded deoxyribonucleic acid
STS ICP	Surface Technologies System inductively coupled plasma
T	Thymine

TBE	Tris borate EDTA
TEG	Triethyleneglycol
UV	Ultra violet radiation
μTAS	Micro total analysis system

Chapter 1

Introduction

1.1 Research Aim

The aim of this research was to produce a microdevice in order to detect specific DNA sequences, for example in disease identification, combining the use of the polymerase chain reaction (PCR) with real-time electrochemical detection in a microfluidic platform. Amplification of short DNA sequences that are specific to a particular bacteria can be used positively identify bacteria within the sample. The overall motivation was to produce a fast, inexpensive, point of care device for specific DNA strand detection. Using a microfluidic platform, it may be possible to develop a device with a decreased reaction time, without any loss of analytical performance from the PCR. It is also hoped a reduction of cost may be possible by reducing reactant consumption.

An electrochemical assay for the detection of DNA was invented by Molecular Sensing plc, Melksham, who funded part of this work. The assay utilises ferrocenylated single stranded DNA molecules (ssDNA) which are detected by an electrochemical cell within a sample solution. It was proposed that using the assay within a micro PCR device, it would provide a low cost solution to identification and quantification of particular DNA sequences.

1.2 Polymerase Chain Reaction

The polymerase chain reaction (PCR) is the enzymatic chemical amplification of DNA. It has become a routine laboratory technique in biology and is used for producing detectable or quantifiable amounts of DNA of specific sequences from either a known or unknown sample. PCR was invented in 1985[1] by Mullis. It was discovered that by using a series of temperature cycles, an enzyme could be used to replicate a sequence of a DNA target strand. This technique became more common place when the original and thermally unstable enzyme, the Klenow fragment,[2] which was a part of DNA polymerase 1 from *Escherichia coli*, was replaced with a thermophile polymerase enzyme, *Taq* polymerase. *Taq* polymerase was extracted from the bacteria *Thermus aquatics*[3] which was discovered in natural hot springs in Yellowstone Park, USA. The enzyme does not denature at the high temperatures required during cycling. The ability of the enzyme to cope with high temperatures enabled the automation of the process, as the enzyme did not need to be added sequentially after each high temperature stage. This later discovery has made PCR a routine molecular biology tool.

1.2.1 Components of a PCR

In order to outline the PCR process, the components of the reaction must be defined and explained.

Template: The template is the double stranded DNA (dsDNA) from which a target section of interest or the complete strand is to be amplified. The target can be a gene or an identifying sequence from the sample DNA;

Primers: Primers are short single strand DNA (ssDNA) that are complementary to the target and binds to the melted template to provide a starting point for the enzyme to extend the primer;

dNTPs: Deoxynucleoside triphosphates (dNTPs) are the four nucleosides that make up DNA, namely deoxyadenosine, deoxyguanosine, deoxycytidine and deoxythymidine;

Polymerase: The enzyme catalyses the addition of the complementary nucleosides of the template to the primer and therefore extends the primer. A number of enzymes have been used, although *Taq* polymerase is the most commonly used;

Buffer: The buffer commonly used is Tris-HCl. The Tris-HCl is buffered at pH 8.5 at 25°C, although the pH varies greatly over the temperature range. Tris-HCl is used more for historical reasons rather than for any other practical reason;

$MgCl_2$: Two magnesium ions are used with the enzyme to coordinate the DNA at the active site. Addition of Mg^{2+} ions increases the selectively of the reaction. An increase in the selectivity of the reaction means that the incorporated base is more likely to be the correct complementary nucleoside.

1.2.2 Workings of PCR

As stated, PCR uses a series of temperature cycles to allow the *Taq* enzyme to amplify the target, see Figure 1.1. There are three steps within each cycle. The first stage involves melting the template, such that the dsDNA helix is broken to form two ssDNA, by heating the reaction to 90-95°C. The temperature is then lowered to 60°C to allow the specific annealing of primers to the two separate ssDNA. The primers provide a starting point for the polymerase enzyme to add complementary bases to the target. Polymerase enzymes have to use dsDNA as a starting point for adding the complementary bases therefore the primers are annealed to the template. To complete the cycle, the temperature is raised to the optimum working temperature of the polymerase enzyme (for *Taq* polymerase this is 72°C).

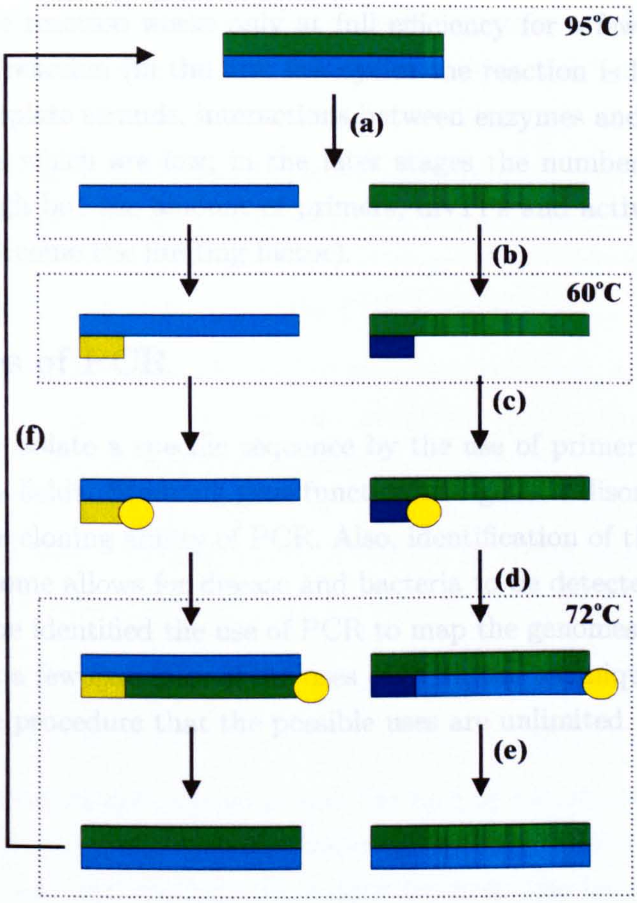

Figure 1.1: Schematic of one PCR cycle: (a) the dsDNA template is melted at 95°C to form two ssDNA; (b) primers attach to the 3' end of the single strand template DNA at 60°C; (c) enzyme attaches to the 3' end of the primer; (d) the enzyme extends the primer at 72°C by addition of the complementary dNTP from the solution; (e) the enzyme extends the primer until it reaches the end of the strand or until the temperature is raised to form 2 exact copies of the template dsDNA; (f) the end of the cycle is reached and the number of template strands is doubled for the next cycle.

At this temperature, the enzyme adds the complementary dNTPs to the primer, to complete the dsDNA. Each cycle in theory doubles the number of the starting strands, such that the total number of strands at the end of the reaction is equal to 2^n, where n is the number of cycles completed.

In practice the reaction works only at full efficiency for a few cycles in the middle of the reaction (in the first few cycles the reaction is limited by the number of template strands, interactions between enzymes and primers with melted targets which are low; in the later stages the numbers of template strands are high but the amount of primers, dNTPs and active enzyme are low, so they become the limiting factor).

1.2.3 Uses of PCR

The ability to isolate a specific sequence by the use of primers makes PCR useful in many fields. Studying gene function and genetic disorders has benefited from the cloning ability of PCR. Also, identification of the presence of particular genome allows for disease and bacteria to be detected. Before the genomes can be identified the use of PCR to map the genomes is invaluable. These are just a few examples of the uses of PCR, the technique has become such a routine procedure that the possible uses are unlimited.

1.3 Microdevices

A microdevice is a miniaturised sensor, instrument or structure, which, in the context of this work may be involved in an analytical, biological or chemical process (including fluidic movement, separation and sensing). Microdevices often contain micrometre sized features which allow the manipulation of low volume samples, to enable the investigation of the composition of a sample or to perform a reaction.

1.3.1 Benefits of Miniaturisation

Converting conventional analytical instruments to microdevices or microsystems delivers certain benefits which drive the area of research. Reduction of the volume of the sample used for analytical purposes makes the system more economically efficient by reducing the amount and hence the cost of the reactants.

An additional reason for trying to reduce the size of instruments is the reduction in analysis time which can be gained through miniaturisation. This arises in PCR due to the reduced thermal mass of the system, such that it is quicker both to heat and to cool the PCR volume.

Due to the fabrication methods used to make microdevices, a number of different structures can be fabricated and integrated within the same device, making a complete miniaturised diagnostic instrument possible. Alternatively, separate devices can be linked or "interconnected" together to preform the desired function. Parallelisation of devices in which several individual sub-systems are linked together can be used to produce high-throughput systems with low volumes. As with silicon transistor microchips, mass parallel fabrication can lead to very cheap individual units, which in this case could enable one-shot, throw-away diagnostic devices to be produced.

Thus, as instruments are reduced in size, the field of miniaturised, disposable point of care diagnostics becomes possible. If devices can include complete sample "work up" and testing, the ability to move the instrument to the patient or to the raw sample becomes a useful possibility. Point of care diagnostics would bring faster diagnosis with the result that effective treatment can be implemented more effectively. With diagnosis being made "on-site" the total cost of the sampling and analysis would be decreased by reduction in the number of steps taken from the start to finish, and the numbers of people involved in the total analysis.

1.3.2 History of Miniature Devices

The first miniature analytical device was a micro gas chromatography device reported by Terry *et. al.*[4] in 1979. A 1.5m long gas chromatography column with a thermal conductivity detector was fabricated on a silicon wafer. However, this failed to inspire further development for nearly a decade due to poor performace. The field did not become widely used until the early 90's when an open column liquid chromatograph was fabricated in 1990 by Manz *et al.*[5] and the phrase miniaturised total chemical analysis systems (μTAS)[6] was first coined. The device was not actually used but theory showed it should be almost comparable to conventional machines. Since then there hve been great improvments in the design and microfabrication leading to a major new technology that is now in widespread use.

1.3.2.1 Capillary Electrophoresis Devices

Capillary electrophoresis (CE) is a technique that lends itself to a microchip format because there is no need for moving parts, integration of electrodes is simple whilst injection plug geometries are easily defined. The first example of micro CE device was published in 1992 by Manz *et. al.*[7] In this case two dyes, calcein and fluorescein, were separated in 300sec using a separation voltage of 3000V. This device proved that micro CE separations were possible without a loss of efficiency. The same group incorporated a sample injection system[8] using a sample channel crossing the separation channel, see Figure 1.2. Building upon this, Harrison *et. al.*[9] fabricated a device which could separate six amino acids in under 5sec, the separation of the amino acids pointed the way for on-chip protein separation. Since then, on-chip CE devices have subsequently been used for medical diagnostics[10,11] and genotyping[12] as well as other applications.

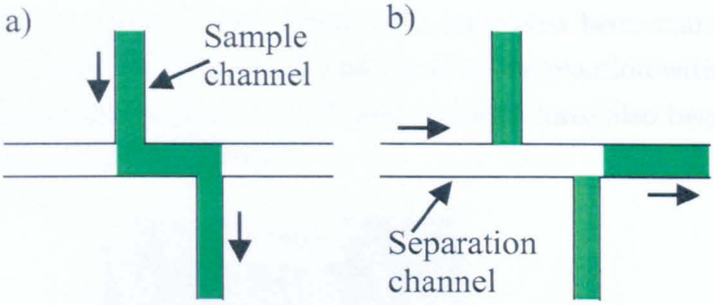

Figure 1.2: Illustration of the mechanism for the sample injection devised by Harrison *et. al.*[8]: (a) the sample is moved by electrokinetic fluid flow through the sample channel crossing the separation channel. The potential moving the sample was switched off leaving a plug within the separation channel; (b) a separating potential is applied along the separation channel and the sample plug moves along the channel and is separated.

1.3.2.2 Other Electrokinetically Pumped Devices

Open channel electrochromatography was published first by Jacobson *et al.*[13] The channel surface was coated in octadecylsilane and electroosmotic pumping was used to move the mobile phase. Three different coumarin dyes were separated in 150s. On-chip separations of DNA using polyacrylamide filled channels with field strengths up to 2300V/cm were achieved by Effenhauser *et al.*[14] in 1994, showing that microdevices could enable fast and effective separations and could be used for the sequencing of DNA. Sequencing was also shown by Woolley *et al.*[15] in 1994.

Electrokinetic devices for separations were first investigated due to the ability to move fluids within the micrometre sized cross-sectional channels by electroosmotic flow. From these initial devices a vast range of different samples and systems have been incorporated on to microchip platforms.

Wilding *et al.*[16] in 1994 showed that human blood, serum and cells could be moved through microchannels and filtered on-chip thus demonstrating that actual biologically relavent samples could be handled within microdevices. The structure of red blood cells was investigated by using a microarray of pillars[17] within a flow device. Other cells have also been manipulated by electroosmotic flow, see Figure 1.3, and lysed by the reaction with a chemical agent in microchannels by Li *et al.*[18] and particles have also been separated within devices by electric fields.[19]

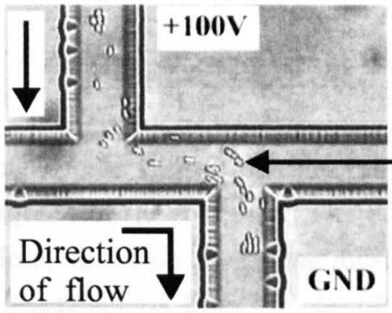

Figure 1.3: Picture of yeast cells being moved through a microfluidic channel by electroosmotic flow within a device fabricated by Li *et. al.*[18] 100V was applied across the length of the channel with the cells moving from the high voltage towards the ground.

1.3.2.3 Mixing Within Microsystems and Mixing Devices

Fluids moving within a microchannel are described as having a low Reynolds numbers. The Reynolds number[20] of a system relates to the dimensions of the channel, diameter d, in which the fluid is flowing as well as the velocity, v, of the flow and the kinematic viscosity, ν, see Equation 1.1.

$$Re = \frac{vd}{\nu} \tag{1.1}$$

A low Reynolds number, considered as being below 2000, will normally describe a fluid flow which is predominantly laminar flow (where there is limited turbulent mixing). For Reynolds numbers above 4000, the flow regime is turbulent, and inbetween these values a third phase is said to be in flux between the two states. As stated, fluid within laminar flow regimes flows in streamlines with all streamlines travelling parallel to each other. Due to this turbulent mixing of reactants within microchannels is not possible. As there isn't any turbulent mixing between stream lines, increasing the surface interfaces within microfluidic devices increases the rate of diffusion, therefore the rate of reactions is not limited by lack of mixing. The time taken (t)[21] to diffuse a distance (x) is directly proportional to the square of the distance and the diffusion constant (D), see Equation 1.2.

$$t = \frac{x^2}{2D} \tag{1.2}$$

As the distance needed to diffuse doubles, the time taken for the diffusion increases as the square of the distance. Therefore for reactions to take place within microdevices, diffusion distances must be kept at a minimum. A reaction device, described by Bessoth *et. al.*[22] decreases the width of the channel to reduce the diffusion distance. This resulted in fast mixing of fluids by diffusion, see Figure 1.4.

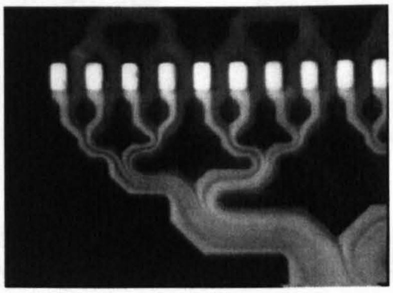

Figure 1.4: Micromixer fabricated by Bessoth *et. al.*[22] showing the diffusion of fluorescein and rhodamine B across streamlines formed within a laminar flow regime. At this flow rate, 50μl/min, the time scale of this picture was ~9ms.

1.3.2.4 Biological Samples Within Microdevices

Many reactions involving enzymes within microchip devices have been published for a variety of purposes, only a few examples for illustrative purposes are discussed here. In 1996 Jacobson *et. al.*[23] used an enzyme to digest a DNA strand. The enzyme and the DNA were electrokinetically migrated into a reaction chamber, 0.7nl in volume, see Figure 1.5. The reactants were held within the reaction chamber for 2-3min, with the small volume of the reaction chamber allowing efficient enzyme substrate interaction, by diffusion. Digested DNA was then separated by CE and detected. The whole reaction and separation took 5min.

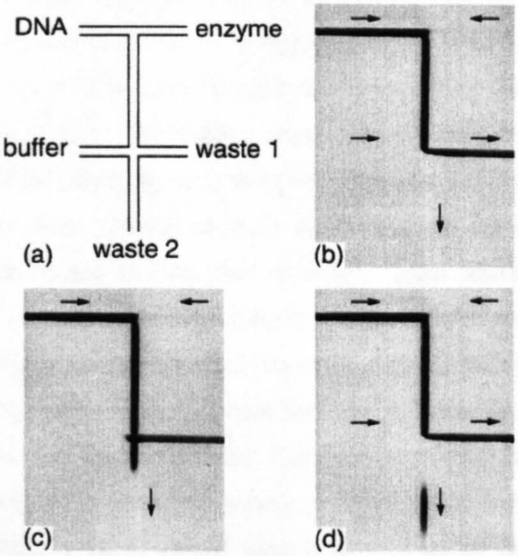

Figure 1.5: a) Schematic of the channel structures used by Jacobson *et. al*[23] for the digestion of DNA by restriction enzyme and sizing of the products along the separation channel (labelled waste 2). b),c) and d) Show the generation of a plug of reaction mixture for separation and sizing. All fluid movement is by electroosmotic flow, so a precise volume of digested enzyme can be separated each time the reaction process is run.

Haad *et.al.*[24] studied the reaction kinetics of a reaction between β- galactosidase and the substrate resorufin β-D-galactopyranoside, to produce resorufin as a fluorescent product, on a microchip format. By controlling the flow of the substrate precisely, by electroosmotic flow, different amounts of substrates were continuously diluted and then reacted continuously with the enzyme, in a 6.5nl volume reaction channel. The amount of product produced was measured optically. Diffusion across the 17μm wide channel took ~11s with a 20min reaction time. Using this information, the reaction kinetics of the system were described and were found to be comparable to the routine assay. Yakovleva *et. al.*[25] used chemiluminescence to detect the light produced by the reaction of horseradish peroxidase (HRP) which was captured on immobilised antibodies. The assay worked on the basis that the analyte was in direct competition with a HRP tagged analyte for binding sites, and that the amount of light collected when the HRP reacted with luminol and H_2O_2 was related to the amount of sample analyte. The system showed that chemiluminescence could be used within a microdevice format with limits of detection as low as 1ng/l. Soybean peroxidase was also used by Srinivasan *et. al.*[26] to polymerise phenols to form polyphenols within a microfluidic device. The reactants were moved along a flow channel by electroosmotic flow and the reaction occurred within the channel. This model reaction demonstrates the use of microfluidic platforms in combinational chemistry which lead to the possibility of being able to coat the surfaces of microchannels with polymers. Schilling *et. al.*[27] reported the fabrication of a device which lysed bacterial cells and then detected the presence of β-galactosidase within the cells by running a fluorogenic assay on the chip, see Figure 1.6. Cells debris was continuously introduced into a microfluidic channel and reacted with a commercial lysis reagent. The cells were separated from the flow by means of a T-junction with solid material travelling along one arm and the proteins extracted traveling along the other. The extracted β-galatosidase was then reacted with resorufin β-D-galactopyranoside to form a fluorescent product which was detected along another microfluidic channel. 10% of the total amount of β-galatosidase within the cells was detected.

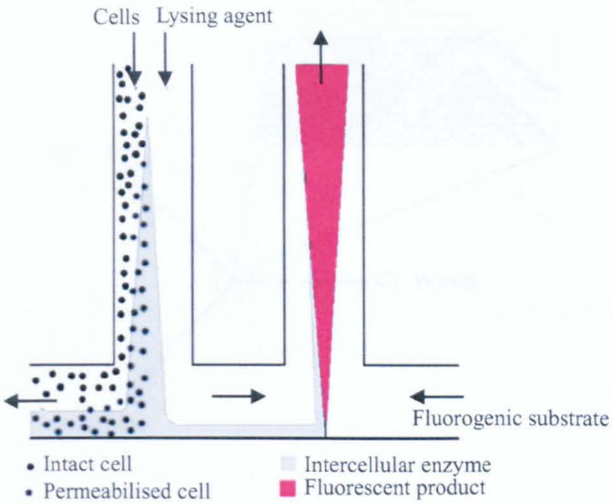
Cells
Lysing agent
Fluorogenic substrate
• Intact cell
• Permeabilised cell
Intercellular enzyme
🟥 Fluorescent product

Figure 1.6: Schematic of the double T-junction used by Schilling *et. al.*[27] to lyse cells, extract β-galatosidase and react the enzyme with a fluorogenic substrate. The cells were chemically lysed in the channel at the interface, working within a laminar flow regime, between the cell flow and lysing agent flow. At the T-junction the two streamlines split because of the laminar flow regime, the extracted proteins flow towards the enzyme substrate. The resorufin was released from the substrate at the interface of the two streamlines and was detected within the second flow channel.

A device which performed a stopped-flow enzyme assay was fabricated by Burke *et. al.*,[28] see Figure 1.7. A micromixer was used to investigate the reaction kinetic constants of β-galatosidase with the fluorescent substrate, fluorescein mono-β-D-galatopyanranoside. The reaction volume was 6nl with the mixing taking place in under 1s. Under these conditions, the reaction constants could be calculated in 60s and compared favourably to the results gained by conventional stopped-flow techniques.

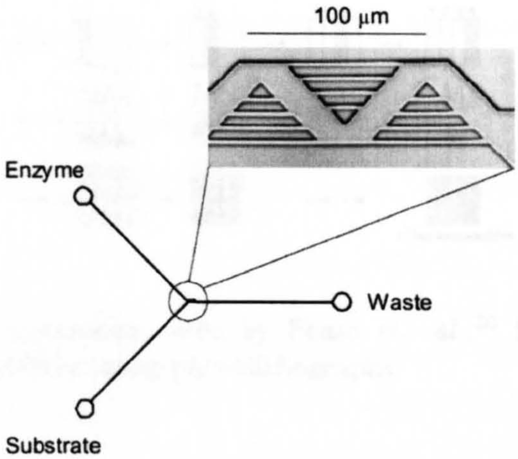

Figure 1.7: Schematic and image of the micromixer used by Burke *et. al.*[28] to find the reaction constants of enzyme reactions with fluorescein substrates. The network of microfluidic channels at the junction between the channels decreases the diffusion distance and therefore the time for the reaction to happen enabling fast reaction analysis.

Using immobilised ascorbate oxidase on a pillar array within a microfluidic channel, by Hayashi *et. al.*,[29] were able to remove L-ascorbic acid to allow for the detection of catecholamine. The pillars were used to increase surface area and the chance of reaction between the mobile and solid phases. The removal of L-ascorbic acid allows for catecholamine to be detected, electrochemically, with a limit of detection of 1nM when ascorbic acid was present in the sample. With this pretreatment of the sample, the limit of detection was low enough for the device to be able to detect catecholamine in blood samples.

Due to the fabrication techniques of the devices, spatial positioning of ssDNA on surfaces is also possible and has been used to form DNA arrays for sequence analysis. Probe ssDNA was immobilised by photolithography,[30] see Figure 1.8, or by electric fields[31] and the target ssDNA was washed across the array. Complementary sequences hybridise were detected therefore the sequence of the target DNA was discovered allowing for on-chip gene expression studies. A more complete disscusion of this topic is outside of the scope of this thesis.

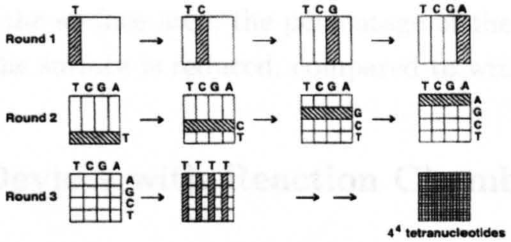

Figure 1.8: Basic procedure, used by Pease *et. al.*,[30] for building up an array of oligonucleotides using photolithography.

1.4 PCR Microdevices

The advantages to be gained by performing PCR experiments on microdevices, as with all chemical and biological systems, are considerable. Any method or system which can improve the efficiency and reduce the cost of a standard procedure is an inviting prospect. In the literature there have been many examples of microdevices which attempt to amplify DNA by PCR. The level of the amplification varies widely from device to device but none so far have compared favourably to conventional PCR devices.

A review of the current state of technology in the field of PCR microdevices is presented. In general, the devices can be divided into two major categories. Devices which utilise a reaction chamber in which the reactants are temperature cycled and those that use a flow through device to cycle the reactants. Also, examples of devices which do not fit within these two categories are discussed along with devices which incorporate detection of the products.

The general problem encountered with PCR microdevices is the high surface to volume ratios of the devices. Template, amplified DNA and the polymerase enzymes tend to adhere to the surface of the devices. This lowers the efficiency of the reaction, with the result that the devices do not perform as well as conventional thermal cyclers. Adhesion to the surface happens within all PCR tubes used with conventional thermal cyclers but as the volume is large compared to the surface area, the percentage of the DNA and enzyme which adheres to the surface is reduced, compared to within microdevices.

1.4.1 PCR Devices with Reaction Chambers

One of the first reports of a microfabricated PCR device was by Wilding *et al.*[32] in 1994. This device was a 17 x 15mm silicon and glass rectangle that was thermally cycled by a computer controlled Peltier effect heat pump. This system showed that the PCR process was possible within a microdevice but the efficiency of the reaction was lower than that of a conventional thermal cycler due to adhesion of the products and enzyme to the surface of the device. Following on from this initial device, the group has since investigated surface coatings[33] and improved the efficiency of the PCR device but efficiency and the consistency of amount of product still did not compare with conventional systems.

A number of systems have since been fabricated that perform PCR within a single chamber. Different materials have been used to fabricate the devices. Silicon and glass devices[34,35,36,37,38,39] have been extensively used because of the fabrication techniques used. Microfabricated wells, which use oil as a cover, have been fabricated with volumes as low as 86pl,[34] with a SiO_2 layer on the surface of the silicon to attempt to stop adsorption. An array of wells were used to perform single molecule PCR, unfortunately, the amplification in the low volumes less than doubled the amount of initial template. Microfabrication of small volume wells in silicon substrates allowed for chambers to be thermally isolated[35] from each other to produce faster cycling times, again with a SiO_2 layer to passivate the surface, see Figure 1.9. Other materials used to fabricate PCR chambers include poly(dimethylsiloxane) (PDMS)[40,41] which were fabricated by moulding the PDMS on microfabricated moulds and surface passivation using oxidised layer of PDMS[40] and parylene.[41] Epoxy-resin SU-8,[42] which is a photosensitive polymer, has been used to form a PCR chamber device with results that compared to silicon micro PCR devices. Many other devices have been fabricated in plastics[43,44] with similar results. Single chamber devices have been used to amplify and detect hepatitis C virus[37,38] and *Eshericha coli*[43] (*E. coli*) and *Salmonella tyhimurium*[44] to name a few but all with indifferent results.

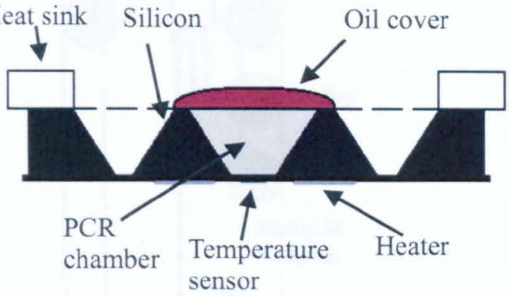

Figure 1.9: Illustration of a silicon chamber fabricated by Daniel *et. al.*[35] which was thermally isolated from the rest of the wafer to produce rapid thermocycling.

Most devices have used a single chamber in which the PCR was a batch process. Several devices have also incorporated separation, detection and different fluidic control mechanisms on to the same microdevice. The addition of capillary electrophoresis to provide on-chip separation and detection of PCR products was described by Woolley *et al.*[45] A electrophoresis channel was fabricated in glass and then an etched silicon PCR chamber positioned above the channel, the system could cycle through a PCR in 20min, and then separate and detect the products by fluorescence. Waters *et al.*[46] fabricated a device that ran 4 separate PCR experiments simultaneously, then separated them individually and detected all PCR products on the same device, see Figure 1.10. Bacteriophage λ and *E. coli* DNA were amplified and detected simultaneously showing that a higher through-put was possible.

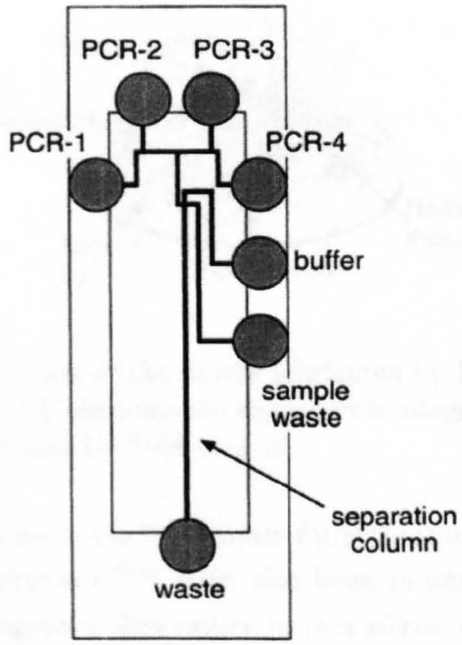
PCR-2
PCR-3
PCR-1
PCR-4
buffer
sample
waste
separation
column
waste

Figure 1.10: Illustration of the device layout used by Waters *et. al.*[46] to cycle 4 PCR experiments at once and then individually separate the products all within the same device.

This group has since published other devices on a range of DNA samples[47] and concentrated the DNA[48] using a porous frit. With on-chip electrophoresis, a number of devices have been fabricated that automatically take the sample through the various parts of the device. Other systems have included mechanical valves,[49,50] see Figure 1.11, and gel valves[44] for fluidic control before and after the PCR cycling.

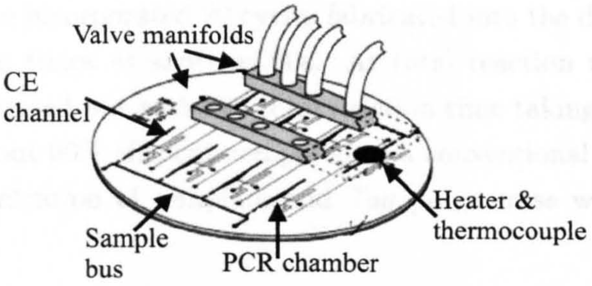

Figure 1.11: Illustration of the device fabricated by Lagally *et. al.*[49] 8 separate chambers and CE channels are shown with integrated heaters and pneumatic valves for automatic fluid control.

As well as devices using electrophoresis for separation, detection devices using real-time fluorescence[51,52] have also been published. Schabmueller *et. al.*[51] used two integrated fibre optics in to a silicon chamber, one to illuminate the sample and the other to collect the fluorescence. PCR products could be detected but running a PCR experiment within the chamber was never carried out successfully. Belgrader *et. al.*[52,53] published a device which incorporated solid state optics for real-time fluorescence monitoring of PCR reactions. *Erwinia herbicola* and *Yersinina pestis*[52] and viruses[53] were detected during PCR with comparisons to conventional real-time instruments being favourable with some systems. Electrochemical detection[54,55] has been incorporated in to PCR devices, which are discussed later within this Chapter.

1.4.2 Flow-Through PCR Devices

The use of a continuous channel, which crosses and then re-crosses three different temperature zones with a constant flow rate, can create the thermal cycling necessary for PCR. This method is different from that of the general system of changing temperature over time. This method of flowing the reaction solution over three discreet temperature zones was first achieved by Nakano *et. al.*[56] by passing a single capillary through three oil baths. Following this a glass microdevice was fabricated by Kopp *et al.*,[57] see Figure

1.12. This device incorporated 20 cycles fabricated into the device and could amplify DNA in times as short as 90s. At total reaction times of 90s no product was detected but with the total reaction time taking 20min, the device became about 90% efficient compared to a conventional thermal cycler. A higher concentration of template and *Taq* polymerase were used in the microdevice.

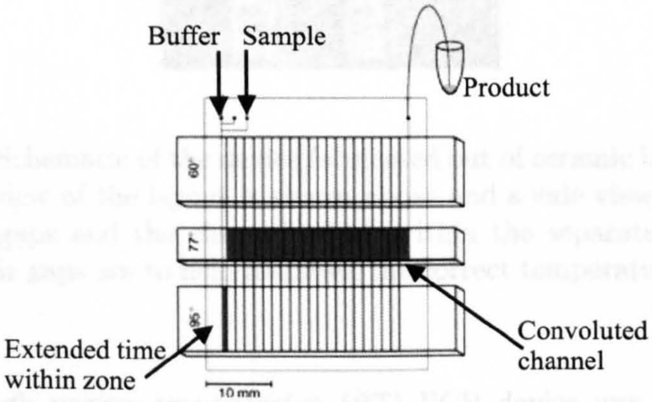

Figure 1.12: Illustration of the flow-through device fabricated by Kopp *et. al.*[57] in which the one channel crosses three separate temperature zones to thermally cycle the PCR. In order for the reactants to extend the time within the extension zone a convoluted channel is used within that region. To ensure all the template was melted the first melt stage is extended by the same method.

Chou *et. al.*[58] fabricated a microdevice that performed continuous flow PCR. This device was fabricated from high pressure and temperature fired ceramic layers with air gaps between the different temperature zones to isolate each temperature zone. The time within each zone was changed by adjustment of the width of the channel, see Figure 1.13. One cycle was fabricated into the device with the reaction mixture being recycled 20 times through the device by a peristaltic pump. 30 cycles took 40min with a total reaction volume of 19μl. The efficiency was comparable with a conventional thermal cycler when a higher concentration of template and enzyme was used within the device.

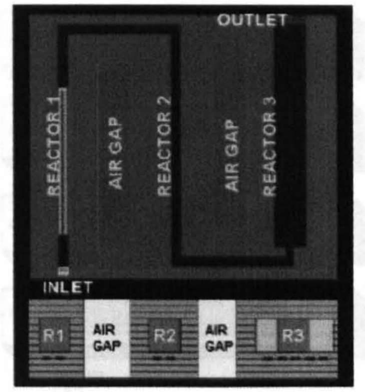

Figure 1.13: Schematic of the device fabricated out of ceramic layers by Chou *et. al.*[58]. A view of the layout is shown above and a side view of the device showing air gaps and the channel width within the separate temperature zones. The air gaps are to help maintain the correct temperatures across the device.

A flow-through reverse transcription (RT) PCR device was fabricated by Obeid *et. al.*[59] RT PCR is a method of amplifying a RNA sample using reverse transcriptase. The device was fabricated from glass with a choice in the number of cycles that the PCR was cycled through. 20 to 40 cycles were used, see Figure 1.14. Both RT PCR and PCR were achieved within the device. A single cycle took 13s with 40 cycles taking 17min for a 10μl sample.

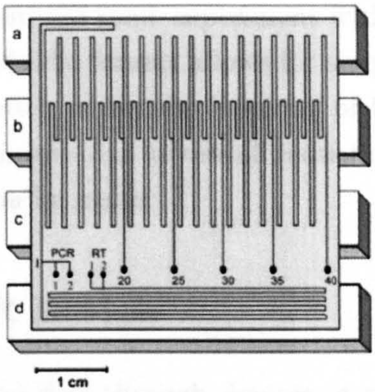

Figure 1.14: A schematic of the device fabricated by Obied *et. al.*[59] The device contains separate inlets for the PCR and RT PCR and the outlets for cycling the reaction through the different number of cycles. With the different temperatures being the various steps a) melting, b) extension, c) annealing and d) for the transcriptase enzyme to preform the RNA copying.

Fukuba *et. al.*[60] designed and fabricated a flow-through PCR microdevice using glass and silicone rubber (PDMS). Temperature sensors were integrated on the glass substrate and the flow channel was moulded into the silicone elastomer. The surface passivation of the silicone rubber channel was important due to the channel being 3m long, having a high surface to volume ratio, and the high adsorbance of the polymerase enzyme and template to silicone rubber. Surface passivation was achieved by using a 2-methacryloyloxyethyl phosphorylcholine silane polymer. Genomic *E.coli* DNA was amplified directly from cells within the device by chemical lysing cells at the high temperature stage. The device was fabricated with 30 cycles which took less than 30min.

A flow-through system has advantages over that of a reaction chamber. As the channel cross sectional area is small, the temperature of the fluid inside the channel rapidly reaches the temperature of the channel surface. Therefore no time is taken in varying the temperature, allowing for faster cycling. Larger sample sizes can easily be handled within the flow-through format because the sample can be continuously flowed into the channel. Multiple samples can be run within the same experiment without the need for device parallelisation. A microfluidic format allows for simple addition of microfluidic work ups and detection protocols. Removal of heaters which vary their temperature with time means that an overall reduction in the control systems needed for the device can be made.

1.4.3 Other PCR Devices

As well as chambers and flow-through devices, a number of other devices that utilize different ways of thermal cycling and sources of thermal energy have been published. Using an analogous idea to the flow-through devices, three separate temperature zones were used in devices with different layouts. Bu *et al.*[61] fabricated a device which used three chambers each set at one of the temperatures needed for the thermal cycling. The reaction mixture was moved from one well to the next, by a bi-directional peristaltic pump, to perform the thermal cycling of the reaction. As with flow-through devices the time taken to change temperatures was small, less than 1s. Liu *et al.*[62] used a circular channel, with three separate temperature zones, see Figure 1.15, in which the PCR reactants were pumped around, cycling through the temperatures. The mixture was flowed continuously within a closed loop until the reaction was completed. Human β-actin gene was flowed around the circular device for 30min, and detected in real-time using a fluorescent PCR assay. Compared to a commercial thermal cycler the amplification was just less than 80%.

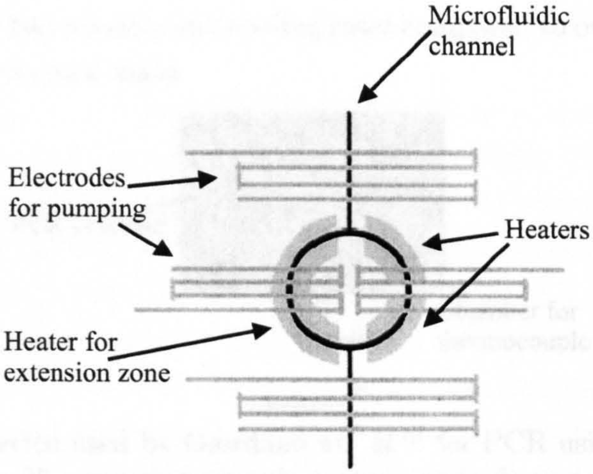

Figure 1.15: Illustration of the rotary PCR device fabricated by Liu *et. al.*[62] The microfluidic channel is shown along with the position of the heaters dividing the loop into different temperature zones. Electrodes are used for electrokinetic pumping of the fluid within the microfluidic channel.

So far the devices that have been discussed have been heated by contact heaters, which heat the reaction mixture externally of the solution, by using peltier effect heat pumps, heating blocks or thin film heaters. A number of other devices have been published where the thermal energy has been generated by alternative methods. Pal and Venkataraman[63] heated a PCR reaction chamber by induction heating. A primary coil heated a metal ring (a secondary coil) on which four 1mm diameter chambers were positioned. This produced a simpler device to fabricate, which had a lower power consumption due to the method of heating with the four chambers being heated by one 12V lead acid battery.

A further method of heating was the use of radiative process, such as an IR lamp. The use of an IR lamp as the thermal heat source was demonstrated off chip by Oda *et al.*[64] and then on-chip by Giordano *et al.*[65] The device was a polyimide device with two chambers, one for the PCR reaction and the other for temperature measurement, see Figure 1.16. A focused IR lamp was used to heat the device and a fan was used to force cool it. The benefit of this was very fast heating and cooling rates compared to other devices due to the reduced thermal mass.

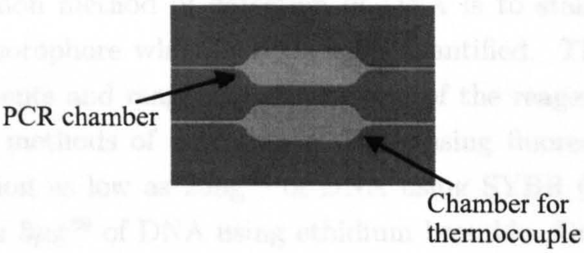

Figure 1.16: Device used by Giordano *et. al.*[65] for PCR using IR mediated thermocycling. The reaction chamber were made from polyimide with a volume of 1.7μl.

Kopf-Sill *et. al.*[66] used electrolytic resistance heating, also known as Joule heating, to cycle PCR reactions. The reaction solution was heated by passing current directly through the mixture between two electrodes. A potential was applied between the electrodes generating thermal energy within the solution. Measuring the conductivity of the solution gave an indication of the temperature of the reaction, which could be monitored and controlled precisely by changing the current applied. This method for heating is well suited to a microfluidic device because only electrodes within the solution are required and no external heating system is necessary. Joule heating of PCR microdevices is covered by US patents held by Caliper Technologies, CA, USA.

Another deivce design was presented by Hardt *et. al.*[67] This device uses a reservoir of a ferrofluid, which is controllable under the effect of external magentic fields, to move a plug across three distinct temperature zones to cycle the PCR. The temperature zones are aligned in a striaght line with respect to the other temperature zones.

For more recent devices in the field please refer to a recent review[68] in to the subject.

1.5 Electrochemical Detection of DNA

The most common method of detection of DNA is to stain or "label" the DNA with a fluorophore which can then be quantified. This relies on expensive instruments and reagents, with several of the reagents being highly toxic. Routine methods of detection of DNA using fluorescence can have limits of detection as low as 25ng[69] of DNA using SYBR Gold (Molecular probes, USA) or 5μg[69] of DNA using ethidium bromide. Detection of DNA by electrochemistry has been shown to be sensitive and there are also other advantages to using electrochemical methods. Electrochemical detection can be performed with an electrochemical cell within the sample solution with no expensive optics required. Some analytes can be detected without any additional labelling. The potential at which the electron exchange happens is dependant on the electronic environment so that different analytes or chemical environments can be distinguished. There are, of course, some associated problems in using electrochemical methods for detection. Electrochemical detection is effected considerable by "dirty" samples but can be used in many samples in which fluorescence detection is not possible, ie cell debris. The number of electroactive analytes is small, so again expensive labelling is generally required.

1.5.1 Introduction of Electrochemical Cells and Potentiostat

An electrochemical cell comprises of an electrolyte, the solution within the cell, and at least two electrodes. Current is passed between the electrodes passing as ions within the electrolyte.[21] Two half reactions occur at the surface of the electrodes, addition of the half reactions together give the full chemical reaction which takes place within the cell. In order to reference the potential of the system to other electrochemical cells a reference electrode is added to the cell. This third electrode has, by convention, an electrode potential of 0V.[21] The half reaction under investigation takes place on the working electrode with the other electrode being called the counter electrode.

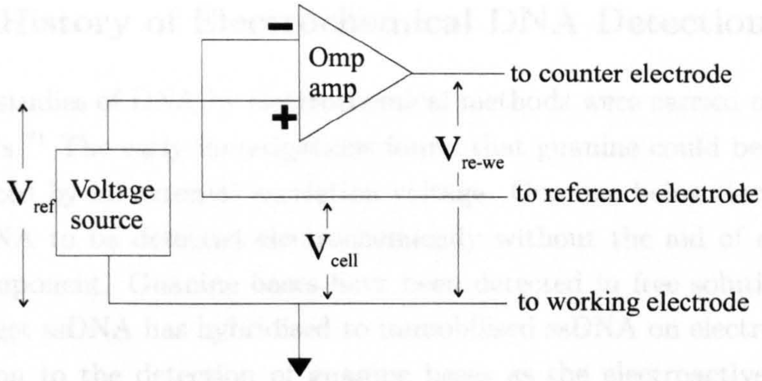
Omp amp
−
+
to counter electrode
$V_{re\text{-}we}$
V_{ref}
Voltage source
to reference electrode
V_{cell}
to working electrode

Figure 1.17: Circuit diagram of a potentiostat.

The half reaction, at the working electrode, is studied by applying a potential difference across the working and counter electrodes while relating the potential to the reference electrode. Voltages are applied by the use of a potentiostat. The current through the electrochemical is measured either as a function of voltage or time. Also the current could be held constant and the voltage varied. A number of techniques can be used to study the half reaction in question.

A basic circuit diagram of a potentiostat is shown in Figure 1.17.[70] The potential across the electrochemical cell is calculated by:

$$V_{cell} = A(V_{ref} - V_{re-we}) \tag{1.3}$$

Where A is the gain of the operational amplifier. If A is high then:

$$V_{re-we} \simeq V_{ref} \tag{1.4}$$

Adjustment of the output from the amplifier controls potential applied across the electrochemical cell.

1.5.2 History of Electrochemical DNA Detection

The first studies of DNA by electrochemical methods were carried out in the late 1950's.[71] The early investigations found that guanine could be oxidised and reduced by an external excitation voltage. Guanine being electroactive allows DNA to be detected electrochemically without the aid of an added redox component. Guanine bases have been detected in free solutions,[72] or when target ssDNA has hybridised to immobilised ssDNA on electrodes.[73] [74] In addition to the detection of guanine bases as the electroactive species, the sugar backbone[75] has also been used, taking advantage of the fact that copper surfaces catalyse oxidation of sugars.

The sensitivity of DNA detection was increased using the technique of adsorptive stripping.[76,77] Free DNA in solution was adsorbed on to the electrode and detected by the redox activity of the guanine bases present. The sensitivity is gained by baseline correcting after the detection by removing the DNA from the surface electrochemically.

The detection of redox active labels is another route by which DNA has been detected electrochemically. Addition of a label either by directly attaching the label or by intercalating a label to dsDNA allows the detection of the label by the electrodes within the electrochemical cell. A few examples of labels are presented below. A common method is to utilize metal colloid particles. Gold colloid is the most widely reported. Probe ssDNA is attached to the gold colloid[78] the probe DNA hybridises to target ssDNA which has been immobilised to a surface. If the probe DNA hybridises, the gold which is present can be dissolved by oxidising the gold atoms to $Au^{(II)}$ ions in an acidic solution[79] wash (bromine solution is often used). The ions are then detected using carbon paste electrodes. Using a similar method, gold with iron centred colloid[80] has been used which released Fe^{3+} in to the solution by the same mechanism. A similar process of DNA detection has been published using silver colloid,[81] with silver colloid attached to probe DNA hybridised to ssDNA attached to gold colloid. Gold colloid was used to increase the amount of DNA that could be attached on a surface to produce a limit of detection of 5pM.

Other labels have been reported for electrochemical detection of DNA, including, for example hexaamineruthenium$^{(III)}$,[82] methylene blue[83] and the addition of multi-walled carbon nanotubes[84] to the electrodes for hybridisation. Proteins and enzymes have also been used as labels for DNA. Daunomycin[85] is an electroactive protein which will intercalate with dsDNA allowing the detection of the DNA. HRP[86] has been attached to biotin modified probe DNA and then the electrochemical detection of the change in oxidation state of a HRP substrate.

Transition metals are commonly used[87] as labels for electrochemical detection due to their range of oxidation states the metals can posses and the ease with which they can be obtained. A popular choice is iron, as it has two redox states, Fe^{2+} and Fe^{3+}. The addition of two cyclopentadienyl rings around a Fe atom produce the compound ferrocene. This complex can be oxidised by the loss of electrons to form the stable ferricinium ion[88] $[Fe^{(III)}(\eta^5\text{-}C_5H_5)_2]^+$. The ring structures introduce convenient chemistry for further functional chemistry, allowing the attachment of ferrocene as an electrochemical label.

The most common method is the direct attachment of ferrocene to DNA. Ferrocene was first covalently bonded to the 5' end of 5'-aminohexyl-terminated oligonucleotides by Takenaka *et. al.* to detect dsDNA when hybridised.[89] dsDNA was detected by forming a triple-helix with the dsDNA[90] (a triple-helix is formed by the ferrocene tagged oligonucleotide fitting in to the major grove of the dsDNA, see Figure 1.18). The ferrocene oxidation potential changed when the triple-helix was formed allowing for detection of the dsDNA.

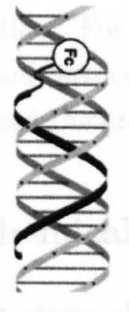

Figure 1.18: Illustration of the triple helix formed, by Ihara *et. al.*,[90] to detect dsDNA by ferrocenylated oligonucleotide.

Uto *et. al.*[91] used 5'-aminohexyl-terminated oligonucleotides as primers for PCR experiments. Using ferrocenylated primers allowed for an increase in sensitivity as the initial target DNA was amplified and each copy of the template was electrochemically active due to the addition of a ferrocene moiety within the primer.

Ferrocenylated oligonucleotides have also been synthesised chemically using aminoferrocene[92] or by modifying the sugar structure of the bases with ferrocene[93] and added into the DNA strand using an automated DNA synthesiser. Ferrocene tagged analogues of dTTP have been introduced to dsDNA by using the dTTP analogues in PCR reactions.[94] Naphthalene diimide intercalates with dsDNA and the addition of ferrocene to the intercalator on a carbon chain spacer[95,96] allows for the detection of dsDNA. The sensitivity of using ferrocenylated oligonucleotides was increased by attaching probe ssDNA to gold colloid which was attached to gold electrodes by Cai *et. al.*[97] The increased surface generated by the colloid allowed for a higher current density on the electrodes, as more ferrocene was in electrical contact with the electrodes. Hybridisation of ferrocenylated oligonucleotides to the immobilised DNA allows for the electrochemical detection with higher sensitivity.

Ferrocenylated oligonucleotides have also been used within a sandwich type assay[98] for increased selectivity. This sandwich assay used an immobilised ssDNA immobilised to a gold electrode, which was complementary to one end of a target ssDNA. The other end of the target DNA was complementary to the ferrocenylated oligonucleotide. For the ferrocene to be close to the electrode both the immobilised and ferrocenylated oligonucleotides have to be complementary to the target and therefore the selectivity is increased.

1.5.3 On-Chip Electrochemical Detection

Gavin *et. al.*[99] reported the first electrochemical detection (EC) microdevice. It comprised of a microfabricated electrode array on quartz in which a capillary was placed. Capillary electrophoresis of dopamine and catechol was carried out within the capillary and the separated analytes flowed into the device and over the electrode array. The electrokinetic potential was decoupled from the electrochemical cell by applying the voltage across the capillary and placing the electrode array downstream of the cathode. Integration of electrochemical detection and CE channels has been achieved in a number of other devices. Woolley *et. al.*[100] fabricated a CE channel with microfabricated counter and working electrodes. An external reference electrode was placed within the exit hole. Multiple working electrodes and dual working electrodes were used for enhanced sensitivity by Martin *et. al.*[101] with external counter and reference electrodes for EC-CE. The decoupling of the two interfering potentials was achieved by placing the electrochemical cell within a detection reservoir, along with the capillary electrophoresis cathode, as close to the channel as possible, see Figure 1.19. Having the cell within a wide detection reservoir decoupled the voltages as the separation voltage was dissipated across the reservoir.

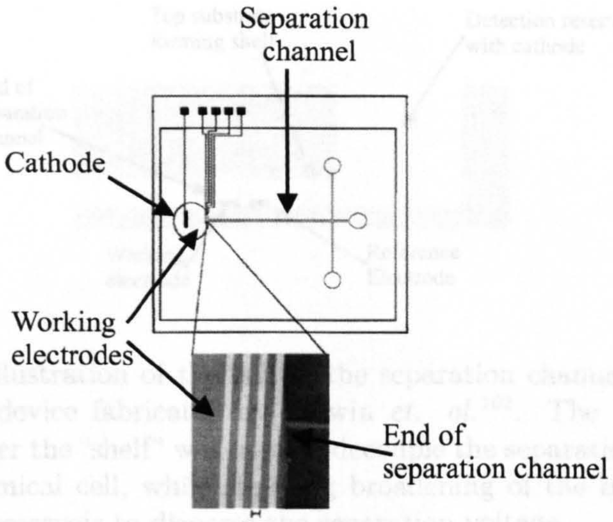

Figure 1.19: Martin *et. al.*[101] fabricated a device for CE-EC. A layout of the device is shown along with a picture of the electrodes demonstrating their placement compared to the separation channel. Multiple working electrodes were used to increase the sensitivity of the detection.

Balwin *et. al.*[102] decoupled the separation potential from the electrochemical cell in a similar fashion as Martin *et. al.* except in order to reduce band broadening after the dissipation of the electrokinetic voltage, the detection electrodes were within the separation channel but close to the detection reservoir, see Figure 1.20. To decouple the two potentials, Ertl *et. al.*[103] used two extra channels at 30°, with a gravity driven flow to the end of the separation channel. This produced a sheath-flow which focused the analytes together over the electrode, reducing the impact of the separation voltage on the electrochemical cell.

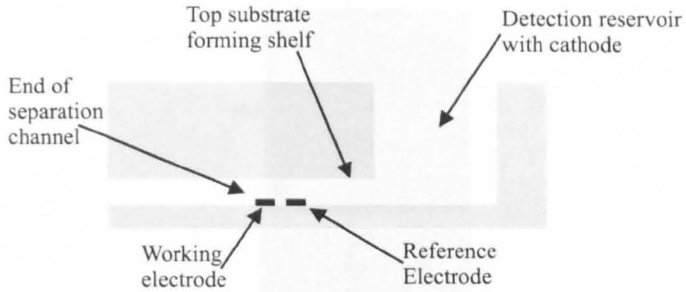
Top substrate forming shelf
Detection reservoir with cathode
End of separation channel
Working electrode
Reference Electrode

Figure 1.20: Illustration of the end of the separation channel and the electrodes of the device fabricated by Balwin *et. al.*[102]. The position of the electrodes under the "shelf" was used to decouple the separation voltage from the electrochemical cell, while stopping broadening of the bands, by using the detection reservoir to disperse the separation voltage.

On-chip electrochemical detection has also focused on utilizing the fabrication techniques to probe small volumes.[104,105] Enzyme activity, oxidases,[106,107] β-galactosidase,[108] creatine kinase,[107] have been investigated using the advantage of small diffusion distances. Horseradish peroxidase was used in a microchip protein assay[109] within a microdevice with microfabricated carbon electrodes. Cai *et. al.*[110] placed heart cells within microfabricated wells and the production of lactate was measured during the pulsing of the heart cell, see Figure 1.21.

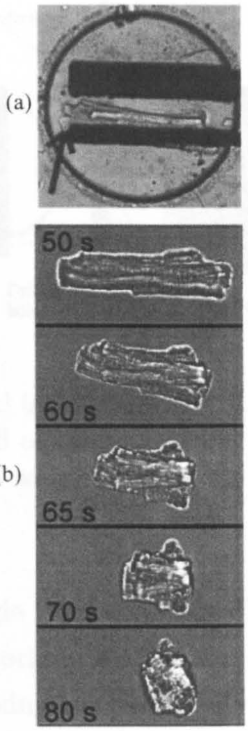

Figure 1.21: Pictures of a) heart cell in microfabricated well with microelectrodes and b) the heart cell be contracted by applied voltage from Cai *et. al.*[110]

1.5.4 Electrochemical DNA Detection Devices

The combination of electrochemical detection with microfabricated devices has been demonstrated by several groups. Woolley *et. al.*[100] separated DNA on the basis of its size and then detected DNA fragments using a CE-EC device, see Figure 1.22. This detection system employed the electroactive Fe(phen)$_3{}^{2+}$ group which intercalates to the DNA. The intercalated Fe(phen)$_3{}^{2+}$ was not detected, instead the reduction of the background Fe(phen)$_3{}^{2+}$ was measured when the DNA passed the detector. This device was reported to have a limit of detection for DNA within the attomol range.

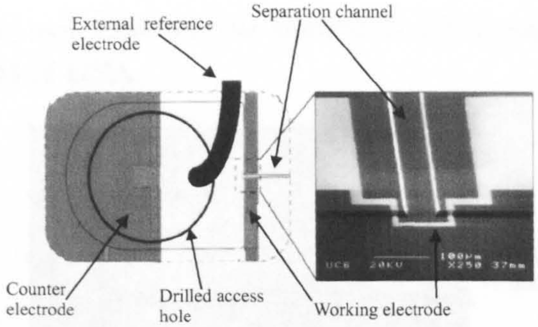

Figure 1.22: Device fabricated by Woolley *et. al.*[100] A schematic of the layout of the electrodes with the end of the separation channel and a scanning electron microscope image of the working electrode at the exit of the separation channel.

Lee *et. al.*[54] fabricated a single PCR chamber which comprised of either gold or indium tin oxide (ITO) working electrodes. ssDNA hybridisation probes were immobilised to the working electrodes. Hybridisation of PCR products to the immobilised probe DNA was electrochemically investigated in two different ways, depending on the type of working electrode. For the gold working electrode, a commercial electroactive intercalating dye was used and detected by the working electrode. Devices which had ITO working electrodes used gold colloid attached to the ssDNA, which hybridised to the immobilised DNA. The gold colloid was then stained with silver and the amount of silver measured using oxidative silver dissolution. Liu *et. al.*[111] detected DNA electrochemically within a polymer flow channel, see Figure 1.23. The silicone surface of the channel was modified to thiol groups by oxygen plasma oxidation and reaction with thiol-silane. ssDNA was attached by acrylamide groups on the DNA to the thiol surface. Biotinylated oligonucleotides were flowed through the channel and were hybridised to the immobilised DNA. Alkaline phosphatase with streptavidin was then bound to the biotin. An array electrode detected the presence of *p*-aminophenol, which is redox active, after the alkaline phosphatase had converted redox inactive *p*-aminophenyl phosphate. The alkaline phosphatase was used to give an amplification of signal by generation of the redox active product which was related to the number of enzyme and therefore the amount of DNA present. The limit of detection was 1nM of DNA.

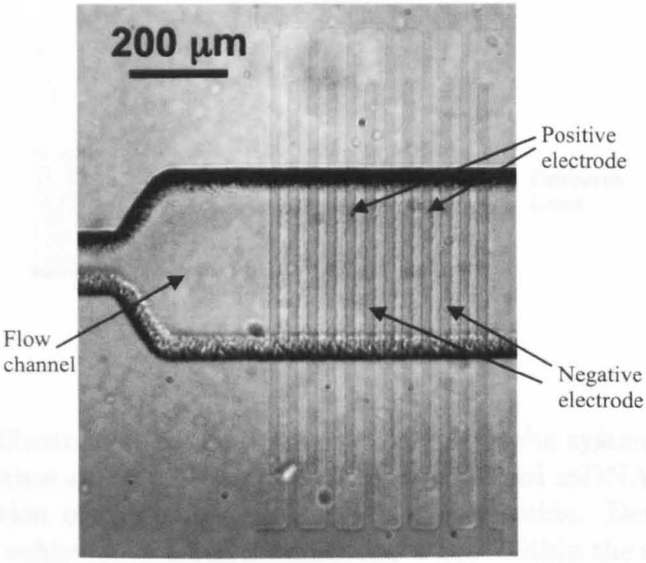

Figure 1.23: Picture of the microelectrode array for the detection of DNA fabricated by Liu *et. al.*[55] within an incubation chamber for alkaline phosphatase, for increasing the sensitivity of the system, in a microfluidic device.

Another device fabricated by Liu *et.al.*[55] detected DNA by using a self assembled monolayer on a gold electrode within a detection chamber, which contained a ssDNA as a capture probe,[112] see Figure 1.24. The capture probe hybridised with a section of the target ssDNA. Once the target DNA was hybridised and therefore immobilised on to the surface, a ferrocenylated ssDNA was hybridised to the other section of the target DNA. The ferrocene was detected by the electrode through the electro-responsive molecular layer on the gold surface.

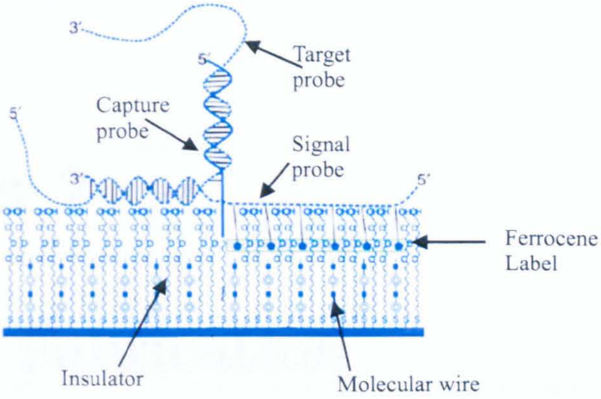
3'
5'
Target probe
Capture probe
5'
Signal probe
3'
5'
Ferrocene Label
Insulator
Molecular wire

Figure 1.24: Illustration of the sandwich capture probe system used by Liu *et. al.*[55] Capture of target ssDNA using immobilised ssDNA, followed by the hybridisation of the a ferrocenylated oligonucleotide. Detection of the ferrocene was achieved by using a "molecular wires" within the self assembled monolayer.

1.6 Conclusion

In summary, the technique of PCR has been discussed. A brief history of microdevices was discussed, especially in relation to PCR microdevices. The diversity of the microdevices used for PCR has been shown along with the problems. In addition, microdevices which utilise electrochemical detection have also been discussed, particularly in the field of DNA detection.

Chapter 2

Device Fabrication

2.1 An Introduction to Fabrication

Microfluidic devices can be fabricated by a number of methods. These require various individual processes but in general there are three basic ways in which devices can be made. The three underlying methods of microchannel fabrication are: 1) moulding; 2) etching and 3) additive methods. The technique that is used for fabrication depends on which materials are to be used and which method would be easiest to fabricate the device.

2.1.1 Moulding Methods

Moulding of microfluidic devices involves using a prefabricated mould or "master" and forming the design within the desired substrate. Pattern replication by moulding can be either by embossing (compression moulding) or liquid resin moulding. Compression molding involves using a hard master (relative to the material to be patterned) which is pressed into a deformable substrate. Often the substrate is heated to make it pliable to the moulding. Liquid resin moulding involves using a liquid polymer hardening over a mould to form the structure. In both cases the mould can be made of a range of materials and can be fabricated in a number of ways.

The advantage of moulding microfluidic devices is that it is a relatively cheap and quick method of fabrication. Generally cleanroom conditions are not required once the masters have been fabricated. The disadvantages of fabrication by moulding are that the master deteriorates leading to imperfections. It is possible that the embossed structure can begin to return to its original form, a process know as memory effect.[113]

2.1.2 Etching Methods

Etching of microfluidic devices is a common method for fabrication. Etching involves removing material from the channels within the device. There are two types of etching namely, isotropic and anisotropic. Isotropic etching is defined by the fact that the material is removed all directions at the same rate, whilst anisotropic etching defines a process in which not all directions are etched at the same rate, resulting in an asymmetric structure.

For example, glass can be isotropically etched by HF acid, whereas silicon can be anisotropically etched by KOH, see Figure 2.1. Despite the difference, both of these techniques are wet etching methods. Dry etching methods can also be employed. Dry etching involves using abrasive or reactive gases to etch the substrate. Dry etch methods can be either isotropic or anisotropic, see Figure 2.1, with the degree of selectivity dependant on the technique used.

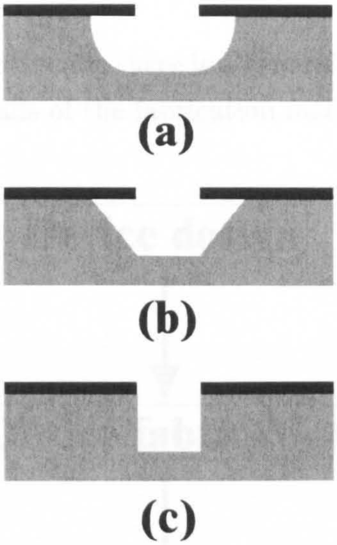

Figure 2.1: Illustration of the etch profiles gained using different techniques: a) glass etched isotropically by HF acid. The shape gained is due to the glass having been removed equally as quick side ways as vertically; b) silicon etched anisotropically by KOH, the silicon has been etched along a crystal lattice edge to gain the well defined shape; c) silicon etched anisotropically using an Surface Technologies System inductively coupled plasma (STS ICP), high selective etching giving a high aspect ratio etch.

2.1.3 Additive Methods

Additive techniques for fabrication of microfluidic devices involve depositing layers onto a substrate. Added layers are patterned to create the desired structures. A number of different materials can be used to build up the device. For example, high viscosity polymers such as PMMA[114] and SU-8[115] can be layered onto the substrate in relatively thick layers and then patterned. The advantages of using an additive procedure is that structures can be applied or added onto other microstructures, such as electrodes within a electrochemical cell. Additive methods are often used because of the ability to gain high aspect ratios with out the need for expensive fabrication equipment.

2.1.4 General Microfabrication Processes

In fabricating microfluidic devices there is a general series of processes, which are carried out of the details of the fabrication method employed, see Figure 2.2.

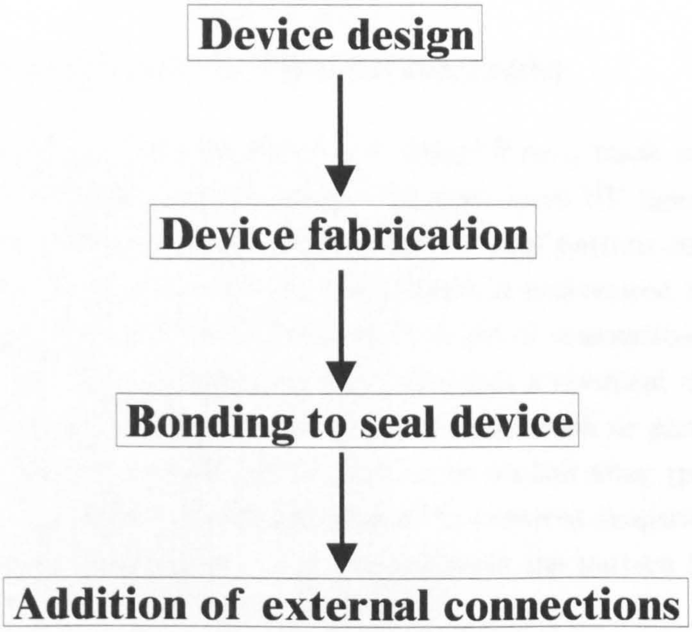

Figure 2.2: Flow diagram to show the general process of device fabrication

The designing of the device defines both the form and therefore the function of the device and necessarily, the materials that will be used. The pattern is first created in a software environment and then used to create a "mask". Generally the pattern is transferred from the mask by photolithography, although other forms of radiation other than light may be used (electron beams or X-rays). Fabrication generally involves photolithography, metal deposition, lift off and etching. To finish a generalised microfluidic device a top layer is often bonded to the device and external connections are added.

2.1.5 Theory of Photolithography

Most fabrication of microdevices involves photolithography at some stage within the processes. In order to understand the methods of fabrication the general principles of photolithography are described.

2.1.6 Introduction to Photolithography

Photolithography involves transferring a design from a mask into a photosensitive thin polymer film using light. In most cases UV light is used, as the short wavelength provides a higher resolution of pattern definition, see Equation 2.1. In photolithography, the pattern is reproduced in a layer of light sensitive polymer, called photoresist. Light is transmitted through a photomask onto the photoresist, which undergoes a chemical change. The photoresist is transformed either by photodecomposition or photopolymerisation, allowing the exposed resist either to be washed away (positive photoresist) or allowing the unexposed resist to be removed (negative resist) by a process called development. After development the pattern is replicated within the photoresist layer, see Figure 2.3.

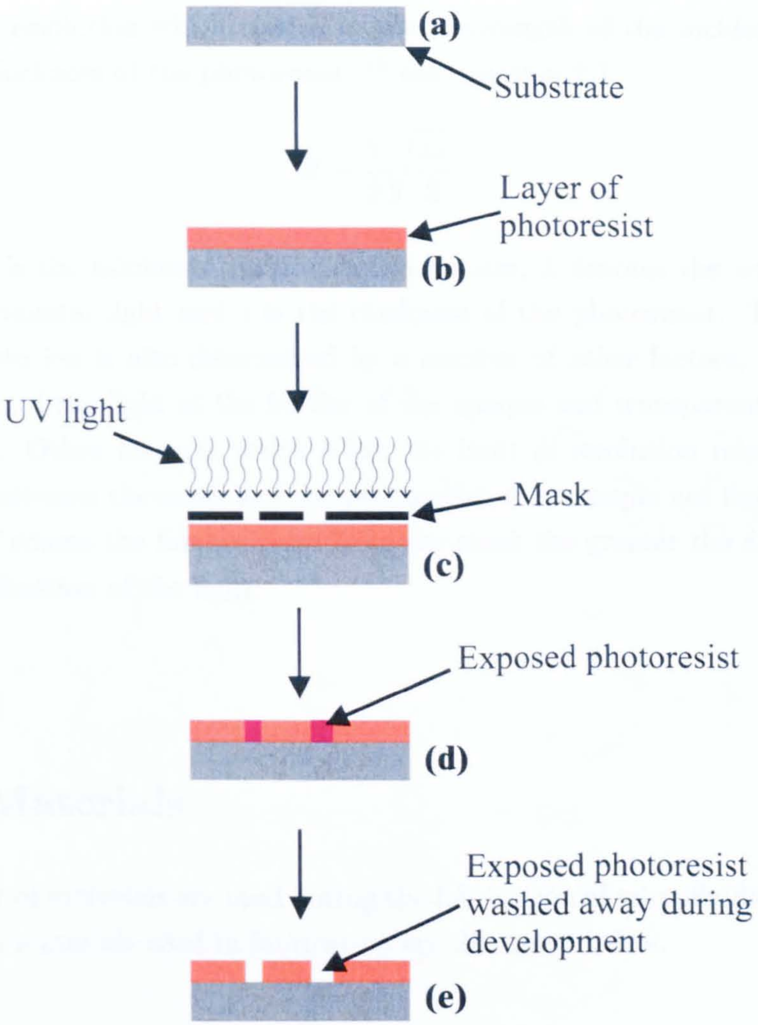
(a)
Substrate
Layer of photoresist
(b)
UV light
Mask
(c)
Exposed photoresist
(d)
Exposed photoresist washed away during development
(e)

Figure 2.3: A schematic of photolithography with positive photoresist: (a) substrate is cleaned; (b) photoresist is spun on to surface; (c) the photoresist is exposed with light through a mask; (d) exposed photoresist has been chemically modified by the light; (e) the pattern is developed, removing the exposed resist which is soluble in basic developer solution.

2.1.7 Why Use Photolithography?

Photolithography provides the ability to form small structures positioned reproducibly and defined accurately time after time. Photolithography has a limit of resolution which relates to the wavelength of the incidental light and the thickness of the photoresist,[116] see equation 2.1.

$$R = \frac{3}{2}\sqrt{\frac{\lambda z}{2}} \tag{2.1}$$

Where R is the minimum resolvable feature size, λ denotes the wavelength of the incidental light and z is the thickness of the photoresist. The minimum resolution is also determined by a number of other factors, including diffraction of the light at the border of the opaque and transparent parts of the mask. Other features which effect the limit of resolution relate to the distance between the mask and the photoresist, for example not flat resist or wafer. Of course the further away from the mask the greater the divergence of the diffraction of the light.

2.2 Materials

A number of materials are used during the fabrication of microfluidic devices. The main materials used in fabrication are discussed below.

2.2.1 Photoresist

Photoresist is a mixture of photosensitive polymer, initiator and solvent, in to which a pattern can be transfered during photolithography. Photoresist is chemically modified during the exposure with UV light, allowing pattern transfer and therefore the selective processing of the substrate. There are two types of photoresist, namely positive and negative resists. Positive resists are modified by the incidental light which allows them to be dissolved by the developer, whereas negative resists are crosslinked by the light and unexposed resist is resolvated by the developer. Only positive photoresists are used and discussed within this thesis.

2.2.1.1 Chemical Bases and Effect of UV

There are two different types of positive photoresist, commonly in use. These are poly (methylmethacrylate) and diazoquinone ester based polymers. The photoresist discussed here is the diazoquinone resist, which is the positive photoresist used in the fabrication of devices in this work. The UV reactive part of the photoresist molecule is a two ring system, called a orthonaphthoquinonediazide group,[117] see Figure 2.4. The diazo bond is changed by the UV light. The actual molecular chain lengths of photoresist may be varied to adjust the viscosity and therefore the thickness of the layer, although in all cases the photochemistry is unchanged. The reaction is that of the diazoketones undergoing ring contraction to form a indenecarboxylic acid.[116]

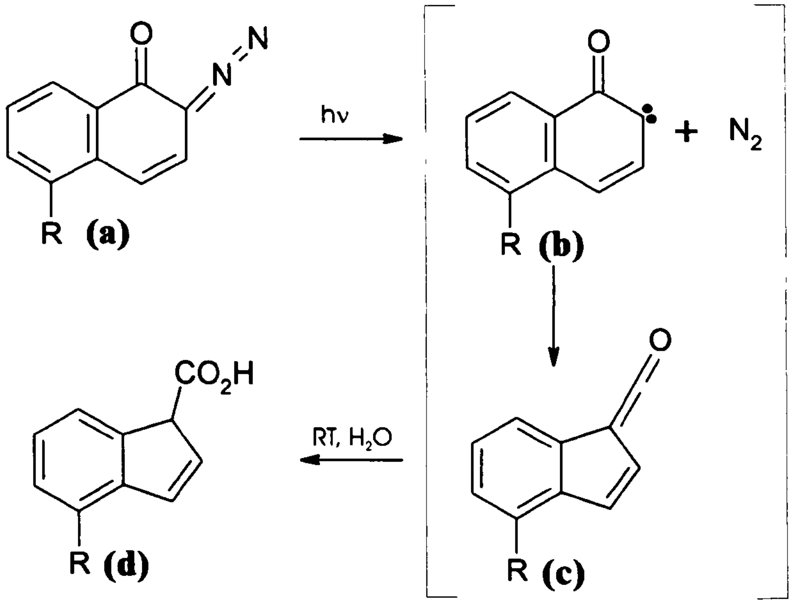

Figure 2.4: Reaction scheme of the reaction undergone by orthonaphthoquinonediazide (a) with UV light[117], through reactive intermediates of firstly a carbene (b), and then rearranging in to a ketene (c). The ketene reacts immediately with water in the atmosphere to form the soluble indenecarboxylic acid (d).

The mechanism through which the UV light converts the orthonaphthoquinonediazide is through the formation of free radicals after the nitrogen molecule is released, see Figure 2.4. This intermediate rearranges to a 5-membered ring to form a ketene molecule,[117] see Figure 2.4, which reacts quickly with water in the air to form the carboxylic acid, (d) in Figure 2.4.

After the exposure of the photoresist, the carboxylic acid containing resist is soluble in the basic developer whereas the unexposed resist remains insoluble in the developer.[117]

2.2.2 Silicon

Silicon wafers are used in the fabrication of microfluidic devices. Silicon wafers have a number of properties which make them idea for microfabrication. As a consequence of the semiconductor industry, photolithography on silicon wafers is well understood, making translation of the process to microfluidic devices easy. Silicon wafers are optically flat with a highly structured crystal lattice, which allows for anisotropic etching, see Section 2.1.2. The surface chemistry is also well understood allowing for easy surface modification. It does have disadvangates, it is a semiconductor so needs to be isolated from external currents or it will conductor. This is a problem with electrophoresis and electrochemical cells. Also it is not chemically inert so cannot be used with all reagents.

2.2.3 Glass

Glass is a common substrate for microfluidic devices. Glass is used because it is relatively cheap and optically clear allowing for optical probing of the device. It is also more robust, it is easier to handle, than silicon and as with silicon, the surface chemistry can be easily modified.

2.2.4 PDMS

Polydimethylsiloxane (PDMS) is a siloxane based elastomer, which can be cured solid from a viscous liquid to form structured flexible rubber substrates, see Figure 2.5. The PDMS used in this work was Sylgard 184 (Dow Corning, Michigan, USA). Structures can be formed within PDMS by curing the elastomer on a inversely structured mould, see Figure 2.13.

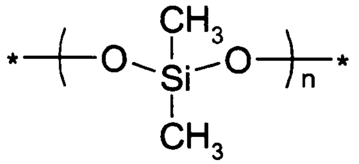

Figure 2.5: Structure of polydimethylsiloxane as a monomer unit.

2.2.4.1 Advantages of PDMS

There are a number of reasons why PDMS has become the material of choice in microfluidics. One of the main reasons is that it is an inexpensive alternative to other substrates (such as Si and glass). This is particularly important in biological, chemical or forensic applications, where it is necessary that devices are disposable. Once moulds have been fabricated, there is little need for cleanroom conditions. Devices can be produced in under an hour, the time taken for PDMS to cure at 60°C. PDMS intrinsically adheres to itself and other polished substrates such as glass and silicon. For many microfluidic applications this natural adhesion is strong enough to seal the channels while in use (even under pressure driven flow).

Other properties of PDMS that make it attractive for use within microfluidic devices are that it is optically transparent at wavelengths down to 300nm and has a low autofluorescence. It is chemically inert and does not adsorb moisture from the air. PDMS is thermally stable up to about 200°C. It is hydrophobic and gas permeable which may be considered useful properties in some cases. It swells rapidly when in contact with non-polar solvents, which may be a disadvantage in some microfluidic applications eg drug discovery. Actively changing the surface properties of PDMS can be achieved although compared with the ease by which the properties of silicon and glass can be changed the process is more difficult. Without changing the surface of the

PDMS it can support electroosmotic flow. The surface can be patterned with metals but again this is more difficult than with other substrates and the adhesion is not as good when compared to them.

2.2.4.2 Structure and Curing of PDMS

PDMS has an inorganic siloxane structure with organic methyl groups attached to the backbone. This siloxane backbone gives more degrees of steric freedom than a linear carbon chain, making the molecule more flexible,[118] enabling more uniform surface properties as the molecule can flex to move the desired groups to the surface. Before crosslinking siloxanes are liquids at room temperature. Crosslinking of siloxanes forms the cured solid elastomer. The PDMS used in this thesis was a two part elastomer, Sylgard 184, Dow Corning. One part is the base component, siloxane with vinyl groups, $SiCH{=}CH_2$, at the ends,[118] whilst the other part is a mixture of a platinum complex, used as a catalyst, and co-polymers of methylhydrosiloxane and dimethylhydrosiloxane, see Figure 2.6. Curing of the PDMS is a hydrosilyation reaction,[116] catalysed by the platinum complex between the vinyl end groups on the PDMS and hydrosilane. PDMS molecules are bound together by the crosslinking hydrosiloxanes forming a complex molecular structure. On formation of this higher structured state the liquid PDMS cures to a more rigid elastomeric solid.

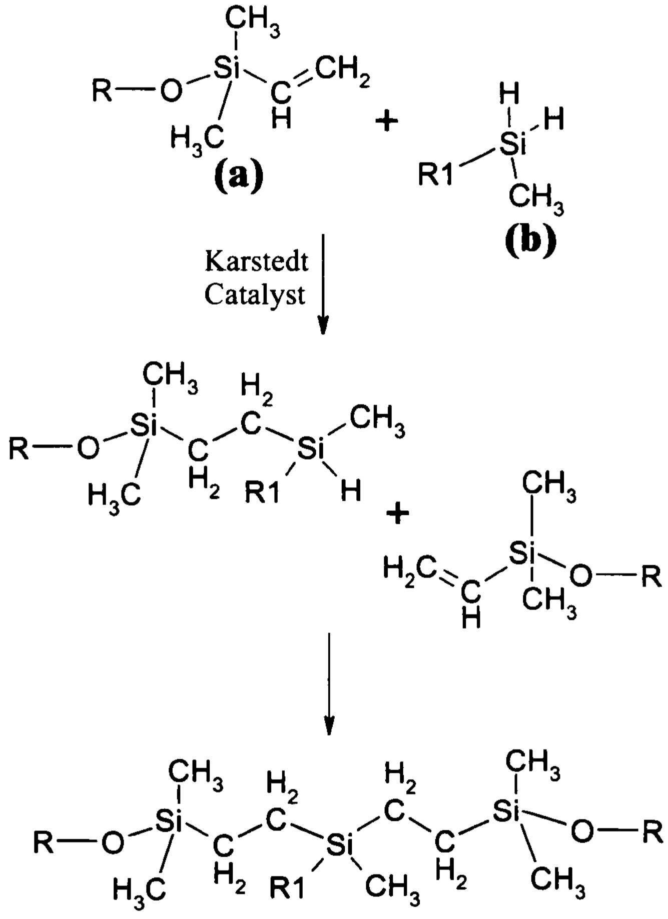

Figure 2.6: The hydrosilyation crosslinking reaction of polydimethylsiloxane (a) via terminal vinyl groups, with hydrosilane groups of methylsiloxanes, (b). Where R is the rest of the PDMS molecule, R1 is either a hydrogen atom or a methyl group.

2.2.4.3 Oxidisation of PDMS Surface

Generating an oxygen plasma using a Surface Technologies System inductively coupled plasma (STS ICP) (Surface Technologies Systems, Newport, UK), see Section 2.3.11.2, can oxidise the surface of PDMS. On oxidising the surface of PDMS, a chemical change occurs and the surface of PDMS, which is made up of -$OSi(CH_3)_2O$- groups, is changed to -$O_nSi(OH)_{4-n}$ after oxidisation.[119] The rearranged surface of PDMS reverts back to its native state over a period of ~45min if left in air.[119] The oxidised state of the surface remains stable for longer (80min), if the surface is covered in deionised water[119].

2.2.5 RTV PDMS

An alternative to PDMS is 3140 RTV (Room Temperature Vulcanisation) silicone sealant flowable, Dow Corning, Michigan, USA. It is a one part PDMS which cures on reaction with moisture in the air. The molecular structure of the sealant is the same as PDMS but the polymer has reactive end groups to bring about crosslinking of the polymer. It has similar physical properties as "two part" PDMS.

RTV PDMS is used instead of PDMS because it will irreversibly bond to surfaces, unlike PDMS. This allows it to be used when moulding around photoresist.

Curing of silicon sealant is by the reaction of water in the atmosphere with oximosilane end groups.[120] The reaction is a condensation reaction producing oxime as a by product, see Figure 2.7. The siloxane cures slowly because the rate of condensation is based upon the rate at which the water can migrate through the sealant.

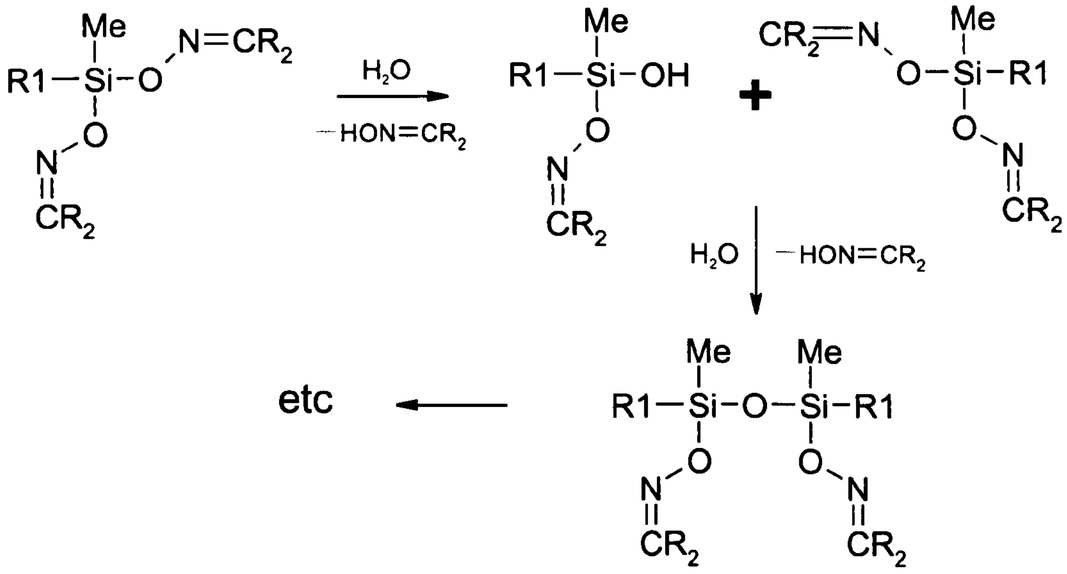

Figure 2.7: The condensation reaction of oximosilane end groups with water to crosslink siloxane polymers during the curing of RTV PDMS. Where R1 and R2 are the rest of the PDMS polymer.

2.3 Procedures Used in this Thesis

2.3.1 Order of Fabrication

In general there is an order in which fabrication is carried out. Whilst the generalised fabrication is shown in Figure 2.2, Figure 2.8 shows the detail of each process used in this thesis. Each stage is considered a separate "process" step.

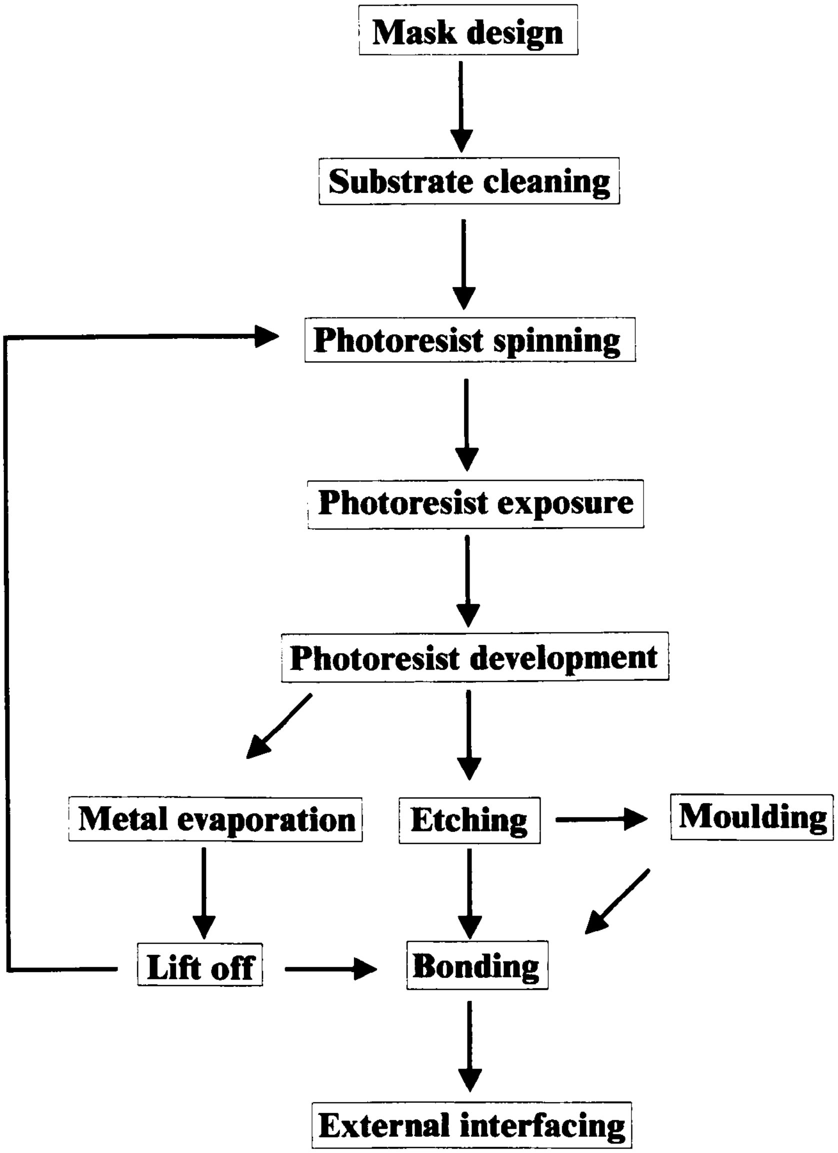
Mask design
Substrate cleaning
Photoresist spinning
Photoresist exposure
Photoresist development
Metal evaporation
Etching
Moulding
Lift off
Bonding
External interfacing

Figure 2.8: Flow diagram showing the general procedure of microfluidic device fabrication.

2.3.2 Mask Design and Fabrication

The initial step of any device fabrication is the design of the device and subsequent mask design. Depending on the complexity of the device, this may require several masks. For example, if the device consisted of electrodes for a electrochemical cell within a microchannel (as is the case in many aspects of this work), at least two masks would be required: one mask to define the electrodes and a second mask to pattern the microchannel.

In general masks are described as being either "dark field" or "light field", see Figure 2.9. With a light field mask, most of the substrate is exposed whilst for a dark field mask, the opposite is true. Which type of mask is used depends on the processing required (including considerations of ease of fabrication or materials and photoresists available).

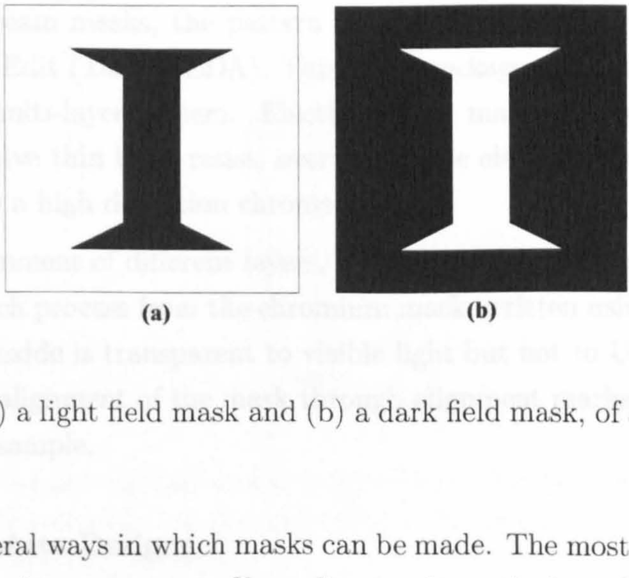

Figure 2.9: (a) a light field mask and (b) a dark field mask, of a "generalised" structure.

There are several ways in which masks can be made. The most common ways are printing designs on acetate films, direct write optical masks and electron beam written masks. Each method has a minimum feature size which is resolvable, see Table 2.1.

Type of mask	Minimum resolution
Printed acetate	~20μm
Directly written	1μm
electron beam written	10nm

Table 2.1: A table to show the minimum possible feature size resolvable by each different type of mask process.

The method of design and construction depends on the size of the smallest feature needed in the mask. For features greater than 20μm, acetate masks can be employed and features of 20μm or smaller direct write or e-beam can be employed.

2.3.2.1 Electron Beam Designs

For electron beam masks, the pattern was designed using a CAD package, in this case L-Edit (Tanner EDA). This CAD package allows for easy layout design on a multi-layer system. Electron beam masks are written using a electron sensitive thin layer resist, over which the electron beam is rastered. This produces a high definition chrome mask.

To enable alignment of different layers, a ferric oxide mask was produced using a metal etch process from the chromium mask, written using the electron beam. Ferric oxide is transparent to visible light but not to UV light, allowing for visual alignment of the mask through alignment marks, with existing layers on the sample.

2.3.2.2 Acetate Designs

For simple line patterns with features greater than 50μm, acetate masks have been found to be suitable. The layout of the acetate mask was drawn using CorelDraw 9 and 10 (Corel Corporation UK). Using a high resolution image setter (5000dpi printer, Scan-Hi, Glasgow) acetate masks were printed.

The benefit of an acetate mask compared to an electron bean mask is the low cost and ease of production. Acetate masks enable rapid and cheap prototyping of a design. The limitation of acetate masks is the low resolution and inability of the resolution to produce curves (due to pixelation). In general feature sizes >20μm can be fabricated using such masks.

2.3.3 Substrate Preparation

After having produced the mask, the next stage involves transferring the pattern on to a substrate (a process which requires the substrate first to be cleaned). Silicon wafers and glass slides were cleaned in a cleanroom by a series of solvent washes, see Figure 2.10. Samples were immersed in acetone and methanol to remove grease and organic debris from the surface. Deionised water was then used to remove remaining particles on the surface.

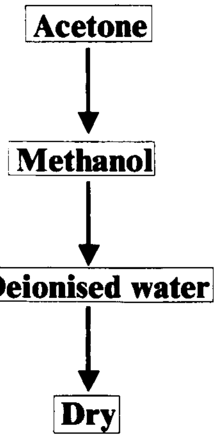

Figure 2.10: Organic solvent cleaning procedure. Samples are sonicated for 3min in each solvent and then rinsed throughly in flowing 18MΩ/cm deionised water and dried under nitrogen.

2.3.4 Spin Coating Thin Films of Photoresist

The application of photoresist to the surface of the substrate was performed by spin coating. Uniformly thin layers of photoresist were produced by spinning samples at high speed with unpolyermised photoresist on the sample substrate. The thickness of the layer depends on the spin speed and the viscosity of the resist.

Samples were first coated with an adhesion promoter, hexamethyldisilane, by spinning (Headway research, TX, USA) for 6s at 4000rpm. Photoresist was then applied and spun. Two different photoresists were used to produce different layer thicknesses, each for different purposes. S1818 (Microchem, MA, USA) was used for defining patterns for metal evaporation, whilst AZ4562 (Clariant UK, Leicester, UK) was used to produce masks for etching. In some cases AZ4562 was spun twice to gain a thicker layer and was subsequently used as a mould. In this latter case photoresist was spun for 30s and after spinning the substrates were baked on a level flat hotplate for 3min at 90°C. The spin speeds used are shown in Table 2.2.

Photoresist\spin speed	4000rpm	1300rpm
S1818	1.8μm	-
AZ4562	6.2μm	12μm

Table 2.2: Table to show the spin speeds used for the different photoresists and different desired thickness.

In order to change the resist profile for improved lift-off, see Section 2.3.9, the photoresist can be hardened by a chlorobenzene soak.[121] Chlorobenzene removes some of the UV sensitive compounds from the resist surface so that the profile of the exposed resist is that of an overhang, see Figure 2.11. Only the surface of the resist is effected by removal of UV active molecules due to the slow diffusion of chlorobenzene in to the photoresist layer. As a consequence the overhang of photoresist aids lift-off by producing a more defined edge to the photoresist.

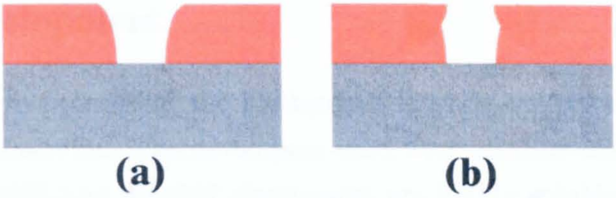

Figure 2.11: A stylised representation of the overhang produced by chlorobenzene in photoresist after exposure and development of the photoresist. The profile of resist after exposure and development: (a) without chlorobenzene soak; (b) with chlorobenzene soak.

2.3.5 Exposure

Photoresist was patterned on a mask aligner (Hybrid Technology Group, CA, USA) which allows manipulation of the mask with respect to the substrate for alignment. Exposure times were normally found out by iterative or empirical measurements. In their detail, they vary with thickness as well as with the different types of resist, see Table 2.3.

Photoresist	Thickness	Exposure time
S1818	1.8μm	11s
AZ4562	6.2μm	25s
AZ4562	25μm	3 x 40s, 20s pause

Table 2.3: Table to show the exposure times for the different photoresists used and at different thicknesses used. Power of the lamp used was 100W.

AZ4562 was spun twice on to a sample at 1300 to produce a thicker layer of photoresist. To expose the resist completely a multiple exposure was needed. To expose thick photoresist multiple exposures are needed because if the photoresist is allowed to relax[122] in between, the depth that can be exposed is increased.

2.3.6 Development

The final step in processing the photoresist layer is the development of the resist on the substrates. The developers used were alkaline solutions in which the exposed S1818 and AZ4562 photoresist are highly soluble in. Substrates are immersed in the developer and agitated to dissolve the photoresist.

Photoresist	Developer	Time
S1818	1:1, concentrate : water	75s
AZ4562	1:4, AZ 400K : water	90s per 12μm of photoresist

Table 2.4: Developer type and time for the different photoresists used.

After development of the exposed photoresist, the substrates were rinsed in deionised water and dried in nitrogen.

2.3.7 Silicon Etching

Reactive ion etching using an STS ICP (Surface Technologies Systems, Newport, UK) was used to etch silicon wafers. This instrument uses highly reactive gases formed in a plasma to etch silicon. The conditions of the reaction are shown in Table 2.5.

Condition	Value
C_4F_8	85sccm
SF_6	130sccm
O_2	10sccm
Coil	600W
Platen	12W
Etching pressure	34mT
Passivation pressure	24mT
Temperature	20°C

Table 2.5: Table of the settings used in etching silicon wafers within the STS ICP

Using this refined protocol gave an etch rate of ~4μm/min. Etch rates vary depending on surface area of device and size of the features to be etched. Individual etch rates where gained for the different devices by etching for a known time, usually 10min, and then measuring the depth of the etch obtained (Dektak 6M Stylus Profiler, Veeco, Cambridge, UK).

2.3.8 Metal Deposition

The fabrication of metal features on devices is necessary for a number of reasons, including the production of resistive heaters, thermocouples for temperature sensing and electrodes for electrochemical detection. Metals were deposited by evaporation. Samples together with the metals to be evaporated were held at low pressure, ~10^{-7}mT. The metal was then melted, to produce a vapour pressure within the chamber. Two ways of melting the metals were used, electron beam and by passing current through the metal (thermal evaporation).

In this thesis the metals that were evaporated were to form electrodes of an electrochemical cell. Electrodes were made from 10nm Ti, 10nm Pd and 100nm Au deposited at a rate of 0.4nm/s in one process step using a plassys system (electron beam evaporation). The interfacial electrochemical surface metal required was gold but gold does not adhere to either glass or silicon so an adhesion layer of titanium was deposited first. To stop titanium from alloying in to the gold and changing the electrochemical properties of the gold electrode, a protective layer of palladium[123] was deposited.

Silver was deposited on to the gold surface. It was evaporated to a depth of 100nm at a rate of 20Hz/s. (The rate is measured in Hz as the thickness is measured using the frequency of a quartz crystal microbalance, where Δ10Hz = 0.1nm.

2.3.9 Lift Off

After the evaporation of metals on to the surface of the substrate with photoresist, metal completely covered the whole substrate. To realise the metal structure, the resist was removed by acetone. After the photoresist was removed the metal features were exposed in a process called lift off, see Figure 2.12. The thickness of the photoresist must be considerably larger than the thickness of the metal depoisted,[116] to make sure that the metal on the surface is separate from the resist which is on top of the photoresist. The resist is removed almost instantly by the acetone but better lift off was gained by soaking for a few hours. Silver lift off was left overnight due to poor adhesion of silver to gold.

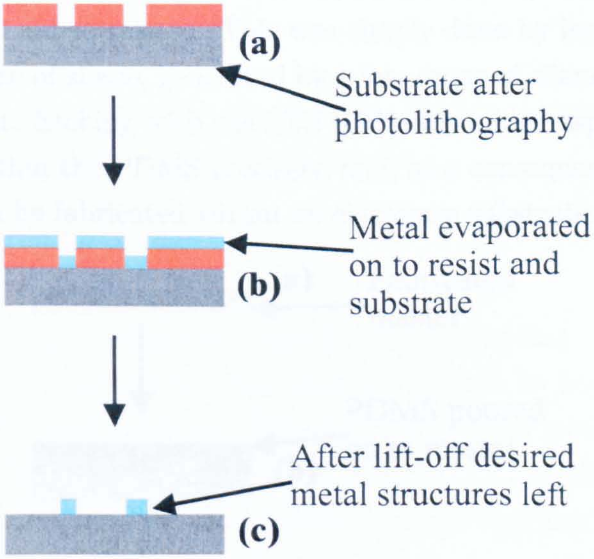
(a)
Substrate after photolithography
Metal evaporated on to resist and substrate
(b)
After lift-off desired metal structures left
(c)

Figure 2.12: A schematic of the process to gain structured metal patterns on the substrate: (a) the substrate already had a layer patterned layer of photoresist on the surface; (b) metal is evaporated on to the whole of the surface, forming a uniformly thick layer; (c) photoresist is removed from the surface by organic solvent, lift off, leaving only the metal that was in contact with the surface of the substrate.

2.3.10 Moulding

Depending on the type of silicone used a different type of moulding was used.

2.3.10.1 Moulding of PDMS

For the moulding of PDMS, silicon wafers were first etched in the STS ICP to form an inverse of the desired pattern. The PDMS was mixed in the ratio of 10:1 base to initiator by weight and air bubbles were removed under vacuum. The solution was then poured on to the mould and allowed to cure at 60°C for 1 hr, see Figure 2.13. To release the cured PDMS from its mould, it was simply peeled away. Most moulds were generally silanised, using hexamethyldisilane (Sigma-Aldrich, Poole, Dorset, UK) on the surface as an additional aid to release. This was simply done by leaving the mould in an atmosphere of silane, generated by a few drops of silane in an enclosed vessel, overnight. Etching with the STS ICP gives a high aspect ratio which is replicated within the PDMS precisely, and, as a consequence, high aspect ratio copies can be fabricated within an elastomer substrate.

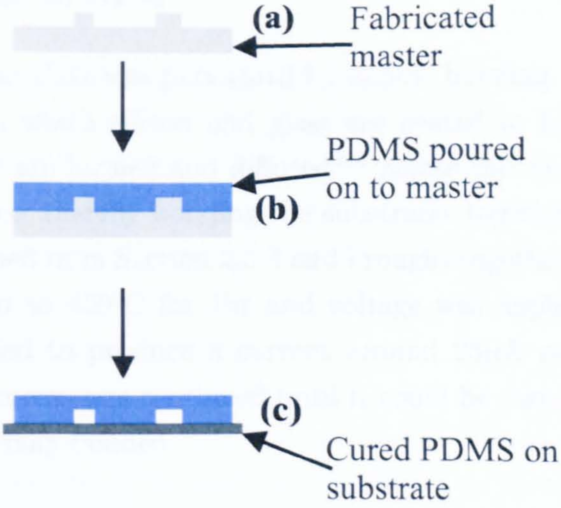

Figure 2.13: Illustration of PDMS moulding using a master (a). PDMS was poured on to the mould (b) and PDMS once cured after 1hr at 60°C was peeled off the mould and adhered to a flat substrate (c).

2.3.10.2 Moulding of RTV PDMS

RTV PDMS was moulded around "thick" patterned photoresist. AZ4562 was spun twice to a thickness of 25μm and patterned using a light field mask. RTV PDMS was then poured onto the sample and spread across the surface by hand. It was cured at room temperature on a horizontal surface overnight.

Once cured the ends of the channels were opened up manually and the sample was soaked in ethanol to remove the photoresist. Acetone was not used as it affected the RTV PDMS. The sample was held vertically within the ethanol to stop pooling of the dissolved resist in the device. The time taken to remove the photoresist depended on the feature shape and amount of photoresist.

2.3.11 Bonding

Capping the device to seal the channels was done in a number of ways depending on the materials used in the fabrication

2.3.11.1 Silicon to Glass

Bonding silicon to glass was performed by anodic bonding. Anodic bonding is a technique in which silicon and glass are heated to high temperatures and then cations are formed and diffused[124] across the surface interface by an applied voltage, thereby bonding the substrates together. The glass and silicon were cleaned as in Section 2.3.3 and brought together. The substrates were then heated to 450°C for 1hr and voltage was applied. The voltage applied was varied to produce a current around 25μA passing across the interface. The process was continued until it could be visually seen that the device had been fully bonded.

2.3.11.2 PDMS Plasma Bonding

Bonding PDMS to PDMS, glass or silicon was preformed by oxidation of the surface of the PDMS, see Section 2.2.4.3, using an STS ICP. When the surface of the oxidised PDMS was brought in to contact with either Si, Si-O- or Si-OH groups an irreversible bond is formed between the two surfaces.

Both PDMS and the second substrate (Si or glass) were cleaned with ethanol and dried in nitrogen. Both parts of the device were placed into the STS ICP and oxidised. The protocol for the oxidisation of PDMS within a STS ICP machine[125] is shown in Table 2.6.

Condition	Value
O_2	100sccm
Coil	100W
Platen	12W
Time	10s

Table 2.6: Table showing the settings used within the STS ICP for the oxidisation of PDMS

After the process, the two samples were brought together and gently pressed together and left for 20min. Once bonded, the bond was sufficiently strong that the bulk PDMS would fail before the interface was pulled apart.

2.3.12 External Fluid Interfacing

A number of different ways of introducing fluids have been used depending on the materials the device was made from and the pressure drop across the device. Methods of interfacing are discussed by material accordingly:

2.3.12.1 Thin Layers of PDMS

When a PDMS layer had been bonded to an etched silicon channel the inlets and outlets are fabricated by cutting the PDMS to open up the channel. The PDMS was removed from covering the end of the channel and from the area around the channel end. A fused silica capillary, 375μm outer diameter, 150μm internal diameter (Composite Metals Services, Ilkley, UK), was then inserted into the channel and glued into place using RTV PDMS.

2.3.12.2 Thick Layers of PDMS

For moulded PDMS devices the inlets and outlets were made by punching holes with a modified syringe needle, gauge 21, from the structured side. The needle was modified by filing down the point to a trancated taper end. This removed a core of PDMS rather than piercing a hole through the PDMS.

The external attachment was achieved by a wider, gauge 23, filed down syringe needle inserted in to the hole, see Figure 2.14. As the inserted needle was larger than the punched hole, a seal was formed that was tight enough to allow the moderately high pressure addition of fluids in to the channel.

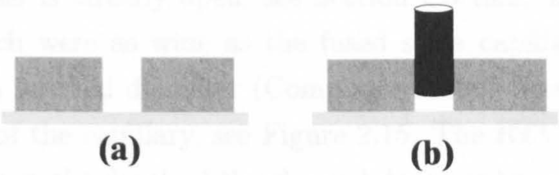

Figure 2.14: Illustration of using a syringe needle to interface with PDMS: (a) PDMS is cored using a modified gauge 21 syringe needle; (b) insertion of a blunted gauge 23 syringe needle to attach tubing to a PDMS device.

2.3.12.3 Glass

For devices made of glass/silicon or just glass, the attachment of a fused silica capillaries was made using a graphite ferrule which provided a mechanical support for the external tubing. Before the device was bonded together either by glue or by anodic bonding, holes were drilled through the glass. If the device comprised of structured glass, the holes were drilled, 1mm diameter, (dentist drill bits) (Diama, London, UK) through from the structured side, to make alignment of both parts of the device easier before bonding.

After bonding of the device, graphite ferrules were glued over the holes. Depending on the final use of the device, different glue was used. For devices which were not heated UV cured glue, loctite 350 (Welwyn Garden City, UK) was used. It was cured under a 30W UV lamp for 20min. For devices which were to be heated, a thermally stable epoxy (TBS, Electrolube, Swadlincote, UK) was used. Fused silica capillary 375μm outer diameter, 150μm internal diameter (Composite Metals Services, Ilkley, UK,) was inserted in to the ferrule and glued in position with thermally stable epoxy (TBS, Electrolube, Swadlincote, UK). This method of attachment allows for higher pressures to be applied to the device.

2.3.12.4 RTV PDMS

For devices using RTV PDMS, because of this method of fabrication, the end of the channel is already open, see Section 2.3.10.2. Designing ends of the channel which were as wide as the fused silica capillary, 375μm outer diameter, 150μm internal diameter (Composite Metals Services, Ilkley, UK) allows insertion of the capillary, see Figure 2.15. The RTV PDMS stretches over the capillary so the depth of the channel does not have to equal the capillary diameter. The channel was sealed by RTV PDMS. Using this method of interface the device was used at lower pressure.

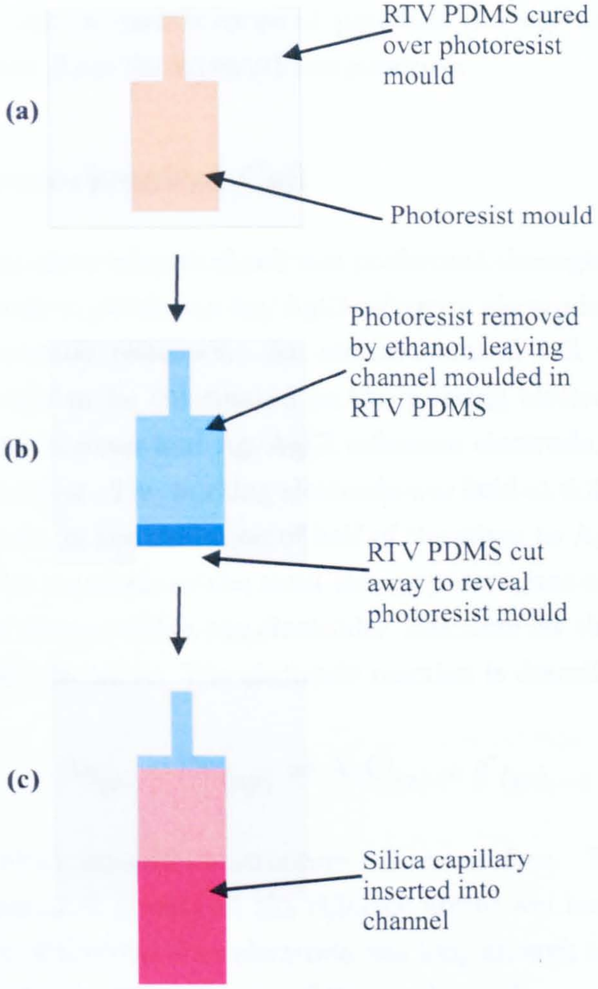
(a)
RTV PDMS cured over photoresist mould
Photoresist mould
Photoresist removed by ethanol, leaving channel moulded in RTV PDMS
(b)
RTV PDMS cut away to reveal photoresist mould
(c)
Silica capillary inserted into channel

Figure 2.15: Illustration of the capillary interface into a RTV PDMS moulded channel: (a) RTV PDMS covering the resist filled channel; (b) RTV PDMS cut away and resist removed with ethanol; (c) capillary inserted in to widened channel.

2.3.13 Electrical Connections

Bonding pads were designed within the mask, together with the actual electrodes. The bonding pads were typically 3-5 millimeters across. Wires were attached with silver paint and then glued over with epoxy to keep secure.

Soldering could not be used because of potential damage to the electrodes within the channel from the elevated temperatures.

2.3.14 Electrochemical Cell

Completion of an electrochemical cell was preformed through the oxidisation of a silver electrode to produce a Ag/AgCl reference electrode. This provided a standard microscale reference. An electrochemical cell was setup with the silver electrode to be chlorinated as the working electrode with macro external platinum counter and Ag/AgCl reference electrode. 0.1M HCl was used as the electrolyte. The working electrode was held at 0.2V for the length of time that results in the oxidation of half of the silver to AgCl. As half the silver needs to be oxidised, so the total charge passed was equal to half the number of silver atoms within the electrode. The time for the oxidation was adjusted for each electrode. The electrode reaction is described below:

$$Ag_{(s)} + Cl^{-}_{(ag)} \rightleftharpoons AgCl_{(s)} + e^{-}_{(m)}$$

AgCl forms a black crystalline structure on the surface. The thickness of the electrode increases greatly as the chlorine atoms are incorporated. The working lifetime of the reference electrode was long enough to run the experiments, though the working lifetime of these eelectrodes can be limited to a number of hours.[126]

2.4 External Instrumentation

2.4.1 Pumps

A Kloehn M6 (Kloehn, Las Vegas, NV, USA) precision syringe pump was employed for fluid manipulations. Precise flow rates and volume could be dispensed by controlling the pump using an in-house developed program running through Labview (National Instruments).

2.4.2 Tubing and Pump Fittings

PTFE tubing (Cole-Parmer, Hanwell, UK) was used to connect devices to the pump. Dimensions of the tubing were internal diameter 0.012" with outer diameter of 0.03". The tubing would fit tightly around the capillaries from the devices for low pressures to be used. For higher pressures MicroTight adaptors (Upchurch scientific, Washington, USA) were used. The capillary was tightened into one end of the adaptor using a sleeve around the capillary and the PTFE tube was tightened in to the other end. This tubing had an internal dimension of 0.012" and an external dimension of $\frac{1}{16}$ of an inch, (Cole-Parmer, Hanwell, UK) which was the standard size of screw fittings for the pump valve.

When the device was fabricated from PDMS, the syringe needles were inserted in to the 0.0009" walled PTFE tubing. This formed a good seal due to the much wider syringe needle.

2.4.3 Potentiostat

The potentiostat used was an in-house made instrument. Data collection was performed by an in-house designed MS-DOS program. Both the instrument and software were designed and made by Dr Andrew Glidle.

Chapter 3

Immobilisation of Polymerase Enzymes

3.1 Introduction

The selective positioning (or "immobilisation") of polymerase enzymes within microdevices offers certain advantages. Localisation of the enzyme within the enzyme's working temperature, within a microfluidic PCR device, would be beneficial because the enzyme would not denature at high temperatures. Even with *Taq* polymerase being thermophilic it does only have a half-life of 30min at 95°C[127] and there has been shown to be improvement in PCR when *Taq* polymerase has been exposed to a reduced time at high temperatures.[128] This would give an increase in the working lifetime and reusablilty of the enzyme. As the enzyme is not heated to high temperatures the possibility of using enzymes which are not thermally stable could be used. Using other polymerase enzymes can bring other properties, such as fast incorporation, proof reading or ability to extend longer strands, to the PCR which *Taq* polymerase can not. All PCR devices discussed within this report use the immobilisation of the polymerase enzyme within set locations to improve the system with the generic benefits of having the enzyme on a solid substrate.

Two different polymerase enzymes were used in immobilisation and subsequent PCR experiments. *Taq* polymerase was used as it is the standard enzyme used within PCR experiments at present. T7 DNA polymerase, from bacteriophage T7, was used as an alternative to *Taq* polymerase as it has been successfully used on a solid support[129] and therefore offers a possible comparison of methods and results.

3.1.1 Structural and Mechanistic Discussion of *Taq* Polymerase

3.1.1.1 History of *Taq* polymerase

Thermus aquatics is a thermophilic bacteria, which means it can live at hot temperatures (>70°C). Proteins extracted from this bacteria are thermophilic in nature, and are not readily denatured by higher temperatures. *Thermus aquatics* Type 1 DNA polymerase (*Taq* polymerase) was extracted[3] from this bacteria. The use of this enzyme provided the opportunity to use elevated temperatures within PCR.[130] The benefit of this was to simplify the running of PCR. *Taq* polymerase has two functions, it has polymerase activity and 5' nuclease activity but does not have the proof reading 3'-5' exonuclease activity. The lack of 3'-5' exonuclease activity differs from the original enzyme used in PCR, *Escherichia coli* DNA polymerase (Klenow fragment).

3.1.1.2 Basic Structure of *Taq* Enzyme

Crystallography investigations of *Taq* polymerase showed it was almost identical to the Klenow fragment.[131] The general structure of the enzyme can be described as a right hand,[131] see Figure 3.1. The active site is situated in the palm region of the enzyme, and comprised of three carboxylic acid residues,[131] Asp 610, Asp 785 and Glu 786. A cleft is formed between the fingers and thumb, with the active site sitting at the bottom of the cleft.

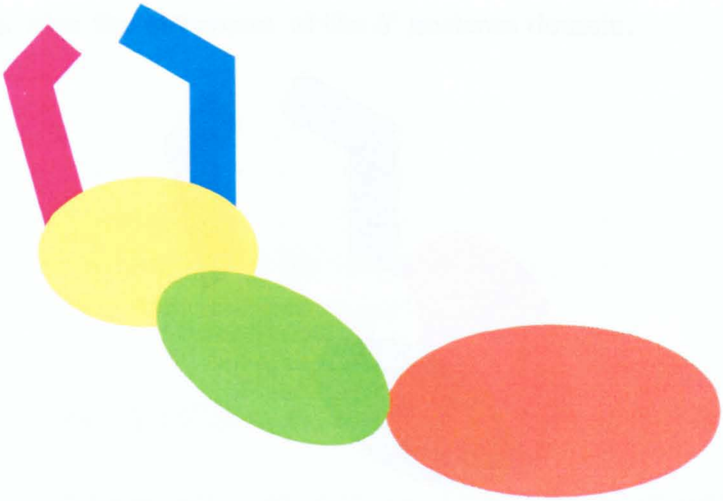

Figure 3.1: Schematic of the structure of *Taq* polymerase. The right hand is described because of structures being called the fingers (red) and thumb (blue) around the palm (yellow). The palm is where the active site is situated. The hand makes up the polymerase activity domain of the enzyme. 5' nuclease activity domain (orange) is loosely attached to the inactive 3'-5' exonuclease activity domain (green).

3.1.1.3 Conformational Change With and Without DNA

Incorporation of the DNA causes a conformational change in the structure of *Taq* polymerase.[132,133] There are two separate conformations of the enzyme: an open conformation when the DNA is not in the cleft;[132] and a changed conformation, which is the "closed" structure, when DNA is in the cleft.[132] In the closed form, the angles of the fingers and thumb move relative to the palm inwards. This conformation change is the rate limiting step of the reaction (the chemical reaction to add the dNTP is quick compared to the conformation change).

In the closed form, the 5' nuclease domain moves around "behind" the polymerase domain cleft.[133] This aligns the active site of the 5' nuclease domain with the DNA after moving through the cleft from the 3'-5' exonuclease side, see Figure 3.2. The enzyme therefore takes on a smaller shape when in the closed form with the movement of the 5' nuclease domain.

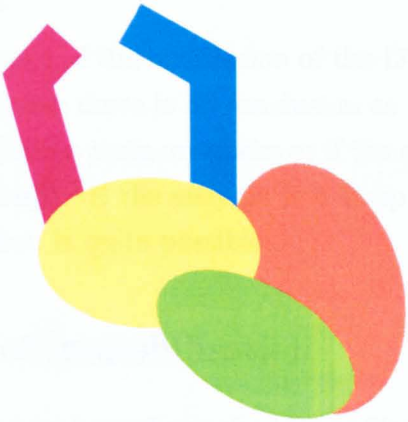

Figure 3.2: Schematic of the change of position of the 5' nuclease (orange) domain when bound to DNA within the closed conformation. The 5' nuclease is now situated behind the palm (yellow), fingers (red) and the thumb (blue) but is still attached to the inactive 3'-5' exonuclease domain (green).

3.1.1.4 Translation of DNA Through Polymerases

The molecular movement of the DNA template through the cleft is not by a screw motion but by a straight translation.[134] Evidence for this translation of DNA through the cleft within polymerase enzymes is from RNA polymerases and additional evidence from other DNA polymerase rather than *Taq* polymerase itself. The driving force of the translation of the DNA through the cleft is little understood but it is believed to involve a ratchet-like mechanism,[135] which has also been described as a worm-like movement.[136] Both descriptions came from the same mechanistic evidence.

During the extension of the primer, the DNA helix changes from the A type helix form to the B type helix form and back to the A form afterwards. The spacing between the bases is larger in the B form than the A form. The DNA changing from A to B and back to A is described as the ratchet movement[135] which implies that the enzyme is holding onto the strand and moving along the strand. This worm-like movement[136] uses the information of the change in nucleotide spacing and conformational change of the enzyme to move the DNA through the cleft.

From the worm-like theory of the translation of the DNA strand through the cleft of polymerase enzyme, there is no conclusion as to whether the enzyme moves along the strand like a train on tracks or if the enzyme is a hoop which the enzyme moves through. If the enzyme is a hoop then movement either with respect to the other, is quite possible.

3.1.2 Methods of Immobilisation

Four methods were used to investigate the immobilisation of polymerase enzymes onto surfaces. In all cases, microspheres were used as the support substrate, to allow the PCR to be carried out within a conventional thermocycler using regular PCR tubes, also due to beads being easy to wash and handle. Coupling through free amine groups in Lysine groups was achieved by two methods, involving n-hydroxysuccinimide ester (NHS) attachment of a biotin molecule with final immobilisation using streptavidin coated on to the bead surface or by using glutaraldehyde bonding to amine coated beads. Attachment via free carboxylic groups in glutamic acid and aspartic acid was also investigated by using carbodiimide and amine coated beads. Passive adsorption was finally used to immobilise the enzyme. The reaction schemes by which these attachment procedures work are described below.

3.1.2.1 Biotin-Streptavidin

A standard method to immobilise or tag proteins is to exploit the strong affinity of the vitamin biotin to the protein streptavidin. Streptavidin is a protein isolated from *Streptomyces avidinii* bacteria.[137] Streptavidin and biotin have a low dissociation constant (Ka) of $\sim 10^{-15}$M. Biotinylation of a protein allows it to retain its biological activity. The easy attachment of streptavidin to a surface makes the application of this system particularly useful. The method is experimentally easy to perform, which increases the chance of immobilisation. The use of the biotin-streptavidin couple has become widely used in enzyme immobilisation, some examples of enzymes immobilised by streptavidin are endonucleases,[138] proteases[139] and uricases.[140] To show how the biotin and streptavidin can be used to immobilise proteins a schematic is shown in Figure 3.3.

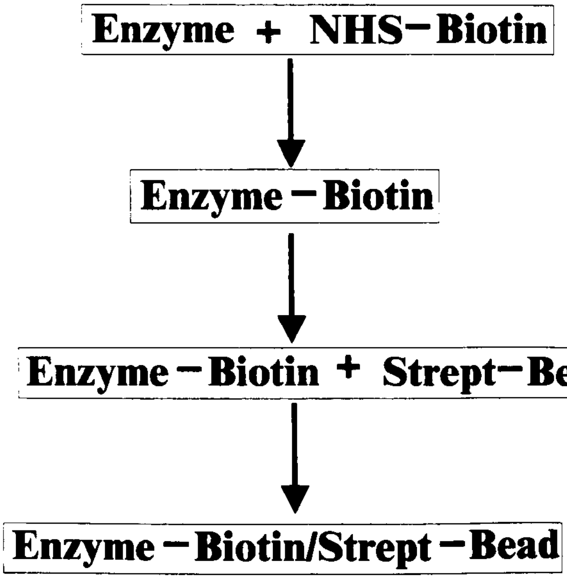

Figure 3.3: Flowchart to show the way in which enzymes are attached to beads using the biotin/streptavidin couple.

Biotin can be coupled to a protein by a number of chemical reactions. The reaction scheme depends on which of the amino acids are involved. The free primary amine group in Lysine is often used as a linkage point. In this case, in order to attach the biotin, a *n*-hydroxysuccinimide ester was used.

The mechanism of the attachment to the *n*-hydroxysuccinimide is a simple nucleophilic attack of the carbonyl by the amine, see Figure 3.4. The succinimide group acts as a good leaving group to drive the reaction forward.

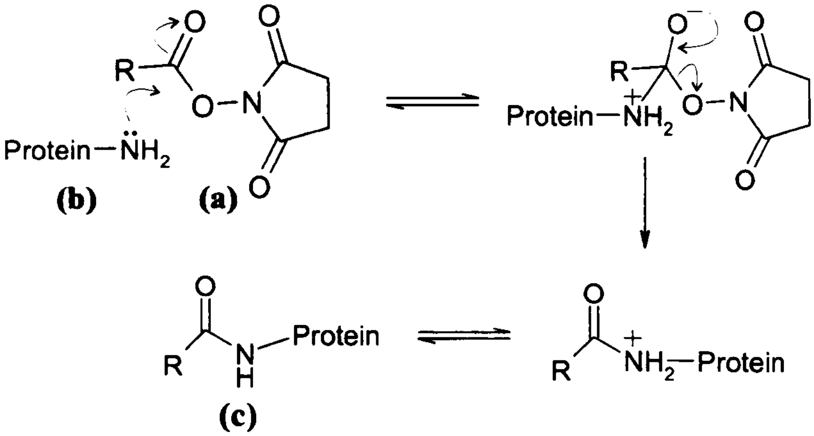
Protein—NH2
(b)
(a)
Protein—NH2
Protein
(c)
NH2—Protein

Figure 3.4: Mechanism of the free amine (b), in protein, to hydrolyse on *n*-hydroxysuccinimide ester (a) to form amide bond in final product (c). Where R is the spacer and biotin molecule.

3.1.2.2 Carbodiimide

The water soluble carbodiimide, *n*-(3-Dimethylaminopropyl)-*n*'- ethylcarbodiimide (EDAC) was used to immobilise the enzyme through free carboxylic acid groups on the protein to amine groups on the surface of the beads, see Figure 3.5.

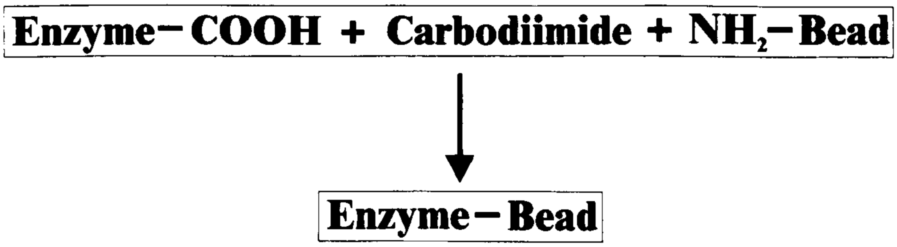
Enzyme−COOH + Carbodiimide + NH2−Bead
Enzyme−Bead

Figure 3.5: Illustration of carbodiimide reaction used in the immobilisation of polymerase.

Carbodiimide has been used to immobilise a range of different enzymes including glucose oxidase,[141] amino acid oxidase[141], alcohol oxidase[142] and laccase,[143] to name a few. This happens through an *O*-acylisourea intermediate.[144,145] Protonation of EDAC, by the reaction with H^+ ions within water in this case, results in a carbocation. This then reacts with carboxylic acid groups that are present to form a Schiff base. This further reacts with H^+ ions to form the *O*-acylisourea intermediate, see Figure 3.6. Nucleophilic attack of the carbonyl group on the intermediate by an amine group moves the reaction through to form an amide bond. This amide bond forms a stable link between the enzyme and the bead surface.

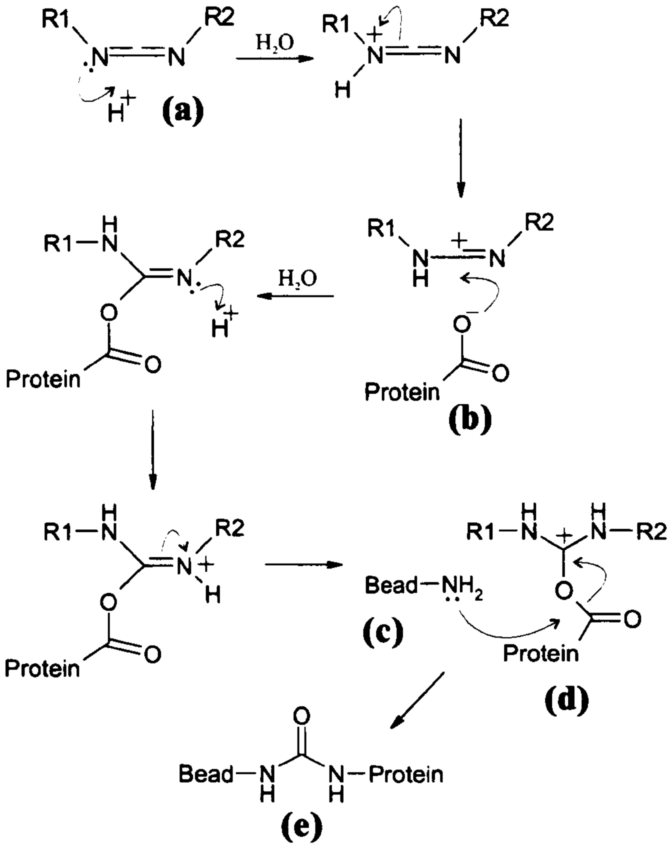
R1
R2
H₂O
H+
(a)
R1
R2
H
H₂O
R1
R2
H
O
Protein
O
(b)
Protein
R1
R2
H
Bead–NH₂
(c)
R1
H
N–R2
O
Protein
(d)
O
Bead–N
N–Protein
H
H
(e)

Figure 3.6: Mechanism by which carbodiimide (EDAC), (a), react with carboxylic acids (-COOH), (b), from the protein, and amine groups (-NH_2), (c), on the beads. The reaction passes through a carbocation intermediate, *O*-acylisourea intermediate (d). Amide bond formation occurs by the nucleophilic attack on the intermediate by the amine group on the bead to from the final desired product (e). R1 and R2 represent the rest of the EDAC molecule not involved in the mechanism.

There are a number of drawbacks with this immobilisation reaction. The reaction will couple proteins to proteins as well as to the solid support. Also *O*-acylisourea intermediates can be formed with the reaction with phenolic groups of tyrosine and *S*-cysteinylisourea with cysteine groups,[146] which could inactivate the enzyme and reduce the efficiency of the coupling.

3.1.2.3 Glutaraldehyde

Glutaraldehyde is a bifunctional cross-linker that attaches two amino groups together from different molecules. Beads with amine functionality on the surface are used for immobilisation of the enzyme via glutaraldehyde. Enzymes have been immobilised using glutaraldehyde with retention of functionality, including alcohol oxidase,[147] peroxidase,[147] diaphorase[148] and β-lactamase,[149] for example.

The mechanism by which the glutaraldehyde couples protein to a surface or to another protein is not as simple a mechanism as reactants and products suggest. Glutaraldehyde is not just a single molecule in aqueous solution: in acidic pH it forms a cyclic hemiacetal[146,150] but at neutral or higher pH it undergoes an aldol condensation to form α,β-unsaturated aldehydes.[151] Reactions between aldehydes and amino groups often produce Schiff's bases although the reaction is reversible, whilst the reaction of amines with glutaraldehyde is not reversible. α,β-Unsaturated aldehydes, which form similar products to a double Schiff's base, react with two amine groups through a Micheal type addition mechanism,[151] see Figure 3.7, to couple or immobilise proteins. The use of amine coated microspheres provides the second amine group for the reaction which immobilises the enzyme to the surface. The length of the spacer between the protein and the bead cannot be identified precisely due to the polymerisation of the glutaraldehyde in solution. The advantage of this method of immobilising via an amine group is the reduced "steric" bulk of the system, when compared to using the biotin/streptavidin couple.

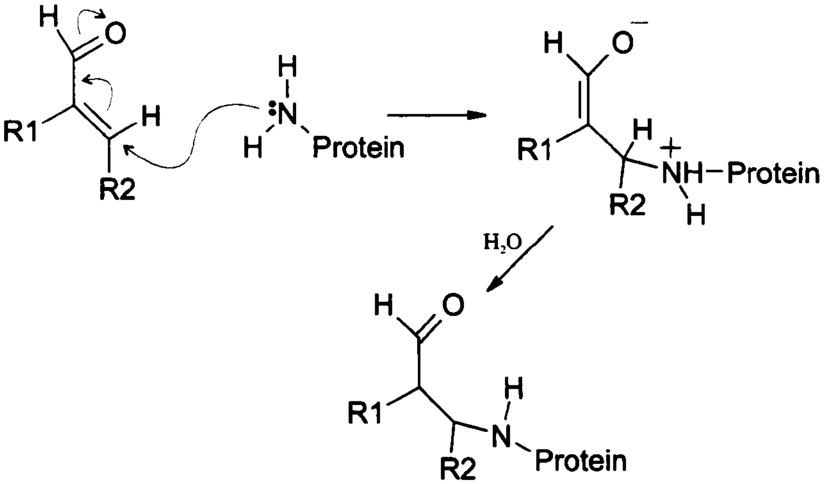

Figure 3.7: The α,β-unsaturated aldehyde (a) reacts with the free amine (-NH_2) of lysine groups within the protein by means of a Micheal type addition. R1 corresponds to the rest of the glutaraldehyde polymer including another α,β-unsaturated aldehyde group which reacts to an amine group, with the same mechanism, on the bead surface to couple the protein. R2 represents the non functionalized part the glutaraldehyde polymer.

3.1.2.4 Passive Adsorption

A simple method of immobilisation of proteins such as enzymes to surfaces is by passive adsorption. Passive adsorption of the protein to a surface is by intermolecular forces. These forces are generally weak intermolecular interactions such as Van Der Waals forces from hydrophobic interactions between the surface and hydrophobic regions of the protein.[152] As with all the immobilisation methods used, a range of enzymes have been previously immobilised by passive absorption, a few examples of enzymes immobilised are horseradish peroxidase,[153] penicillinaze[154] and cholestrol oxidase.[155] Bead materials employed are common polymers such as polystyrene spheres, which are hydrophobic. Beads with hydrophilic groups such as carboxylic acid groups and amine groups, can be used for passive adsorption with the interactions being ionic based.[152]

For control over ionic interactions, adsorption of the proteins is normally performed at pHs near the isoelectric point (pI) of the protein. If the sole interaction between the bead and protein is ionic, a change of pH can result in desorption from the surface.[152] The disadvantage of this method is that there is no control of the orientation of the protein on the bead, where as for the other covalent methods one can promote the orientation of the enzyme on the surface. The method is technically easy but less robust with respect to numbers of enzyme attached to the bead and the stability of the attachment.

3.1.3 Estimating the Amount of Enzyme Per Bead

In order to achieve a monolayer of enzyme on the surface, the amount of protein that could fit on to the bead was calculated for each bead. This is related to the physical dimensions of the bead and the protein binding capacity of the bead[152]. The estimation for the amount of protein per bead was by using Equation 3.1.

$$S = \frac{\sigma C}{\rho D} \tag{3.1}$$

Where S is the amount of protein, in mg, that can fit on to the bead per g of support. σ is surface area of the microsphere, m^2/g, ρ is the density of the microsphere, g/cm^3, D is the diameter, mm, and C is the protein binding capacity of the bead, mg protein/m^3.

3.2 Materials

Taq polymerase, DNA ladder and loading dye were supplied by Promega (Southampton, Hampshire, UK). T7 polymerase was supplied by New England Biolabs (Hitchin, Hertfordshire, UK). Streptavidin coated polystyrene beads with magnetic cores were from Dynal Biotech (Semstad, Norway). Primer and template mix was purchased from Microzone Ltd (Haywards

Heath, West Sussex, UK) as part of a kit, OK Kit, which is used to test the efficiency of thermocyclers. Gensieve LE agarose was purchased from Flowgen (Wilford, Nottingham, UK). All other chemicals and beads were sourced from Sigma-Aldrich (Poole, Dorset, UK). Dialysis cassettes were Slide-A-Lyser 3500MCW 0.1-0.5ml from Pierce and spin columns were from Biorad (Hemel Hempsted, Hertfordshire, UK).

Different NHS-Biotin molecules, purchased from Sigma-Aldrich, were used, which vary by the length of the spacer arm. The structures of these molecules are shown in figure 3.8.

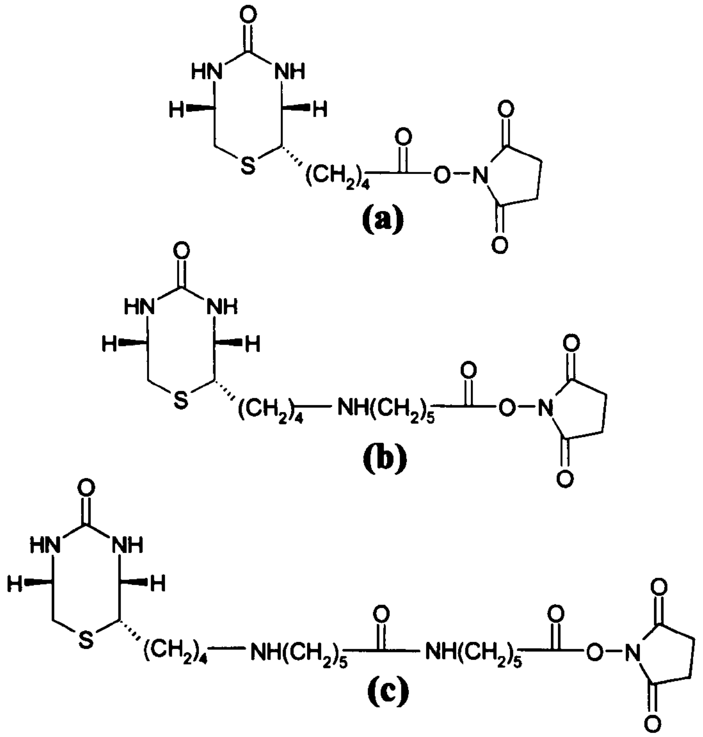

Figure 3.8: Structures of NHS biotin molecules used in the immobilisation of *Taq* polymerase: a) biotin N-hydroxysuccinimide ester, denoted as -, with no spacer; b) biotinamidohexanoic acid N-hydroxysuccinimide ester, denoted as -X-, which contains a 6 atom spacer arm; c) biotinamidohexanoyl-6-aminohexanoic acid N-hydroxysuccinimide ester, denoted as -XX-, which contains a 14 atom spacer arm.

3.2.1 Buffers

The buffers used were prepared as follows: PCR buffer was made up of 20mM Tris-HCl pH=8.0 at 25°C, 100mM KCl, 0.1mM Ethylene diaminetetraacetic acid disodium salt (EDTA), 1mM DL-Dithiothreitol; biotinylation buffer comprised of 50mM $Na_2CO_3/NaHCO_3$ pH=8.5 at 25°C, 0.1 EDTA; Phosphate buffered saline (PBS) contained 0.01M phosphate buffer with 2.7mM KCl and 0.137M NaCl at pH 7.4 at 25°C; 1X Tris Borate EDTA buffer (TBE), 90mM Tris, 90mM Boric acid, 2.6mM EDTA; MES buffer, used for passive adsorption, contained 10mM 2-(N-Morpholino)ethanesulfonic acid pH=6.1 at 25°C, 50mM KCl; phosphate-cirate buffer, used in colourmetric test of immobilisation, contained 50mM phosphate-cirate pH=5.0 at 25°C, 0.014% H_2O_2.

3.3 Methods

The methods of immobilisation of both enzymes and subsequent PCR experiments are described. The methods used are modified procedures adapted from standard protein immobilisation techniques. Adjustment of the procedures allows for the smaller size of the enzymes compared to most proteins used for immobilisation.

3.3.1 Immobilisation of *Taq* Polymerase

Taq polymerase was immobilised using biotin-streptavidin couple, carbodiimide, glutaraldehyde and by passive adsorption.

3.3.1.1 Biotin-Streptavidin Immobilisation

The first step in the immobilisation process was the biotinylation of the *Taq* polymerase. Enzyme stock solution was diluted 10-fold, resulting in an activity of 50units/100μl in PCR buffer. The buffer was changed by microdialysis to biotinylation buffer, see Section 3.2.1. This buffer change was necessary to remove the tris buffer which contains primary amine groups (NHS will react with any amine). To ensure the NHS reacts only with primary amines in the enzyme, an amine free buffer was need. The biotinylation buffer was adjusted to pH 8.0 to allow the deprotonation of the free amine group in the lysine residues. A lower pH would allow a higher percentage of deprotonated lysines but at pH 8 the NHS does not immediately hydrolyse as it would at lower pH. The result was a higher efficiency of the immobilisation as more NHS reacts with the protein rather than the water. After dialysis 1x10^{-10}mol of NHS-biotin ester in 10μl of DMF was injected into the dialysis cassette to initiate the reaction. The cassette was shaken and incubated at 4°C for 3hrs. The reaction was run at 4°C to minimise the NHS being hydrolyzed by the water (by limiting the energy within the system, the more energetically favourable reaction with the free amines happens faster than the hydrolysis with water) and to try to promote the interaction towards the least sterically hindered lysine. The least sterically hindered lysine is favoured at low temperatures because the energy within the system is too low to force reactions over sterically hindered energy barriers,[156] ie less sterically hindered lysines have a lower intermediate energy barrier to react and produce products. Three different biotin molecules were used, each differed in the length of the spacer between enzyme and surface to minimise steric hindrance, see Figure 3.9. The different spacers were denoted as either -X-, -XX- or as -, with no spacer, see Section 3.2 for structures. Once the reaction was complete, the buffer was changed to PCR buffer by dialysis overnight at 4°C, removing unreacted biotin from the solution. Biotinylated *Taq* in PCR buffer was removed from the cassette and stored at 4°C.

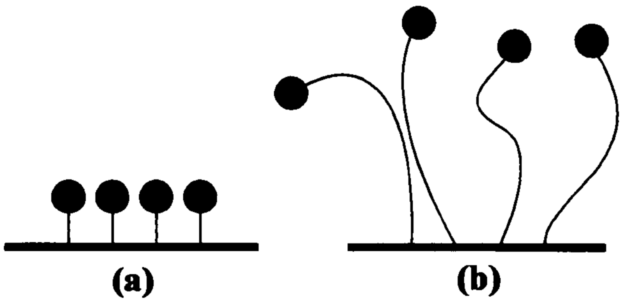

Figure 3.9: Illustration of how a shorter spacer arms (a) is more sterically hindered compared to a longer spacer arm (b). It can be seen that longer the spacer the more degrees of freedom of movement for the enzyme.

After the enzyme had been biotinylated, the next stage was to attach it to the surface of the streptavidin coated beads. The beads were 2.8μm diameter streptavidin coated magnetic beads. 5x10^{-5}g of beads were used to immobilise 48 units of biotinylated *Taq* polymerase. The number of the beads used was estimated by determining the amount of protein possible to attach to each bead, see Section 3.1.3. The beads had a surface area of 4-8m^2/g and had a density of approximately 1.3g/cm^3.

0.5μl of bead stock solution was washed 3 times in PCR buffer. The beads were resuspended in a minimum amount of buffer and added to the biotinylated *Taq* in 120μl of PCR buffer. The bead slurry was shaken for 3hrs at room temperature. The beads were then washed 3 times in PCR buffer and stored at 4°C

3.3.1.2 Carbodiimide Reaction

Attachment of *Taq* polymerase via the carbodiimide method was performed in a one pot reaction in which the beads and the enzyme were simultaneously reacted with the EDAC. This was done to ensure that the EDAC did not react only with the amines on the enzyme without interaction with the amine coated beads. The EDAC reacts with the carboxylic acid groups of the enzyme and then with the amine groups on the surface beads.

The whole procedure was performed in 10mM PBS pH 7.4 buffer. The first step was an exchange of buffers from the storage buffer of *Taq* to PBS buffer using a spin column. 8μl, at 2x10^9 beads/ml, of amine coated beads, 2.8μm in diameter, were washed 3 times in PBS buffer, then suspended in 200μl of 0.1M EDAC in PBS buffer. 5units of *Taq* were added to the reaction "pot" and shaken for 2hrs at room temperature. 5units of *Taq* on 16x10^6 beads allowed a spacing of 1 protein per 50nm^{2}of bead surface[129]. The reaction was quenched with excess glycine. The beads were then washed in PBS buffer and stored at 4°C.

3.3.1.3 Glutaraldehyde Reaction

Firstly, the beads were activated with glutaraldehyde. 8μl of amine coated beads (2x10^9 beads/ml stock solution and 2.8μm in diameter) were then washed 3 times in 10mM PBS buffer pH 7.4. The beads were then activated at room temperature by a 1% glutaraldehyde in PBS for 2 hours by shaking and then at 4°C overnight.

Taq polymerase underwent a buffer exchange from the storage buffer to 10mM PBS buffer, pH 7.4, using spin column. The activated beads were washed in PBS and resuspended in 40mM cyano borohydride ($NaCNBH_3$) in PBS buffer. 5units of *Taq* in PBS buffer were added to the cyanoborohydride solution and left to react overnight at 4°C. 16x10^{6}beads were used with an estimated 1 protein per 50nm^{2}of bead surface[129]. Once complete, the beads were washed in 1% bovine serum albumin (BSA) in PBS buffer and stored at 4°C. BSA was used to block the remaining active sites on the beads.

3.3.1.4 Passive Absorption Method

Two different types of beads were investigated for adsorption of *Taq* polymerase, they were made from silica beads and polystyrene. Silica beads contained polar silioxyal groups for hydrophilic attachment of the enzyme. Polystyrene beads have hydrophobic surfaces, due to the alkane surface groups, for hydrophobic immobilisation of *Taq*. All beads were 1μm in diameter, the bead diameter varied compared to streptavidin coated beads due to availability of smaller diameter beads allowing for better retention within the solution. Using Equation 3.1 the maximum mass of protein that could be adsorbed on the beads, was estimated.

Two different buffers were used during the physical adsorption of the enzyme to the solid support, Tris-HCl pH 7.2, 1mM EDTA at room temperature and MES buffer pH 6 at room temperature. MES at pH 6 was used to match the isoelectric point of the protein. From the literature the isoelectric point of *Taq* was found to be pI 6. Three methods of passively adsorbing *Taq* on to silica beads were implemented.

1. 0.5μl of silica bead stock solution was suspended in 200μl of 50mM Tris-HCl pH 7.2, 1mM EDTA with 50units *Taq* polymerase for 1 hr at room temperature. This was used as the basic passive adsorption method.
2. 0.25μl of silica bead stock solution was suspended in 5μl, 25units, of *Taq* polymerase stock solution, Tris-HCl buffer, for 1 hr at 4°C. The reaction volume was reduced to promote adsorption of the enzyme to the beads. The immobilisation was carried out at 4°C to reduce the thermal instability of the adsorption.
3. 0.25μl of silica bead stock solution was suspended in 75μl of MES buffer pH 6 with 25units of *Taq* polymerase for 1hr at 4°C. To investigate the difference in absorption at the isoelectric point the buffer was changed to pH 6.

Taq polymerase was also physically adsorbed on to polystyrene beads using the MES buffer method, as described for the silica beads, number 3 above, except 0.4μl of polystyrene bead stock solution was used for 25 units of *Taq*. After the immobilisation steps all the beads were washed 3 times in PCR buffer and stored at 4°C.

Experiments were also carried out to investigate the thermal stability of the enzyme on polystyrene beads. The format for these was immobilising the enzyme on to polystyrene beads, as before, then heating the beads in PCR buffer, to 95°C for 10min. After the beads had been heated the beads were washed three times in PCR buffer and stored at 4°C. The beads were used within PCR experiments in order to discover if the enzyme was removed from the beads at high temperature.

3.3.2 PCR Reaction with *Taq* on Microspheres

Once the *Taq* polymerase had been attached to the microspheres, a PCR reaction was performed. These experiments were run using a conventional thermal cycler (MJ 100PTC, MJ research inc., Bio-rad, Hemel Hempsted, Hertfordshire, UK) in standard 200μl PCR tubes. A standard PCR protocol was used, it was the same procedure for all bead configurations. For the final PCR concentrations see table 3.1.

Reagent	Final conc. in reaction
10x PCR buffer	1X
MgCl2	3.5mM
dNTPS	200μM

Table 3.1: Table to show the final concentrations of reactants in the PCR experiments.

2 μl of template and primers were added together in the PCR tube. The template and primers form products of 360bp, 550bp and 650bp. 1μl of *Taq* polymerase (5units/μl) was added to the positive control. The *Taq* polymerase immobilised on beads was added in 5μl of PCR buffer to the PCR tube. Water was added to bring the reaction volume to 26μl. For the microspheres larger than 1μl, the reaction was paused every 5 cycles to resuspended the beads by vortexing. The PCR cycle was 15s at 95°C, 30s at 60°C and 30s at 72°C to complete.

Before the first cycle, the reaction mixture was heated to 95°C for 3min to ensure that the template had completely melted to improve the efficiency of the first cycle. 35 cycles were employed in the experiments with the last cycle having an extended extension time of 10min to guarantee that all the copies were extended to the full length. After the cycling was complete the PCR products were stored at 4°C.

3.3.3 Gel Electrophoresis of PCR Products

Products from the thermal cycling were tested using gel electrophoresis. 2% agarose gel in 1X TBE, see Section 3.2.1, was prepared by heating the agarose gel in the TBE buffer. The gels were moulded to form 8 x 10cm gels with wells for the samples. 40V was applied across the gel for 10min to move the samples into the gel. The voltage was then increased to 80V, 8V/cm, (~23mA) for 1hr 45min. Gels were stained afterwards using ethidium brominde (EtBr) or SYBR green. Staining gels with these stains allowed visualisation of the DNA under UV light. EtBr was added as 10μl of 10mg/ml in to 50ml of deionised water and gently agitated for 20min. After staining the gel was washed in deionised water. SYBR Green was diluted 50μl in 50ml of 1x TBE and left for 30min, no washing was required.

3.3.4 Immobilisation of T7 DNA Polymerase

T7 DNA polymerase was also immobilised on to polystyrene beads via the passive adsorption method. The immobilisation was carried out in 50:50 Tris-HCl : Glycerol. This buffer was used by Levene[129] in the adsorption of T7 DNA polymerase. 5units of T7 DNA polymerase was adsorbed onto 0.5μl of polystyrene beads, after the beads had been washed three times in 100μl of immobilisation buffer for 1hr. The estimated spacing of enzymes on the beads was 1 protein per 2.5$\mu m^2$of bead surface. The immobilisation was carried out at two different temperatures, namely 4°C and room temperature. After the immobilisation the beads were washed 3 times in PCR buffer with 0.1% Triton X-100 and 1% BSA and stored at 4°C. Triton X-100 and BSA were used to block any remaining active sites. Triton X-100 was added to help dissolve the glycerol. T7 DNA polymerase is not thermally stable so the reaction was to be carried out in one cycle so a higher concentration of template was needed at the beginning. A standard PCR was run and the products from that used as the template for the T7 DNA polymerase reactions.

Once the PCR had been run, the PCR mixture, without any T7 DNA polymerase, was heated to 95°C, to melt the template DNA strands, for 10min. It was then cooled to 37°C and the beads with immobilised T7 DNA polymerase were added and the free enzyme added to the controls. The reaction mixture was incubated at 37°C for 30min. The samples were then stored at 4°C. Products were tested using gel electrophoresis as described in Section 3.3.3.

3.3.5 Assessment of Enzyme Immobilisation

The immobilisation of the enzymes was assessed in two ways. It was necessary to determine if enzyme, attached by passive absorption, was detaching from the microsphere when heated. Also the immobilisation procedures needed to be investigated to show if the methods inhibited all activity of any enzyme immobilised under these conditions.

3.3.5.1 Protein Staining to Determine Thermal Loss

Amido black staining solution, which stains only proteins, was diluted 1:1 with deionised water. This was used to stain the immobilised enzymes on polystyrene beads by shaking at room temperature in the dark for 1hr. The enzyme was immobilised by passive adsorption only, as described in Sections 3.3.1.4 and 3.3.4. Only passive adsorption was tested in this manner because it appeared that the enzyme might be dissolving back into the solution under heating because of increased thermal energy breaking any physical bond with the surface. The stained beads were then washed in PCR buffer and heated to 95°C for 10min. After the heating, the beads were centrifuged and the supernatant was collected. Using a UV/Vis spectrometer (U-2000 spectrophotometer, Hitachi Scientific Instruments, Wokingham, Berkshire, UK) the absorbance was measured to determine whether amido black was in the buffer. Amido black has a $\lambda_{\max}$ of 630nm. The heated supernatant was compared to the buffer in which the beads were washed before heating as way of a negative control. Plain polystyrene beads were stained with amido black to check the background with no protein attached to show that amido black would only stain the beads if protein was attached.

3.3.5.2 Immobilisation of HRP to Investigate Immobilisation Procedures

The methods for immobilisation were tested to check that it was possible for an enzyme to still remain functional using the protocols used for *Taq* polymerase. Horseradish peroxidase (HRP) was used as a model enzyme because it has a well understood structure and function. HRP has a number of properties ideal for testing the immobilisation, including: a high substrate turnover rate, easy assay and low cost.

The assay used was the oxidization of 2,2'-azino-bis(3-ethylbenzthiazoline-6-sulfonic acid) (ABTS) to ABTS radical cation by its reaction with H_20_2. This reaction gives a green colour product from a colourless starting material, which has a characteristic peak at 415nm in the visible spectrum which can be investigated by UV/Vis (U-2000 spectrophotometer, Hitachi Scientific Instruments, Wokingham, Berkshire, UK).

Due to the difference in size between the enzymes, 44kDa for HRP to 94KDa for *Taq* polymerase, the total mass of the proteins was used to equate the enzymes rather than number of units. 1 unit of *Taq* polymerase equates to 125ng of protein whilst 1 unit of HRP, with respect to ABTS, is equivalent to 880ng of protein. The protocols used were the same as described in Sections 3.3.1 and 3.3.4.

ABTS was oxidised using HRP in the presence of H_20_2 in phosphate-citrate buffer, pH 5.0 with 0.014% w/v H_2O_2 and 0.2M ABTS. Immobilised HRP was added to 200μl of phosphate-citrate buffer and was shaken for 30min at room temperature in the dark and then quenched with 10μl of 0.1% sodium azide. A positive control was established with 1unit of HRP, from the stock solution, added and mixed in the same conditions. The beads were centrifuged and the supernatant collected, the supernatant was then tested in a UV/Vis spectrometer. A negative control, which contained all the reagents included sodium azide, apart from the HRP was investigated with the UV/Vis spectrometer.

3.4 Results of PCR Using Immobilised Enzyme and Discussion

3.4.1 Results of PCR Amplification Using Immobilised *Taq* Polymerase

Short strands of DNA were used, as the template, to limit problems of steric hindrance when investigating the interaction between enzyme and template. Shorter templates are most likely to be able to find the correct orientation and would take less time to be extended if the enzyme was not working at full efficiency. The template forms three distinct bands, 360bp, 550bp and 650bp. For positive results these three bands must be visible in the electrophoresis gel with the band at 360bp expected to be the brightest and therefore the most probable to find a positive result. A 100bp ladder was used as a size reference to interpolate the size of the products on the electrophoresis gel.

3.4.1.1 Biotin-Streptavidin Immobilisation

Taq polymerase was biotinylated and immobilised on microspheres. Once immobilised the enzymes were used within a PCR experiment to amplify the template. Figures 3.10 and 3.11 show the products gained separated by gel electrophoresis. The three expected bands can be seen in the +ve controls and in the enzyme which is biotinylated but not attached to the bead. Enzymes attached to microspheres via the biotin-streptavidin couple showed no bands.

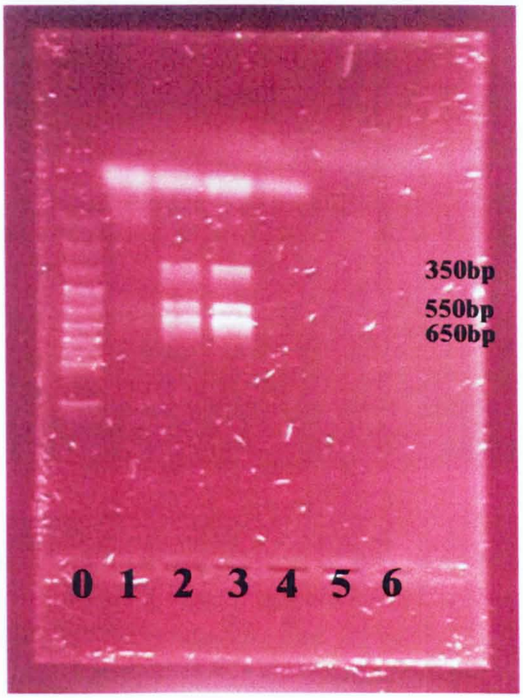

Figure 3.10: Image of gel after separation of products from a PCR. Lane: 0, 100bp ladder, 1, +ve control, 2, biotin-X-*Taq*, 3, biotin-XX-*Taq*, 4, unrelated experiment, 5, bead-biotin-X-*Taq*, 6, bead-biotin-XX-*Taq*.

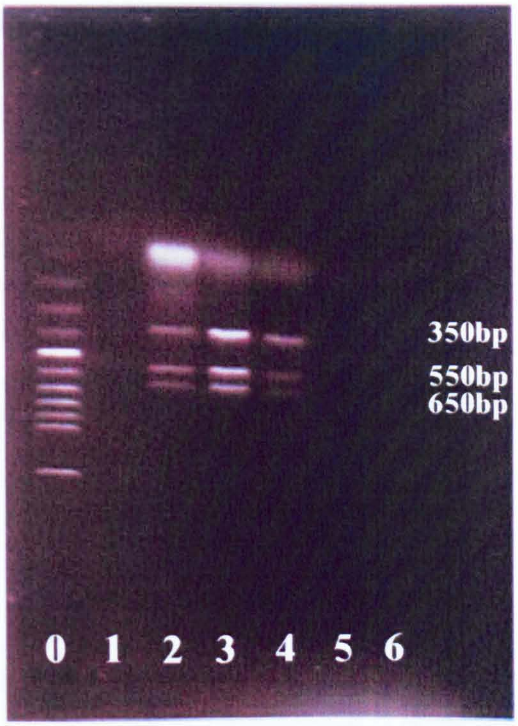

Figure 3.11: Image of gel after separation of products from a PCR. Lane: 0, 100bp ladder, 1, -ve control, 2, +ve control, 3, biotin-*Taq*, 4, biotin-XX-*Taq*, 5, bead-biotin-*Taq*, 6, bead-biotin-XX-*Taq*.

The appearance of the three distinct bands at 360bp, 550bp and 650bp for the biotinylated enzyme shows that the addition of the biotin moiety and the spacer, if there was one, has no significant effect on the action of the enzyme. In contrast to the activity of the biotinylated enzyme the enzyme attached to beads showed no bands at the expected sizes. This implies that once *Taq* polymerase is immobilised onto a surface, the enzyme is unable to function normally. The faint bands in the positive control, in figure 3.10, could be from poor experimental procedure when the experiment was set up, eg not enough template or enzyme.

3.4.1.2 Glutaraldehyde

Taq immobilised to the surface of amine coated microspheres was used to amplify DNA in a PCR experiment. The products were investigated by gel electrophoresis. The separation of products by gel electrophoresis can be seen in Figure 3.12. PCR experiments run using *Taq* polymerase immobilised by the glutaraldehyde method did not show any of the three expected bands at 360bp, 550bp and 650bp.

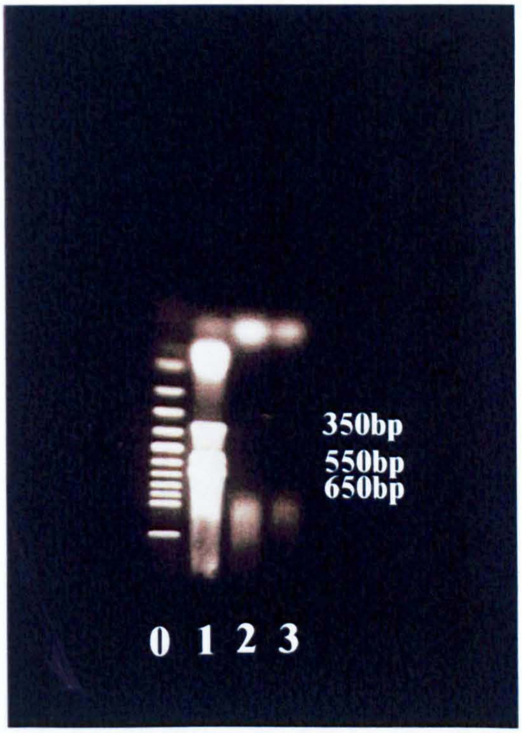

Figure 3.12: Image of a electrophoresis gel showing separation of PCR products from PCR using glutaraldehyde immobilised *Taq* polymerase. Lane: 0, 100bp ladder, 1, +ve control, 2 and 3 reactions using immobilised enzyme.

Lack of any of the three expected bands after the separation implies that the enzyme is unable to amplify the DNA template. It is possible that the presence of the bead close to the enzyme prohibits either the interaction of the template with the enzyme or the ability to add the dNTPs or of course both actions might be unable to occur. The high weight bands in lanes 2 and 3, see figure 3.12, must be due a to a contaminate within the sample, as there is nothing within the experiment to account for those bands.

3.4.1.3 Carbodiimide

Immobilised *Taq* on to microspheres, by carbodiimide, was used in PCR experiments. The separated products are shown in Figure 3.13. The experiments using *Taq* immobilised by carbodiimide do not show either of the three expected bands at 360bp, 550bp and 650bp.

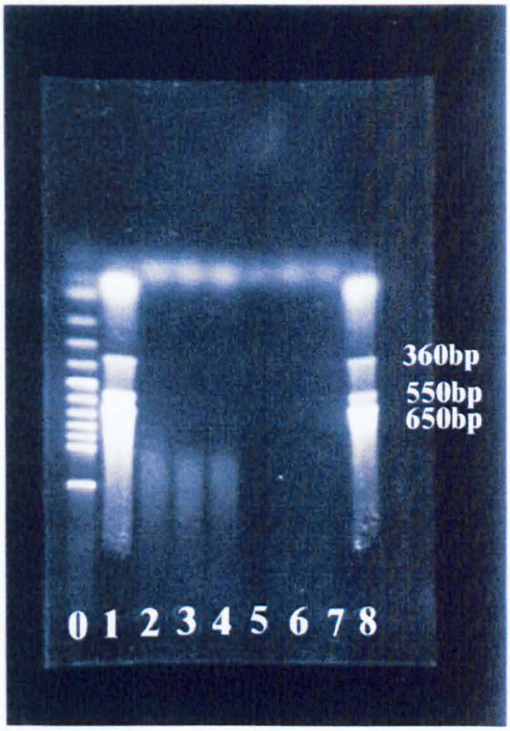

Figure 3.13: Image of gel after separation of PCR products by electrophoresis. Lane: 0, 100bp ladder, 1, +ve control, 2-4, unrelated experiment, 5-7, bead-*Taq* using carbodiimide coupling reaction, 8, +ve control.

As no bands at the correct size for the products are shown in the electrophoresis gel this implies that using carbodiimide to immobilise *Taq* polymerase inhibits the activity of the enzyme. The way in which it loses its activity is probably due to the bead blocking the active sites.

3.4.1.4 Passive Adsorption

Taq polymerase passively immobilised on to silica beads was used in PCR experiments and the products were visualized after gel electrophoresis. The products gained from the first method of absorption, described in Section 3.3.1.4, is shown in Figure 3.14.

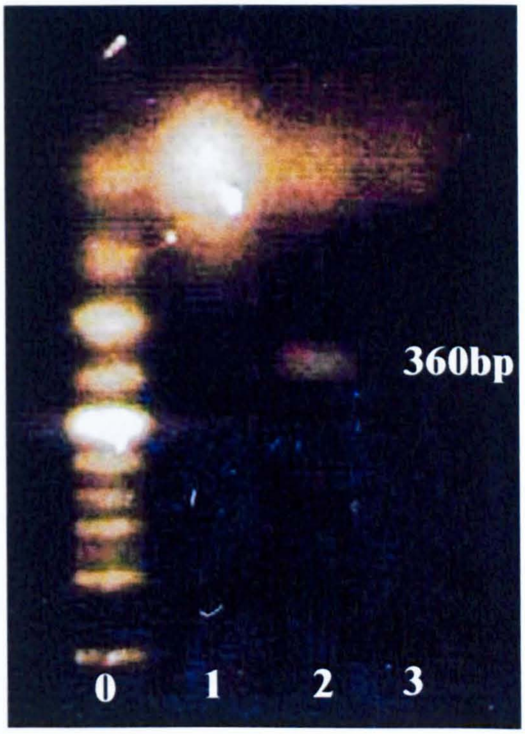

Figure 3.14: Colour enhanced visualization of products of passive absorption of *Taq* polymerase on 1μm silica beads using 50mM Tris-HCl pH 7.2 buffer. Lane: 0, 100bp ladder, 1, +ve control, 2 and 3, bead-*Taq*.

Using silica beads with *Taq* absorbed at room temperature in Tris-HCl showed some of the expected bands in one experiment. In figure 3.14 one band is seen faintly at 360bp. This shows that the enzyme has amplified one of the templates.

The products gained, using *Taq* polymerase adsorbed on to silica microspheres using Tris-HCl at 4°C, are shown to be separated by gel electrophoresis in Figure 3.15. Three out of the four PCR experiments run with immobilised *Taq* polymerase produced the three excepted bands. The expected bands appearing in the correct sizes when separated mean that the enzyme that was adsorbed on to the bead has managed to amplify the templates.

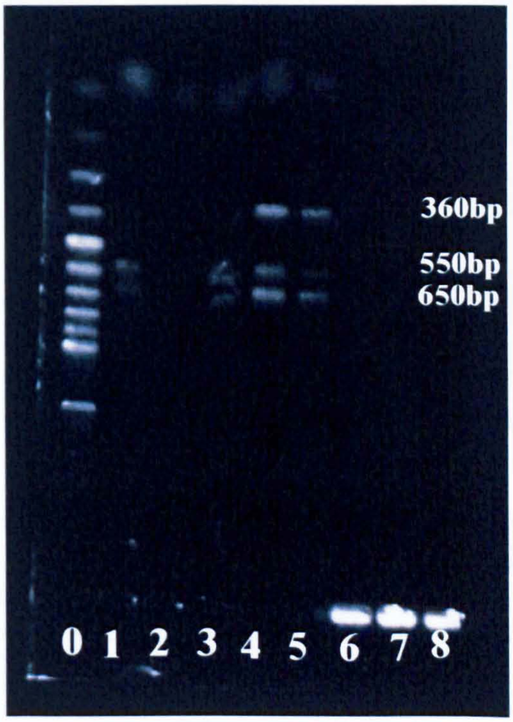

Figure 3.15: Gel of products from physically adsorbed *Taq* polymerase on to 1μm silica beads using *Taq* in storage buffer at 5units/μl. Lane: 0, 100bp ladder, 1, +ve control, 2-5, bead-*Taq*, 6-8, unrelated experiment.

Products from *Taq* polymerase being adsorbed on to silica beads at the isoelectric point of the enzyme, using MES buffer pH 6, see Section 3.3.1.4, can be seen in Figure 3.16. Positive results can be seen by both experiments using *Taq* immobilised on to silica beads. A positive result is given when the 3 bands are observed at 360, 550 and 650bp.

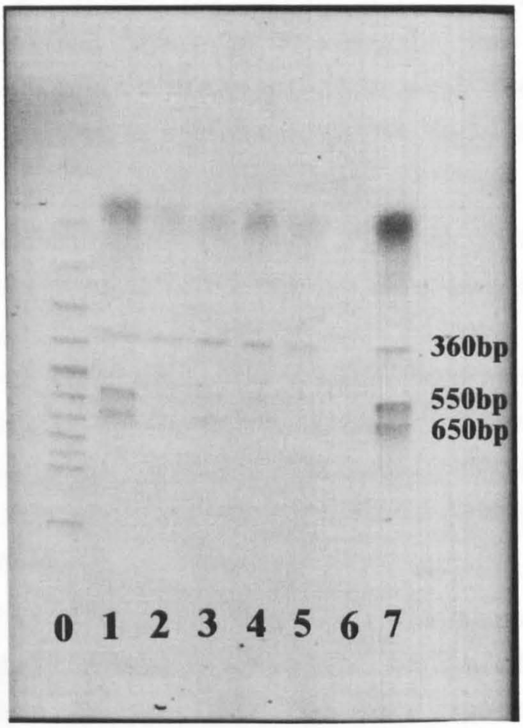

Figure 3.16: Colour inverted, to make viewing clearer, electrophoresis gel of products from the adsorption of *Taq* polymerase on to silica and polystyrene beads at pH 6. Lane: 0, 100bp ladder, 1, +ve control, 2 and 3, silica bead-*Taq*, 4 and 5, polystyrene bead-*Taq*, 6, empty lane, 7, +ve control.

The products, after separation, from the PCR experiments involving *Taq* polymerase absorbed on to polystyrene beads at the isoelectric point and at 4°C are shown in Figure 3.16. In all experiments, using MES as the buffer, the 360bp band is visible. The bands at 550bp and 650bp are not visible. This might be because there was less template within in the starting mixture than for the 360bp. The templates might not of been amplified enough in the number of cycles used to show up in the gel. This shows that *Taq* immobilised at the isoelectric point is still active.

From the results it appears that passive adsorption does not inhibit the activity of the enzyme unlike the other methods of immobilisation. If the presence of the bead prevents the enzyme from functioning fully in three cases but not in another there must be a reason. One reason is that, as the enzyme was only held on to the surface by weak intermolecular forces, when the reaction mixture is heated the enzyme might simply desorb from the bead.

Passive adsorption is dependant on a stable pH. If the pH changes the protein may desorb from the bead. Tris-HCl changes pH greatly as the temperature changes which could allow the enzyme to leave the bead. Also the increased movement of solvent molecules within the protein as the temperature rises could force the enzyme off the surface. A possible reason why the enzyme immobilised at pH 6 only amplified, what is normally, the brightest band may be due to better adsorption on the surface so less enzyme deabsorped back into the solution.

The separation of products gained after PCR experiments using beads which were coated in enzyme by passive adsorption then heated to 95°C for 10min and washed are shown in Figure 3.17. The three expected bands at 360bp, 550bp and 650bp are visible for the experiments that used beads that had not been heated. Whereas the beads that had been heated did not show any of the expected bands. This demonstrates that the positive results gained by passively adsorbed enzyme where due to the enzyme becoming detached from the beads during the initial heating phase rather than still being active still on the bead.

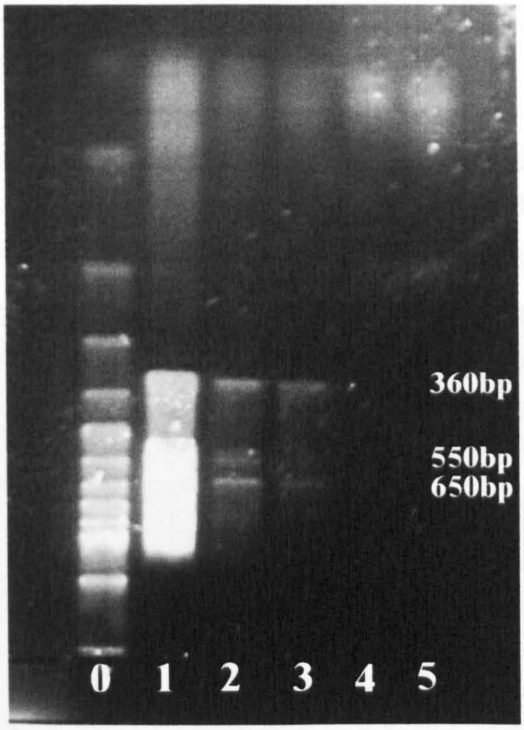

Figure 3.17: Electrophoresis gel of comparison between PCR experiments with beads that have undergone a preheat step and beads with *Taq* that were used directly. lane: 0, 100bp ladder, 1, +ve control, 2 and 3, no preheating of beads, 4 and 5, preheated of beads.

3.4.2 Results of PCR Amplification Using Immobilised T7 DNA Polymerase

The products, after separation by gel electrophoresis, from the amplification of the template by immobilised T7 DNA polymerase are shown in Figure 3.18. The two positive controls show the bands at 550bp and 650bp whilst the experiments that used T7 polymerase passively adsorbed on to the beads show brighter bands, brighter bands could come from the fact that there was less enzyme in the control than in the immobilised samples. This means that the enzyme was able to amplify the template. As shown for *Taq* that was passively adsorbed, the enzyme could become detached from the bead.

This is most likely to have happened in this case as well. It is unlikely that the enzyme amplified the template while attached to the bead due to steric hindrance. There is one difference in this case compared to the passive adsorption of *Taq* and that is that the beads were not heated above 37°C. This temperature is most likely to be high enough to cause desorption through pH changes and increased vibrational energy within the system.

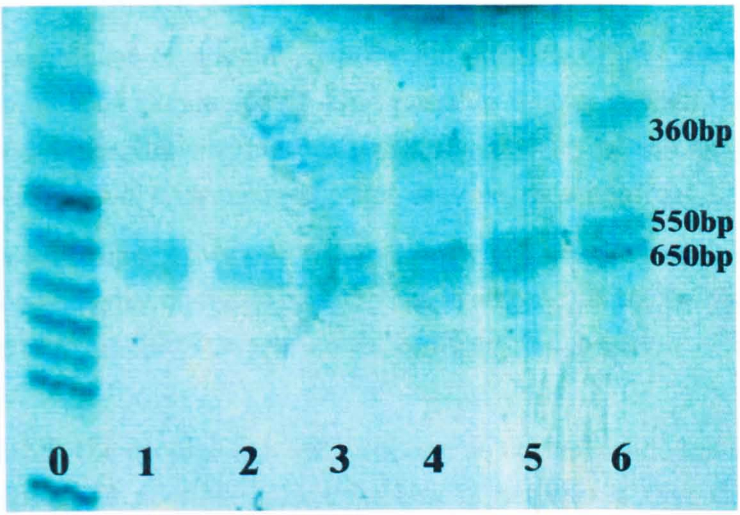

Figure 3.18: Inverted colour image of the gel gained from products of T7 DNA polymerase physical adsorbed on to 1μm polystyrene beads. Lane: 0, 100bp ladder, 1, Control for amount of template DNA, 2, +ve control with free enzyme, 3 and 4, T7 enzyme adsorbed at room temperature, 5 and 6, T7 enzyme adsorbed at 4°C.

3.4.3 Discussion of Immobilisation of Polymerases

Taq polymerase and T7 DNA polymerase was immobilised by 4 methods. *Taq* polymerase was immobilised using a biotin-streptavidin couple, carbodiimide, glutaraldehyde and by passive adsorption. T7 DNA polymerase was attached by passive adsorption. The enzymes were immobilised on to microspheres and PCR experiments were carried out using the immobilised enzyme.

Amplification of the DNA substrates with immobilised polymerases were not successful. Passively adsorbed enzyme produced results that indicated positive results, but it was believed that the enzyme became detached from the bead and was amplifying the template as free enzyme in solution. This was demonstrated by heating the enzyme coated beads before the PCR experiment and then washing the beads and using the beads in a PCR experiment. These heated beads, unlike unheated beads with passively adsorbed enzyme, did not produce positive results.

There are a number of possible reasons for the lack of any activity shown by the immobilised polymerases. One possible reason is that the methods used to immobilise the enzyme destroyed the activity of the enzyme. This scenario is discussed later using another enzyme, as a control.

There are a number of other possible reasons which are the most likely causes of the lack of activity of the enzymes. One is a steric factor, whilst a second is the enzymes inability to cope with addition and position of a chemical moiety.

Assuming that the enzyme can still function as normal while immobilised to the microsphere, a possible reason for lack of activity is that the presence of the bead might make interaction between enzyme, template with primer and dNTPs highly improbable. If this was the case, the efficiency of the amplification reaction would be very low but not necessarily zero. Therefore one might be expected to see a small amount of amplification rather than none which was seen. The lack of activity cannot be solely attributed to the steric hindrance of the attached bead.

In a similar fashion, it is possible that the attachment of the bead might act at a residue that would stop the activity of the enzyme. Evidence against this is the fact that, if this were the case, there would be a percentage of enzyme where the attachment has been a free residue. The numbers of free lysines (providing -NH_2), aspartic acid and glutamic acid (providing -COOH) are not known compared to the number of lysines, aspartic and glutamic in the whole protein. If the position of attachment is the reason for lack of activity then the percentage of enzymes working would be equal to the percentage of free residues. As no activity was seen, then the problem of activity was probably not due to the position of the attachment.

This explanation was supported by the fact that enzyme which has been biotinylated but not attached to the bead was still able to successfully amplify the template DNA during a PCR experiment, shown in Figures 3.10 and 3.11.

After these possible reasons had been eliminated as the probable reasons for lack of activity, there are a few more fundamental reasons for the lack of activity. The first is the effect of the attachment of the bead on the reorganisation of the conformation of the enzyme during the incorporation of the nucleotides. A second is whether the enzyme is active (under the classical view of the enzyme moving along the template strand, it may be unable to "pull" the bead with it, if this is how the mechanism works).

Investigating the conformational changes that occur within *Taq* polymerase during the extension stage of PCR on template and primer, see Section 3.1.1.3, all of the protein is effected upon capture and extension of the primer. By studying the change of the shape of *Taq* polymerase during extension, it has been shown that the two domains not directly used for polymerisation change orientation. For example, the 5' nuclease domain moves to align its active site with the extended DNA. If the protein was immobilised this might limit its ability to re-orientate itself which could cause the enzyme to become inactive. This hypothesis would explain the lack of activity seen from either of the two polymerase enzymes once they were bound to the surface of the beads.

This hypothesis is supported in the literature. Firstly the lack of papers reporting the successful immobilisation of *Taq* polymerase enzymes. However the immobilisation of the enzyme is used in a "hot start" PCR method. "Hot start" is where the polymerase enzyme is restrained from working within a PCR experiment until the reaction mixture has reached the first high temperature melt stage (this has the benefit of reducing nonspecific polymerisation). *Taq* polymerase is adhered to a surface using a his-tag[157] which falls off once heated.

A final question relating to the lack of activity of the immobilised polymerase is whether the enzyme can move along the template DNA (like a train on a track) if it has a bead attached to the enzyme. Central to this explanation is the question as to whether the traditional text book idea of the smaller enzyme having to move along the larger template strand is correct, or does the DNA strand move through the enzyme cleft? If the enzyme does not need to move along the strand then it would seem possible for the enzyme to be immobilised.

In contrast to *Taq* polymerase, T7 RNA polymerase has been immobilised[158] using a hybrid maltose binding/T7 RNA polymerase protein which has been attached via an antibody bridge to protein A and then to a plastic bead. This proved that a DNA strand could be transcribed using an immobilised polymerase. Rates of polymerisation were unaffected by the enzyme being immobilised. Instead of the enzyme being considered a train on a track, the action was described as the enzyme being a nut and the template acting as a screw. Further evidence for the fact that polymerase enzyme could be immobilised comes from *in vivo* cell work, where enzymes are immobilised within membranes[159] and can still function.

For polymerase enzymes it would seem to be the constraint of conformational change that limits the ability to amplify template strands.

In the literature there is one case reported in which T7 DNA polymerase has been immobilised to a surface.[129] From the above hypothesis the enzyme should have lost its activity once in contact with the surface. A possible explanation for this is that the enzyme is not actually attached to the surface. The enzyme was localised within a well but not significantly in contact with the surface. There is the other possibility that as a single polymerase enzyme was being studied at a time then it could be active on the surface but not enough enzymes are activite to produce a detectable amount of product, hence it appears that there is no polymerase activity.

3.5 Control Experiments for the Assessment of Immobilisation

3.5.1 Assessing Enzyme Activity Post-Immobilisation

All the different methods of immobilisation were assessed to investigate whether the method of immobilisation still allowed the enzyme to function. The colour of the reaction solution was scanned using a UV/Vis spectrometer (U-2000 spectrophotometer, Hitachi Scientific Instruments, Wokingham, Berkshire, UK). Absorption was scanned between wavelengths 600nm to 200nm. The ABTS radical cation was detected at 415nm.

3.5.1.1 Biotin-Streptavidin

In this case HRP was used as a model to demonstrate the efficiency of the immobilisation. The UV/Vis spectrum of the ABTS radical cation after ABTS has been converted by immobilised HRP, where the HRP was immobilised by biotin and streptavidin is shown in Figure 3.19. The peaks at 415nm shows that the ABTS radical cation is present in the sample. As the radical cation has been detected this confirms that the HRP was active after immobilisation by biotin and streptavidin. Therefore in principle, not all enzymes lose their activity when immobilised by this particular method. Also the difference between the long spacer and no spacer appears to make little difference to HRP in this particular assay. The maximum absorbance is higher for the immobilised enzyme compared to the free HRP because 5 times as much enzyme was immobilised than in the control. In Figure 3.19 the sharp peaks are caused by the change of the lamps within the UV/Vis spectrometer.

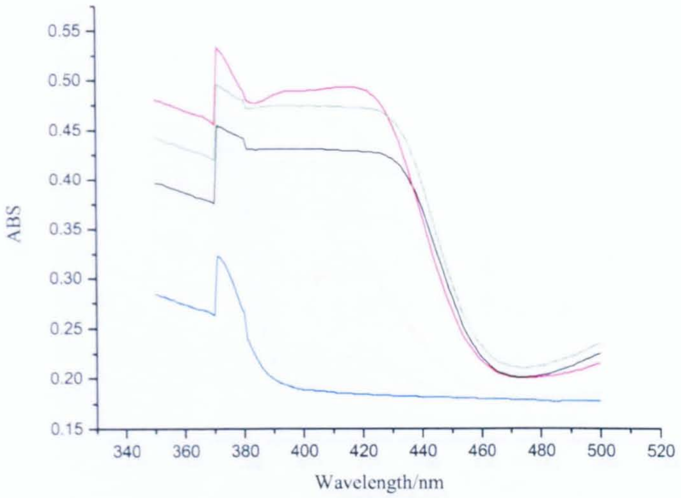

Figure 3.19: UV/Vis spectra of reaction between ABTS and HRP immobilised on beads by biotin-streptavidin couple. The blue trace shows the negative control whilst the red trace shows immobilised HRP by biotin with -xx- spacer. The green trace shows immobilised HRP by biotin with no spacer, whilst the black trace shows the positive control.

3.5.1.2 Carbodiimide

The UV/Vis spectrum of the assay of ABTS, after it has been converted to ABTS radical cation by HRP immobilised by the carbodiimide method is shown in Figure 3.20. The appearance of the peaks at 415nm in both spectrum of ABTS radical cation produced by immobilised HRP by the carbodiimide shows that the enzyme remains active after immobilisation using this particular carbodiimide method. The immobilised HRP did not convert as much ABTS as the free HRP, the positive control, so the efficiency might not be as high as with free enzyme but it still was able to function. As with the sharp peaks in Figure 3.19, the sharp peaks in Figure 3.20are due to the change of lamp with in the spectrometer.

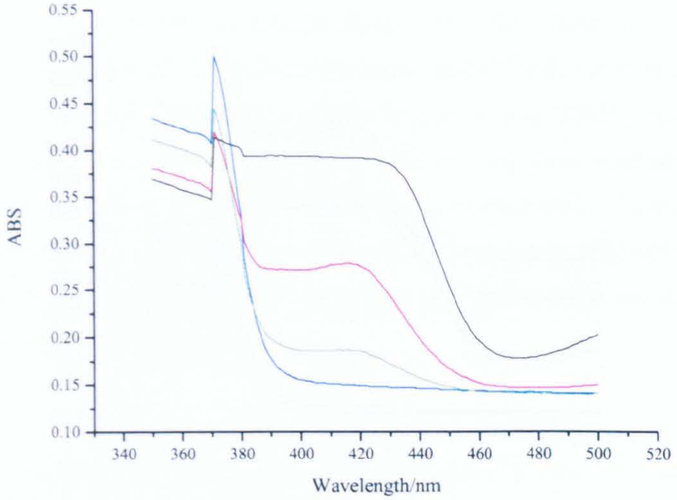

Figure 3.20: UV Vis spectra of ABTS radical cation after reaction with HRP immobilised to microspheres by carbodiimide method. The blue trace shows the negative control with the red and green traces show immobilised HRP using the carbodiimide reaction. The black trace shows the positive control.

3.5.1.3 Glutaraldehyde

UV/Vis spectrum of ABTS radical cation produced by immobilised HRP, immobilised by glutaraldehyde, is shown in Figure 3.21. In the spectrum of the ABTS radical cation, produced by the immobilised HRP, the peak at 415nm can be clearly seen. Therefore the enzyme was still active when immobilised via this particular glutaraldehyde method. Again the sharp peaks in the spectra in Figure 3.21 are due to the lamp changes within the UV/Vis spectrometer.

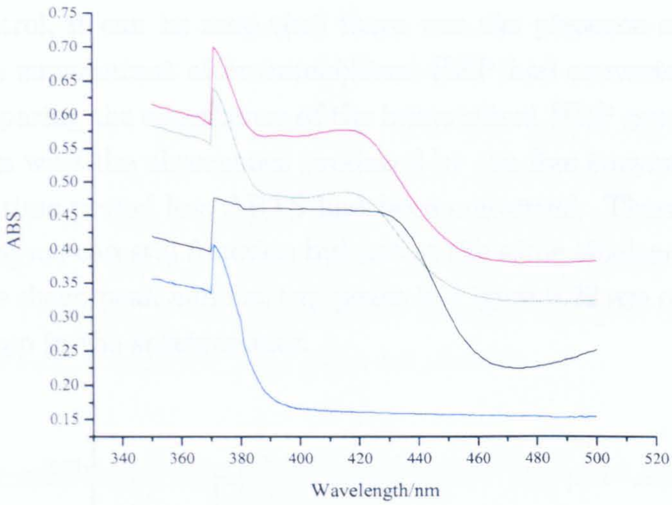

Figure 3.21: UV Vis spectra of reaction mixture from glutaraldehyde immobilised HRP on to amine coated beads. The blue traces shows the negative control control, whilst the red and green traces show the immobilised HRP, using the glutaraldehyde method. The black trace shows the positive control.

The amount of ABTS radical cation produced by the immobilised HRP was more than that generated by the 1 unit in the positive control. This was because 5 units of HRP where immobilised on to the beads and the efficiency of the enzyme was still high enough to produce more product than the 1 unit of HRP in solution.

More ABTS radical cation was generated by the glutaraldehyde immobilised HRP than that generated by the free HRP. The maximum absorbance gained for the positive control is the same in this experiment as in the other positive controls.

3.5.1.4 Passive Adsorption

HRP was immobilised by passive adsorption and the colour of the supernatant measured using UV/Vis. The spectra collected are shown in Figure

3.22. Comparing the two spectra of the ABTS radical cation to that of the negative control, it can be seen that there was the presence of the radical cation in the supernatant after immobilised HRP had converted ABTS for 30min. Comparing the absorbance of the immobilised HRP produced ABTS radical cation with the absorbance produced by the free enzyme shows that in the same time period less ABTS had been converted. Therefore the immobilised enzyme can still function but not at the same efficiency as the free enzyme. The sharp peak and flat top peaks in Figure 3.22 are caused by the change of lamp in the spectrometer.

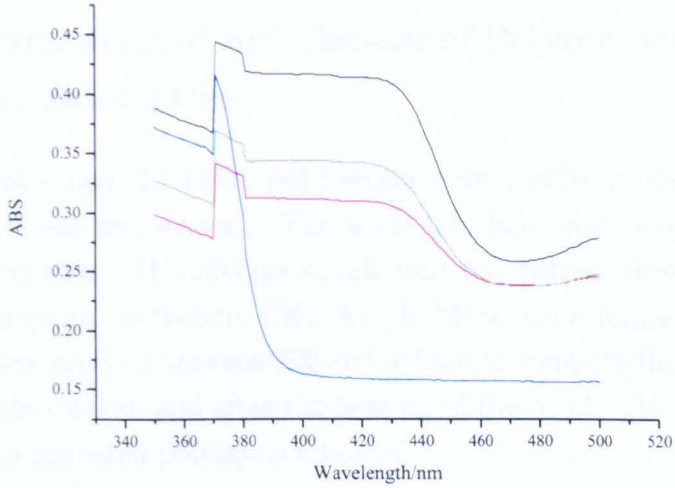

Figure 3.22: UV Vis spectrums of reaction mixtures of ABTS after reaction with physically adsorbed HRP on to polystyrene beads. The blue trace shows the negative control with the red and green traces showing the immobilised HRP, whilst the black trace shows the positive control.

3.5.1.5 Discussion of HRP Immobilisation

Using HRP to convert the substrate to the radical cation while immobilised by the four immobilisation methods shows that the methods used do not inhibit the activity of enzymes in general. As HRP will work immobilised this shows that the actual method by which the polymerase was immobilised did not kill off the activity. The techniques used allowed for enzymes to function but the ability to function depended on the particular enzyme.

A further result to be gained from the successful immobilisation and use of HRP is that the chances of the polymerase enzyme being immobilised is highly likely. An obvious reason for lack of template amplification is that the enzymes might not have been attached to the beads and therefore not in the reaction. As one protein was immobilised by these methods it is probable that the polymerase enzymes were also immobilised.

3.5.2 Assessment of Attachment of Polymerases by Passive Adsorption

Taq polymerase and T7 DNA polymerase were passively adsorbed on to polystyrene beads and heated. The wash solutions were analysed with a UV/Vis spectrometer (U-2000 spectrophotometer, Hitachi Scientific Instruments, Wokingham, Berkshire, UK). Amido black has a λ_{max} at 630nm so the sample was scanned between 700 and 300nm to compare the supernatant from the washes before and after the heating of the beads. Amido black did not adhere to uncoated polystyrene beads.

3.5.2.1 MES Immobilisation of *Taq* Polymerase

The PCR buffer in which the polystyrene beads had *Taq* polymerase passively adsorbed on to the surface were compared by UV/Vis to the PCR buffer used to wash the beads before heating, see Figure 3.23. Compared to the background, the amount of protein within the solution after the heating has substantially increased. The increase of protein in the supernatant after heating shows that the enzyme became detached from the bead surface at elevated temperatures.

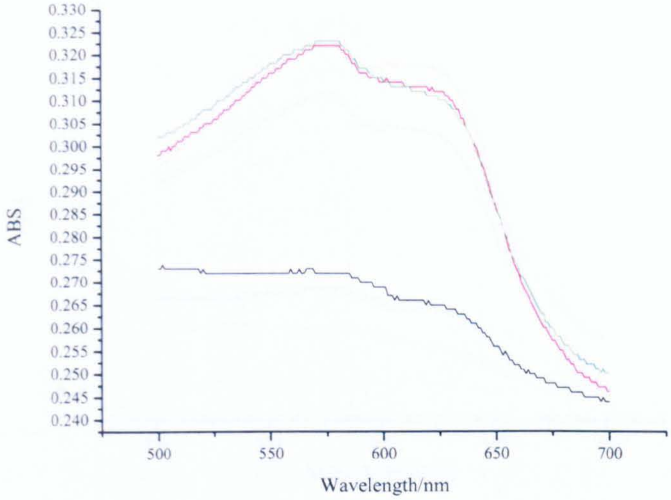

Figure 3.23: UV/Vis spectra of amido black in PCR buffer before (black) heating and after 10min at 95°C (red and green). Immobilisation of *Taq* polymerase was by physical adsorption using MES pH 6.0 as the buffer.

3.5.2.2 Tris-HCl Buffer Immobilisation of *Taq* Polymerase

UV/Vis spectrum of the PCR buffer in which the beads were washed before heating was compared to the supernatant in which the beads were heated. The spectra are shown in figure 3.24. The maximum absorbance is considerably higher for the PCR buffer in which the beads were heated compared to the wash buffer before the heating. This shows that *Taq* desorbed from the surface of the bead during heating.

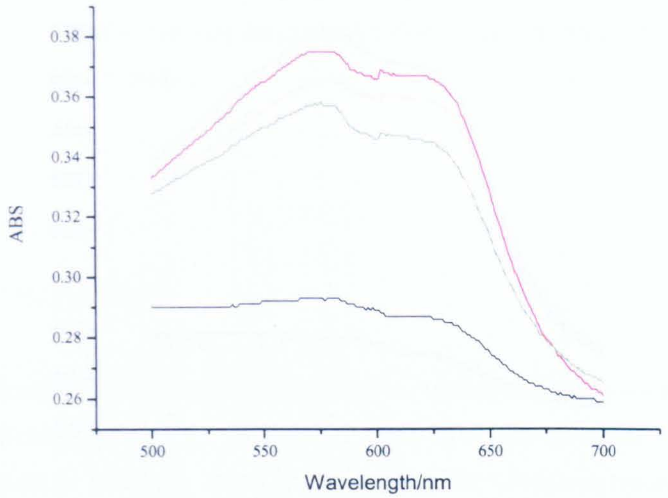

Figure 3.24: UV/Vis spectra of amido black in PCR buffer before (black) heating and after 10min at 95°C (red and green). Immobilisation was by physical adsorption carried out in Tris-HCl buffer, pH=8.0 at 25°C, of *Taq* polymerase.

3.5.2.3 T7 Polymerase Immobilisation

Comparisons of UV/Vis spectra of the wash buffer and the PCR buffer supernatant in which the enzyme coated beads were heated are shown in figure 3.25. The maximum absorbance was higher for the heated supernatant compared to the pre-heating wash. This implies that there was more amido black in the solution after heating which shows that protein had come off the beads during heating.

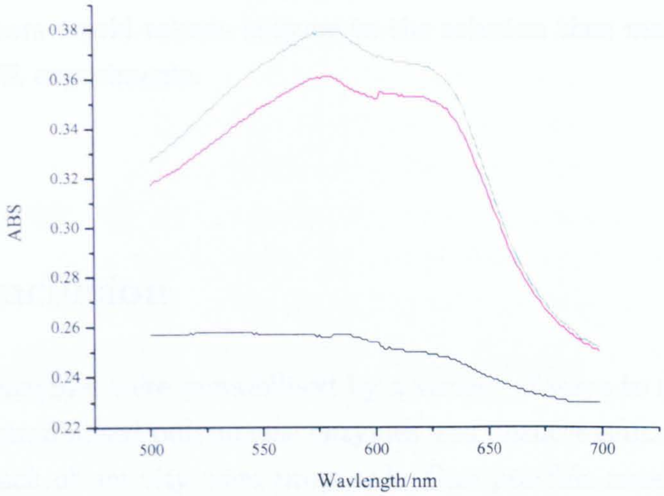

Figure 3.25: UV/Vis spectra of amido black in PCR buffer before (black) heating and after 10min at 95°C (red and green). Immobilisation was by physical adsorption carried out in the Tris-HCl buffer, pH=8.0 at 25°C, of T7 polymerase.

3.5.2.4 Discussion of Heating Passively Absorbed Polymerases

It has been shown that when heated, the two polymerases desorbed from the surface of the beads. This would explain the results of passively adsorbed enzyme coated beads when used in PCR experiments. PCR experiments using these beads gave positive results when the other methods for immobilising beads did not. If on heating, the enzyme desorbed from the bead, the enzyme was then in solution and free to extend templates as normal.

The increase in temperature changes the pH of the buffer considerably for Tris-HCl buffers. pH remaining constant is an important factor in passively adsorbed protein remaining attached.[152] As well as the change in pH, the increased thermal motion may also force the enzymes to move off the bead surface and into solution. Other factors could include the increased convection within the tube and the movement of the beads and wash, which might also be able to remove the loosely bound enzymes from the bead surface. All these factors would release enzyme to the solution thus making positive results in PCR experiments.

3.6 Conclusion

Polymerase enzymes were immobilised by a variety of ways to microspheres. PCR using immobilised polymerase enzymes was unsuccessful. A number of reasons for lack of activity were proposed. One possible reason was steric interactions between the bead and the enzyme making it impossible for the reactants to reach the enzyme. The conformational change that takes place in the enzyme during the addition of the dNTP might not be able to happen if the enzyme is immobilised. This seems to be the most likely reason of the lack of activity. Another hypothesis for the lack of activity is that the bead stopped the enzyme from moving along the strand but has been shown that this was not necessarily the mechanism by which the enzyme extended the primer. Therefore it might be possible if it were not for the steric interactions, for an immobilised enzyme to copy ssDNA.

Chapter 4

Microfluidic PCR devices

4.1 Introduction

In this chapter the fabrication and use of a novel microfluidic PCR device is presented. A general format for the instrument is presented and a number of devices which fulfill the requirements of such a system are discussed. Fabrication of the designs using several methods are also described and the associated problems with each design and method of fabrication are discussed.

The microfluidic PCR devices discussed within this chapter build on the idea of immobilising the polymerase enzyme within in the device at its working temperature. Within in Chapter 3 the immobilisation of *Taq* polymerase is shown not to work but the discussion of microfluidic PCR devices will still focus on this as an aim of the device.

4.2 Research Outline

4.2.1 Requirements of PCR Microfluidic Device

The fabrication of a device which utilises miniaturisation to enable the implementation of cheaper assays through the reduction of costs of reagents used and the time involved in the running of the assay. A requirement of such a system was to be able to monitor the amplification reaction in real-time using an electrochemical assay. Real-time electrochemical detection was to use a ferrocene tagged DNA assay, invented by Molecular Sensing Ltd, Melksham, UK, and subsequently patented by Osmetech, Roswell, GA, USA. In order for the ferrocene based assay to be detected, the ability to integrate an electrochemical reaction cell within the microfluidic device was an essential requirement of the system. Following on from the key aims, parallelisation of the device or a high throughput system was also desired as a final system but is beyond this thesis. Microfluidics is ideal for making continuous flow PCR system. Continuous flow is desirable became of the attributes perviously mentioned of cost and speed.

4.2.2 Real-Time Ferrocene Assay

This assay, originally developed by Molecular Sensing, uses a short ssDNA which is tagged with a ferrocene moiety, see Figure 4.1. The ferrocenylated DNA strand (the probe) was complementary to a section of the desired sequence to be detected (the target). The ferrocenylated ssDNA hybridises to the target sequence between the two primers, see Figure 4.2, during the annealing stage of PCR. During the PCR extension, the *Taq* polymerase extends the primer, digests and removes the ferrocenylated DNA due to the polymerase activity of the enzyme. Ferrocene is released into free solution where it can be detected electrochemically. On release into the solution, the ferrocene undergoes a change in ionic environment. This change in environment comes about because the positional and chemical environments have changed and therefore the number and distribution of the electrical charge surrounding the ferrocene molecule have also changed. As the distribution of the electrons in the molecule change, the molecular orbitals change and therefore the energy needed to oxidise the molecule differs between the two chemical states of the ferrocene. This change in oxidation energy can be equated to a change in potential required (or electrochemical work) to oxidise the ferrocene.

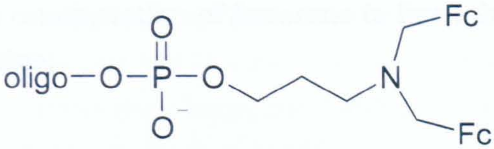

Figure 4.1: Diagram shows two ferrocene moieties (Fc) attached to a oligonucleotide.

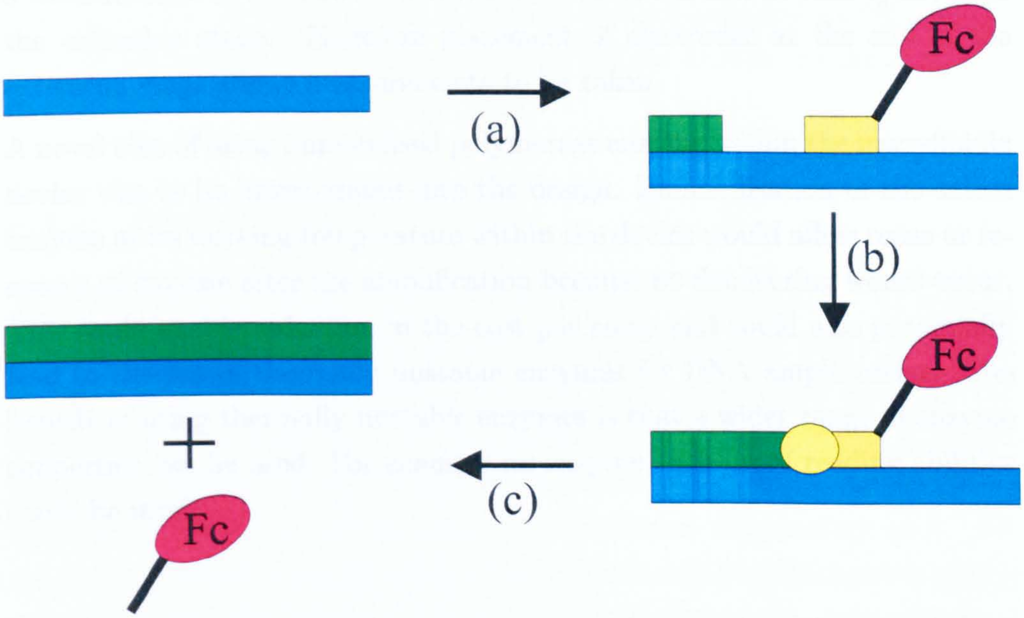

Figure 4.2: Schematic of the ferrocene electrochemical assay for the real-time monitoring of PCR: (a) primer and detection probe ssDNA are annealed to the template during the annealing stage (60°C) of the PCR; (b) enzyme extends the primer and digests the probe strand by polymerase activity; (c) the complete PCR cycle results in amplified template being formed along with free ferrocene. This ferrocene can then be interrogated electrochemically and a measurement of the amount of amplification can be undertaken.

As the oxidation potential is different, between the ferrocene attached to the DNA and free ferrocene, the free ferrocene can be directly detected without interference from the attached ferrocene. The recorded current is directly proportional to the concentration of ferrocene in free solution and hence the degree of amplification.

4.2.3 Considerations in the Designing of PCR Microfluidic Devices

In order to realise real-time electrochemical monitoring of the PCR reaction a measurement of the free ferrocene is desired at the end of each cycle, after the extension stage. Therefore placement of electrodes at the end of the extension stage allows measurements to be taken.

A novel idea of using immobilised polymerase enzyme within the microfluidic device was to be incorporated into the design. Immobilisation of the active enzyme at its working temperature within the device would allow reuse or recovery of enzyme after the amplification because no denaturing would occur. This could enable reduction in the cost per assay and could also potentially lead to the use of thermally unstable enzymes for DNA amplification. The benefit of using thermally unstable enzymes is that a wider range of enzyme properties can be used. For example an enzyme with proof reading abilities could be used.

4.3 Designing of Device

In this section, the design of a number microfluidic devices are presented, together with the motivation and reasoning behind each device.

4.3.1 Fulfilling Basic Requirements

The separation of the device into three distinct temperature zones enables the immobilisation or retention of the polymerase enzyme within its optimum working temperature. This can not be achieved with conventional thermal cyclers. This enables the enzyme to remain at its optimum working temperature, stopping the enzyme from being deactivated at high temperatures and potentially allowing its reuse. Such a design may also enable the possible use of thermally unstable polymerases. With the device being divided into three different temperature zones, the reaction mixture, as a microfluidic sample, needs to be transported between the zones to cycle the reaction. Three basic concepts were considered: a flow-through device; a linear device; and a cyclic triangle device. As there needed to be three distinct temperature regions, the possible placement of the electrodes either within or close to the extension temperature zone, becomes easy.

4.3.2 Flow-Through Device

The first method of using three temperature zones was to have one channel crossing over each of the temperature zones, as previously demonstrated in the literature,[57,58,59,60] see Figure 4.3. For each cycle of the reaction, the channel needs to cross the three temperature zones. The number of cycles possible is defined during the fabrication of the device. This design allows immobilisation of the enzyme within the extension temperature zone. After each extension zone, an electrochemical cell can be fabricated enabling simple real-time detection. As each cycle is completed, an electrochemical measurement can be taken in relation to the number of cycles run. Practically an electrochemical cell after every cell is not needed. Only after about 20 cycles will number of templates be high enough to be detected. After that a number of electrochemical cells could be spaced out throughout the cycles remaining.

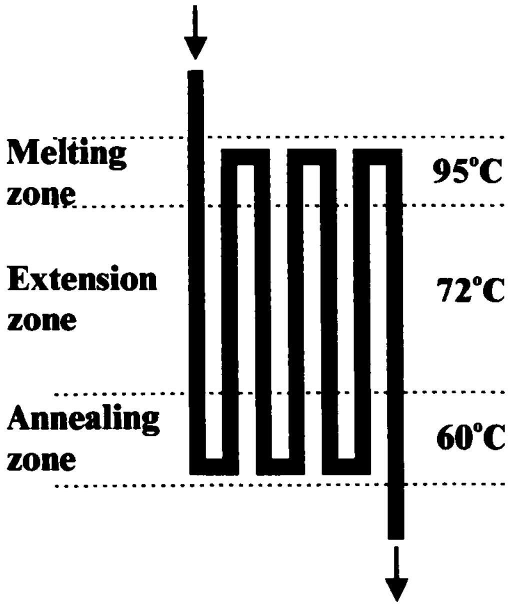

Figure 4.3: A stylized representation of the basic design for the flow through PCR device. This diagram shows a single channel crossing the three temperature zones to form the cycles. Direction of flow is shown by the arrows.

4.3.2.1 Physical Dimensions

With this particular design, there are several variables that need to be considered before fabrication. Firstly, the number of cycles for the reaction. Within a flow-through design, the channel physically crosses each of the temperature zones completing a cycle. As such, the number of cycles are prescribed at the design and fabrication stage. Conventional PCR experiments generally use 35 cycles.[130] Efficiency of the reaction decreases after 35 cycles[130] due to the enzyme being denatured after a number of high temperature stages. Also the primer concentration falls with each cycle and the chance of enzyme coming in to contact with a hybridised primer and target decreases. Therefore using this number should enable reasonable amplification to be obtained.

Consequently, as the number of cycles is physically defined within the device, the ratio of duration times between the three steps of the cycle are also physically determined. In conventional protocols for PCR, annealing and extension takes twice as long as the melting stage. Therefore the selected ratio of times for melting:annealing:extension was 1:2:2 in channel length which relates to the "dwell" time.

With the relative times within each temperature zone having been defined, the actual length of time at each zone should be considered. The time taken to melt the dsDNA, anneal the primers and finally, extend the primer must be considered. Also a consideration of the time taken for an aqueous solution to reach the same temperature as the surrounding temperature zone.

In considering the time taken at each step of the cycle only the extension time needs to be considered because the relative stage times have already been prescribed. The average speed of incorporation for *Taq* polymerase is 65-100 nucleotides a second.[160,161] From this, a dwell time of 4s was needed for target strand of 350bp. Using dimensions constrained on the device by actual physical size of the heaters gave a volume of 30nl, with a square cross sectional area of 50μm sides, for the 4s required.

The time taken for water within a microchannel to reach the desired temperature was investigated by simple simulation. To investigate the time taken for flowing water, entering at room temperature, to reach the desired temperature within a microchannel, one surface was held at constant temperature and the water temperature modelled, see Figure 4.4. Modelling was done using Femlab (Comsol ltd, London, UK) using its chemical:convection and conduction and incompressible Navier-Stokes flow modes. From this simulation it was demonstrated that the time taken for the fluid to reach the desired temperature was negligible. This could be tested experimentally using fluids where the colour is dependant on the temperature. Showing sharp changes in colour when the transistion is made.

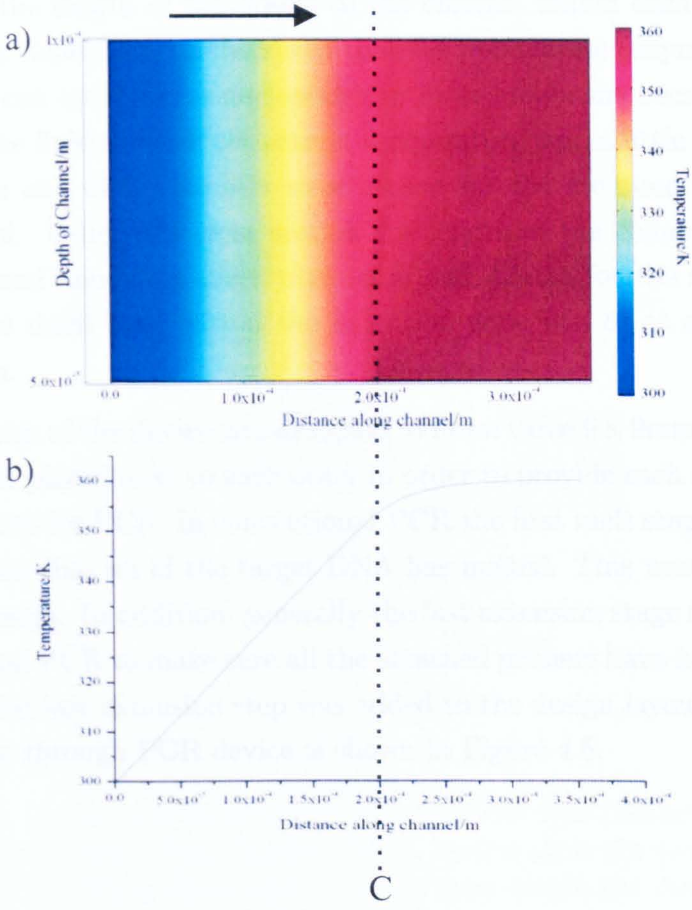

Figure 4.4: Results of simulation a 50μm deep channel, in silicon covered in PDMS, filled with water in Femlab (Comsol Ltd, London, UK) using chemical: convection and conduction and incompressible Navier-Strokes packages. The model was drawn as a 2.2mm long channel (only the first 0.35mm are shown here, with water flowing from left to right, direction of the arrow, at 1μl/min entering at a temperature of 300K). At the dotted line, marked C, the bottom edge of the channel was held at 360K within the model, to represent the device sitting on top of a heater. The physical parameters used for water were ρ 1, Cp 4.2 J/g K, K 0.6W/K m, η 0.001Pa s.
Figure 4.4(a) shows the temperature as a coloured surface across the channel; (b) shows the temperature change as a cross section through the middle of the channel, 25μm deep.

Therefore the length of the design of the channel within each temperature zone is only dependant on the speed that the polymerase enzyme (at a given flow rate) can incorporate nucleotides to form amplicons because the time taken for the fluid to reach the correct temperature was as little as a ~100ms. 50μm wide and deep channels were chosen for the cross-section profile of the channel. Using this cross section the length of the channel within the extension and annealing stage were 9mm and 4.5mm for the melting stage so that the dwell time within the extension zone was 8s at a flow rate of 0.25μl/min.

The footprint of the device was designed to fit on three 9 x 9mm Peltier effect heat pumps placed next to each other in order to provide each of the desired temperatures for PCR. In conventional PCR the first melt stage is extended to guarantee that all of the target DNA has melted. This was incorporated into the design. In addition, generally the last extension stage is extended in conventional PCR to make sure all the attached primers have been extended. An extended last extension step was added to the design layout. The design of this flow-through PCR device is shown in Figure 4.5.

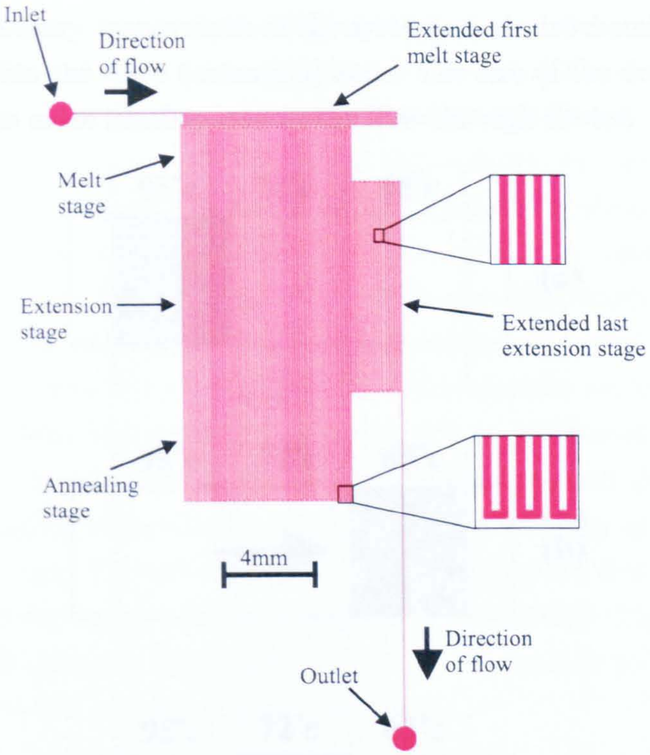
Inlet
Direction of flow
Extended first melt stage
Melt stage
Extension stage
Extended last extension stage
Annealing stage
4mm
Direction of flow
Outlet

Figure 4.5: A diagram showing the layout of the flow-through device from the design software L-Edit (Tanner EDA). Inserts show the parallel channels 50μm wide and 50μm apart and the turns used within the channel.

4.3.3 Linear Device

An alternative device layout was a linear device. This "straight line" device consisted of the three temperature zones but instead of one channel repeatedly crossing the temperature zones, there was one large channel across all three temperature zones, see Figure 4.6. A plug of sample of PCR reactants is flowed across each of the temperature zones repeatedly to cycle the sample. This allows the dwell time at each temperature to be controlled independently of the other temperature zones and the number of cycles to be adjusted, accordingly. As the three different temperature zones are defined, the enzyme could still be immobilised within the extension zone. In addition, to fulfill the sensory requirement of the system an electrochemical cell could be placed within the same (extension) zone. The size of the device was such that it had the same heating area as the flow-through device.

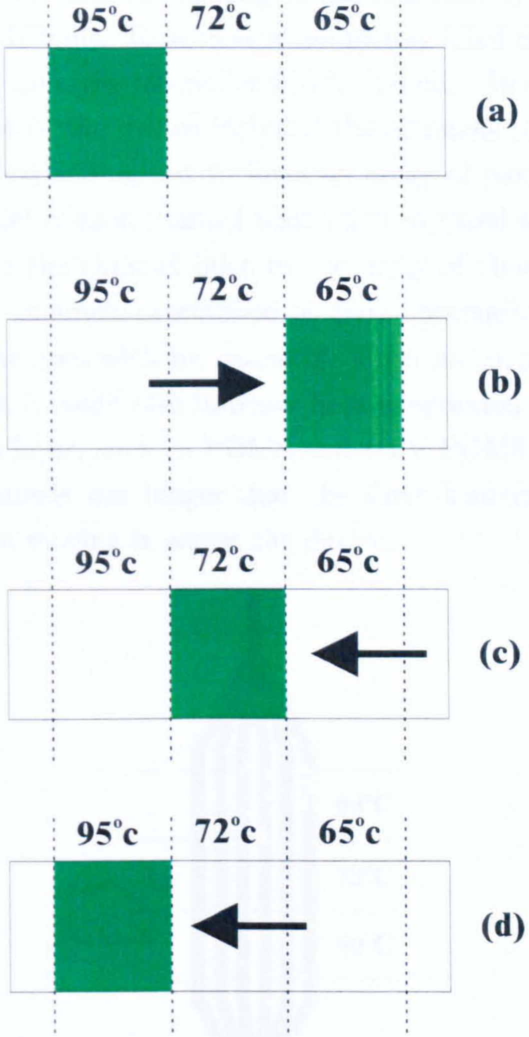

Figure 4.6: A illustration of how a cycle is completed within the linear PCR device: (a) melt stage, the reaction plug lies within the first zone; (b) the plug is moved to the annealing stage passing through the 72°C zone; (c) plug moved back into the extension temperature zone; (d) and finally the cycle is completed by moving the reaction plug in to the melt zone.

Filling such a large volume from smaller inlets proves, from previous experience, to be difficult. Fluid entering a wide channel finds the path of least resistance through, and often does not fill the channel completely. With an incompletely filled channel the cycling of the reaction, by movement of the plug, would prove difficult. To achieve a completely filled channel, the device was designed to be an array of smaller width channels. In order to fill all the channels the layout of the device included the channels starting at a single inlet channel and expanding out to form an array of parallel channels, see Figure 4.7. The inlet of each channel width was adjusted so that the volume was the same from the channel inlet to the array of channels independent of the angle. The channels overlapped as they approached the centre producing a triangular area with no channels. Such an array of channels has the advantage that it could also improve heat conduction into the fluid and support a soft top layer, such as PDMS and RTV PDMS. The total length of the parallel channels was longer than the three heaters to help hold the plug together when moving it across the device.

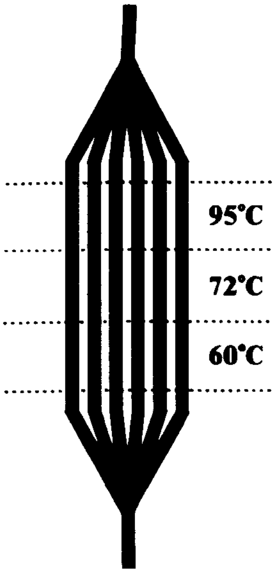

Figure 4.7: Schematic of the linear design PCR microfluidic device. The array of channels crossing the three temperature zones enables a plug of reaction mixture to be flowed backwards and forwards to cycle the reaction.

4.3.4 Cyclic Triangle Device

An improvement on the linear device was that of a cyclic triangle device. In this design, each side of the triangle was held at one of the three temperatures used within the cycle. A plug of PCR mixture flows around the triangle to cycle through the reaction temperatures, see Figure 4.8. The reaction plug was flowed from one zone to another, after being held for the correct length of time at each temperature. This design gives independent dwell times within each temperature zone as fluid was not continuously flowing around the triangle. Again with the separate temperature zones, the immobilisation of the enzyme within its working temperature was possible. The advantage of using a cyclic triangle shape rather than the straight line device was that the PCR reactants were cycled directly from the one temperature stage to the next. This has the advantage of limiting the non-specific annealing of the primers. If the temperature is high enough, the primers can incorrectly hybridise to the wrong sequence in the template leading to non-specific hybridisation. If the temperature is quickly lowered, the possibility of non-specific hybridisation occurring is minimised and therefore the reaction would have a higher fidelity.

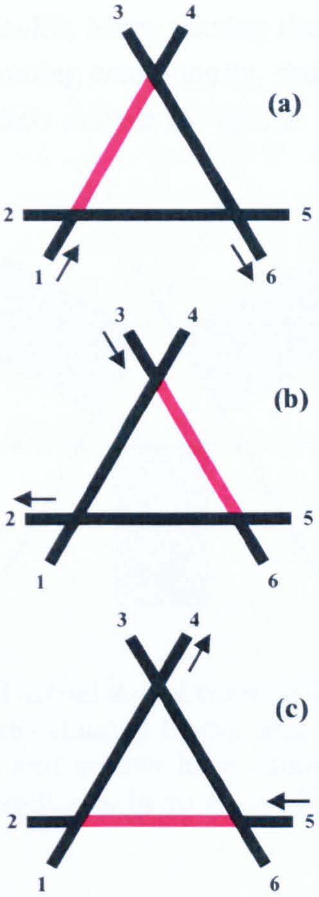

Figure 4.8: An illustration of how a plug of PCR mixture was moved within the triangle device: (a) the plug in one side of triangle starts the cycle, and was moved onto the next side by applying pressure at inlet 1 (with outlet 6 opened to atmosphere); (b) the plug within the second temperature zone was moved onto next stage by pressure being applied along inlet 3 (with outlet 2 opened); (c) to finish the cycle, the plug was flowed back to its starting position by applying pressure to inlet 5 (outlet 4 opened).

The layout of this device consisted of a "triangle" with two channels at each apex to flow the plug around the device, see Figure 4.9. In order to increase the volume of the plug, each side of the triangle was arranged into a serpentine channel to increase its length and therefore the volume, see Figure 4.9. Using inlet and outlet valves, a different side could be opened and the bulk fluid moved in and out of the device, hence moving the reaction plug around the device. With the pump running continuously, changing the positions of the two valves made the plug flow around the device.

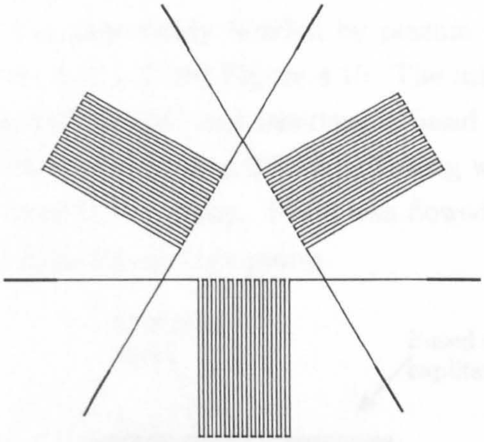

Figure 4.9: The design and actual size of triangle device showing the radiator like channels to increase the channel length and therefore the plug volume within the device. Inlets and outlets have enlarged channels to allow the insertion of fused silica capillaries in to the etched silicon without tearing the PDMS cover.

4.4 Fabrication of PCR Devices

All three devices where fabricated using micro-fabrication methods. The general procedures used are discussed in Chapter 2.

4.4.1 Flow Through Device

Several materials for the flow through device were investigated, including silicon and PDMS (Section 4.4.1.1), glass and RTV PDMS (Section 4.4.1.2) and silicon and glass (Section 4.4.1.3), with the procedures described in Chapter 2.

4.4.1.1 Silicon and PDMS

The microfluidic channel was first etched, 50μm deep, using an ICP STS dry etch machine see Section 2.3.7, in a silicon wafer and a thin, ~500μm thick, PDMS layer was irreversibly bonded by plasma oxidation to enclose the device, see Section 2.3.11.2 and Figure 4.10. The inlets and outlets were made by opening up the channel and inserting a fused silica capillary then sealing with RTV PDMS, see Section 2.3.12.1. Tubing was directly attached to the capillary to connect the pump. Fluid was flowed through the device by positive pressure from the syringe pump.

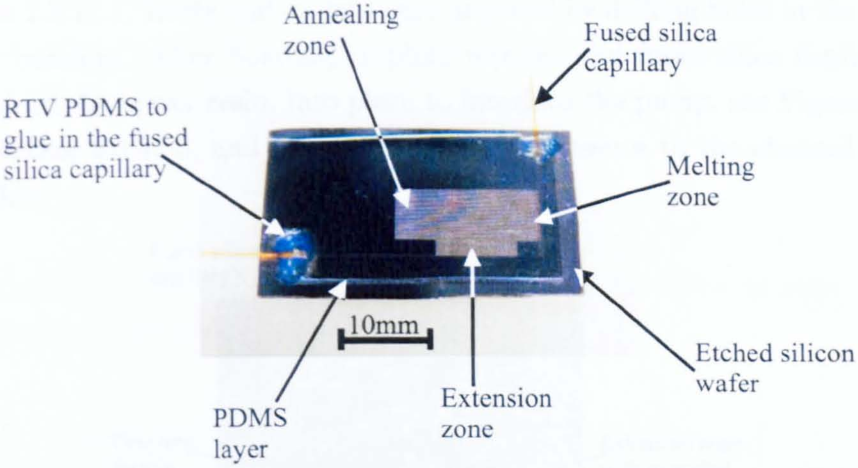
Annealing zone
Fused silica capillary
RTV PDMS to glue in the fused silica capillary
Melting zone
10mm
Etched silicon wafer
Extension zone
PDMS layer

Figure 4.10: A photograph of the flow through PCR device fabricated using an etched silicon wafer with a 500μm thick layer of PDMS. The PDMS was irreversibly bonded using oxygen plasma and the fused silica capillary inserted into the channel.

4.4.1.2 Glass and RTV PDMS

A channel was moulded in RTV PDMS around a re-soluble photoresist, AZ 4562, mould. Photoresist was spun on to glass cover slips, see Section 2.2, to a thickness of 30μm. Cover slips were used for improved thermal conduction over thicker glass slides. RTV PDMS was poured over this photoresist, forming a layer ~500μm, and cured (RTV PDMS and PDMS spread out until, if allowed, it is a minimum thickness of $\sim 500\mu m$ when poured, due to molecular interactions). Opening the end of the channel allowed the photoresist to be dissolved using ethanol, see Section 2.3.10.2, leaving an open channel, and for the insertion and gluing of a fused silica capillary with RTV PDMS, see Section 2.3.12.4.

4.4.1.3 Silicon and Glass

An etched silicon channel, STS ICP to a depth of $50\mu m$, was enclosed with Pyrex glass. The glass was bonded to the silicon by anodic bonding, see Section 2.3.11.1. Inlets and outlets were included by drilling holes in the glass before bonding. After bonding graphite ferrules and fused silica capillaries were glued, by epoxy resin, into place to interface the pump, see Figure 4.11 and Section 2.3.12.3, and to apply a positive pressure to the channel from fluid flow.

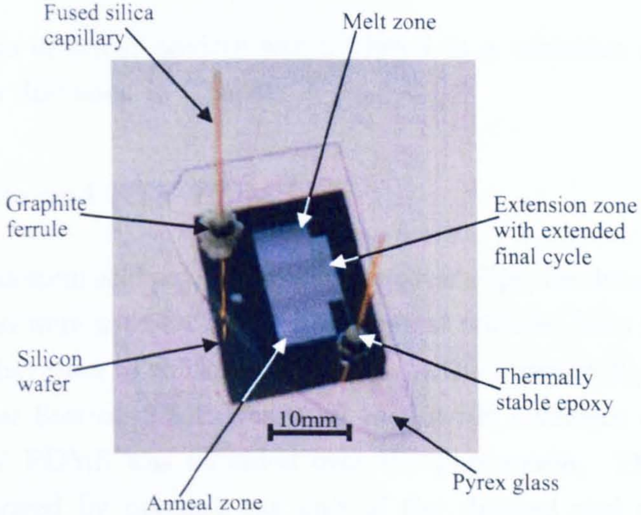
Fused silica capillary
Melt zone
Graphite ferrule
Extension zone with extended final cycle
Silicon wafer
Thermally stable epoxy
10mm
Pyrex glass
Anneal zone

Figure 4.11: A Photograph of a flow-through device fabricated on a silicon wafer. The channel was etched in silicon, and a glass top layer, which was anodically bonded. The inlet and outlet were formed from fused silica capillaries and graphite ferrules.

4.4.1.4 Surface Passivation

In order to stop the non-specific adsorption of the template and the enzyme to the insides of the channel, the sides of the channel were coated in bovine serum albumin (BSA) (Sigma-Aldrich, Poole, Dorset, UK). The BSA non-specifically binds to the surface of the channel, occupying the available absorption sites and minimizing DNA and enzymes from attaching to the surface. Devices made as described in Sections 4.4.1.1 and 4.4.1.3 had the channel surface passivated with BSA. This was achieved by flowing 1% BSA solution in deionised water through the device for 30-60min and then allowing it to stand overnight at 4°C. The channels were then thoroughly rinsed with deionised water. After the channel surface had been coated, the devices were stored at 4°C.

4.4.2 Linear Device

The fabrication of linear devices was achieved in a variation of ways using the techniques discussed in Chapter 2.

4.4.2.1 Glass and RTV PDMS

Photoresist was spun and patterned on glass cover slips, for details see Section 2.2. Cover slips were used for more effective heat transfer from the heaters to the device rather than to thicker glass slides. A thickness of 30μm of AZ4562 photoresist, see Section 2.3.4, was used to provide sufficient depth for the channel. RTV PDMS was moulded over the photoresist. The photoresist was then removed by opening the end of the channel and dissolving the photoresist with ethanol. Fused silica capillaries were inserted to form the inlets and outlets and glued in place with RTV PDMS, see Figures 4.12 and 4.13.

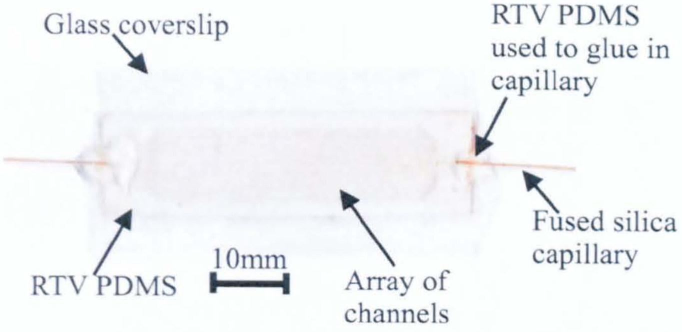
Glass coverslip
RTV PDMS used to glue in capillary
Fused silica capillary
RTV PDMS
10mm
Array of channels

Figure 4.12: Photograph of the complete linear device fabricated by moulding RTV PDMS on patterned 30μm thick photoresist.

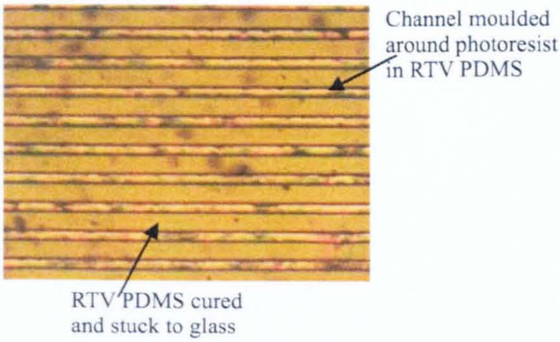
Channel moulded around photoresist in RTV PDMS
RTV PDMS cured and stuck to glass

Figure 4.13: A photograph of the channel array moulded in RTV PDMS by photoresist. The uneven nature of the photoresist can be seen by the change in colours in the channel surface. The uneven nature of the photoresist is due to spinning of the photoresist on top of photoresist, so the surface is considerably less smooth and flat than normal.

4.4.2.2 Silicon and PDMS

The device was constructed by etching the structure in a silicon wafer, using a STS ICP to a depth of 50μm, see Section 2.3.7 and covering the channels with a PDMS layer, $\sim$500μm thick, and irreversibly bonding the layers together using oxygen plasma bonding, see Section 2.3.11.2. Inlets and outlets were formed by insertion of fused silica capillaries, see Section 2.3.12.1, and glued in place using RTV PDMS, see Figure 4.15.

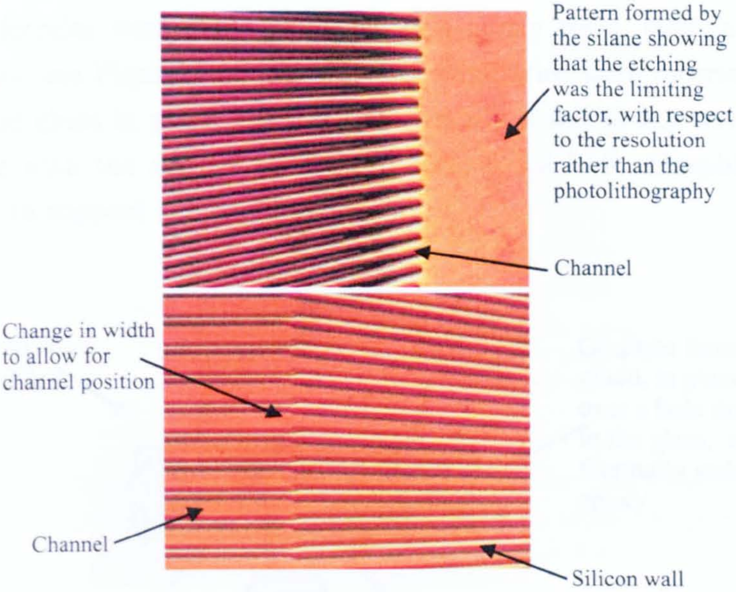
Pattern formed by the silane showing that the etching was the limiting factor, with respect to the resolution rather than the photolithography
Channel
Change in width to allow for channel position
Channel
Silicon wall

Figure 4.14: Photographs of the linear device etched in silicon, showing the precise etching gained using the STS ICP. This device was covered with a PDMS layer, bonded after O_2 plasma activation.

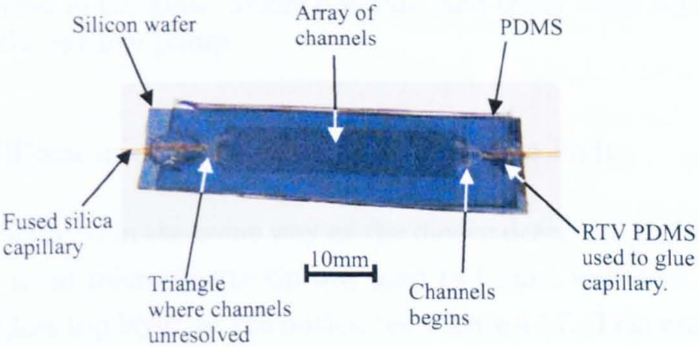
Silicon wafer
Array of channels
PDMS
Fused silica capillary
Triangle where channels unresolved
10mm
Channels begins
RTV PDMS used to glue capillary.

Figure 4.15: A photograph of the complete linear device fabricated with an etched silicon wafer and PDMS cover.

4.4.2.3 Silicon and Glass

Channels were etched in silicon, 50μm deep, and the device was completed by anodic bonding, see Sections 2.3.7 and 2.3.11.1, of 500μm thick Pyrex glass.

Graphite ferrules were glued in place, with epoxy resin, over holes drilled in the glass, see Figure 4.16. Fused silica capillaries were inserted into the ferrules and glued in place, again with thermally stable epoxy resin, to allow interfacing with the syringe pump, see Section 2.3.12.3. Graphite ferrules were used to support the capillaries.

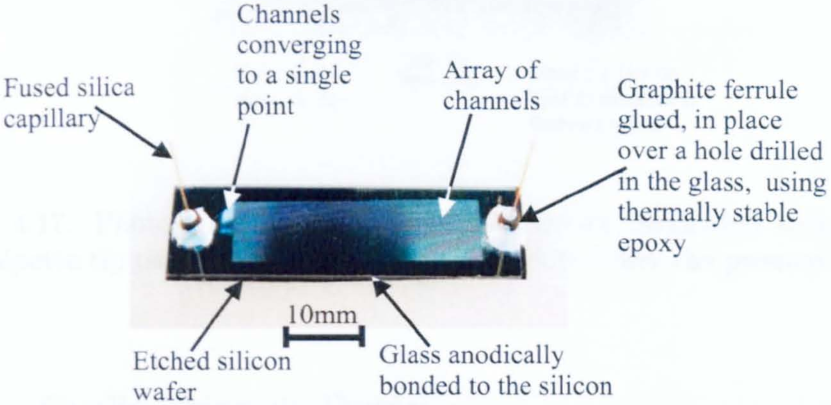
Fused silica capillary
Channels converging to a single point
Array of channels
Graphite ferrule glued, in place over a hole drilled in the glass, using thermally stable epoxy
10mm
Etched silicon wafer
Glass anodically bonded to the silicon

Figure 4.16: A photograph of the straight line device fabricated by anodically bonding Pyrex glass to etched silicon wafer. The inlet and outlet are formed by drilling holes in the glass, before bonding, and using fused silica capillaries to connect the syringe pump.

4.4.2.4 Silicon and Glass with Low Pressure Exit

This was fabricated in the same way as the device described in Section 4.4.2.3 except that a cut micropipette tip was used to form a well over a pre-drilled hole in the glass top layer, at the outlet, see Figure 4.17. This was to promote flow through the device by not restricting the fluid leaving the device, (not forcing it back into a capillary but in to a reservoir of bulk fluid). The inlets were interfaced with fused silica capillaries and graphite ferrules, which were glued over holes in the glass with epoxy resin.

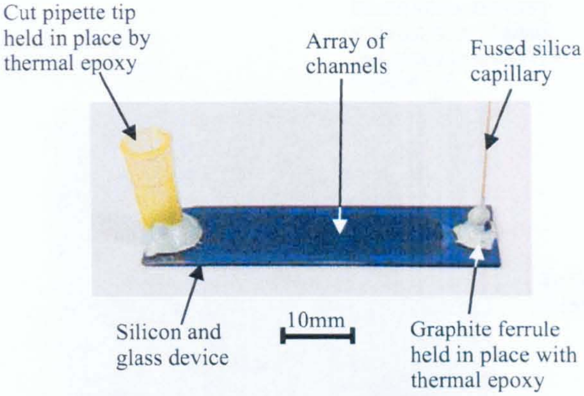
Cut pipette tip held in place by thermal epoxy
Array of channels
Fused silica capillary
Silicon and glass device
10mm
Graphite ferrule held in place with thermal epoxy

Figure 4.17: Photograph of the straight line device fabricated with a cut micropipette tip to form a reservoir at the outlet to lower the pressure at the outlet.

4.4.3 Cyclic Triangle Device

The cyclic triangle device was fabricated by etching silicon wafers using a STS ICP machine, to a depth of 50μm with an etch rate of 4.4μm/min, as described in Section 2.3.7. A lid of $\sim500\mu$m thick PDMS was bonded by plasma oxidation in a STS ICP, see Section 2.3.11.2. Inlets and outlets were formed by insertion of a fused silica capillary in to opened channels and sealed with RTV PDMS, see Section 2.3.12.1 and see Figure 4.18. Microtight adaptors (Upchurch Scientific, WA, USA) were used to link the capillaries to PTFE tubing to allow the interfacing of a pump to the system.

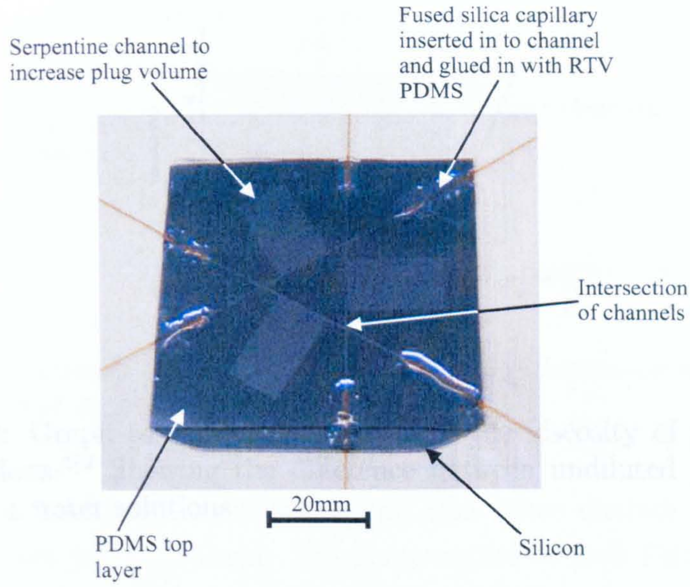
Serpentine channel to increase plug volume
Fused silica capillary inserted in to channel and glued in with RTV PDMS
Intersection of channels
20mm
PDMS top layer
Silicon

Figure 4.18: Photograph of the cyclic triangle device which was fabricated from etched silicon and oxygen plasma bonded PDMS top layer. Inlets and outlets formed by insertion of fused silica capillaries and glued in place by RTV PDMS.

To control fluid flow, two manual valves were used (Omnifit, Cambridge, UK). The inlet valve was a four-way valve. Three outlets from the valve were connected to the three inlets and one to a bulk fluid reservoir. The syringe pump was connected to the inlet valve. The outlet valve was a three-way valve with the outlets of the device connected to it and the outflow of the valve being connected to a bulk fluid reservoir. In order to move the reaction plug within the device, the correct outlet of the device was opened to the reservoir, see Figure 4.8.

In order to form the plug and to pressurise the device, it was completely filled with either a light clear mineral oil or glycerol. Glycerol was diluted with water to adjust the viscosity of the bulk solution. These dilutions of glycerol:water ranged from no dilution to 1 : 1 (the viscosity of the glycerol water solutions vary greatly, see Figure 4.19).

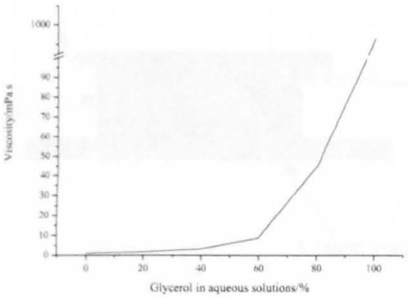

Figure 4.19: Graph to show the variation of the viscosity of glycerol and water solutions.[162] Showing the difference between undiluted glycerol and 1:1 glycerol : water solutions.

4.4.4 Heaters

Peltier heat pumps were used to produce three thermally distinct areas. For each temperature zone, there was a separate Peltier element each with its own temperature controller. The Peltier heat pumps (Melcor, NJ, USA) were 9mm by 9mm, using 17 Peltier couples, with output of 2.4W at 2V and maximum current of 2.1A. The Peltier controllers used were integrated miniature peltier controllers (Hytek microsystems, NV, USA). The temperature was controlled by using a feedback thermistor, with the controller comparing the resistance of the thermistor to an external resistor using an integrated Wheatstone bridge. The external resistor was set to be equal to the resistance of the thermistor at the desired temperature.

The Peltiers were mounted, with thermally conductive epoxy (TBS, Electrolube, Swadlincote, UK), on a flat copper 5 x 5cm square and the thermistors were positioned along side the top of the Peltier heat pump, against the hot side. When the device was placed on to the peltiers the thermistors were in contact with the peltier and the device at the same time with heat sink ensuring good thermal contact, see Figure 4.20.

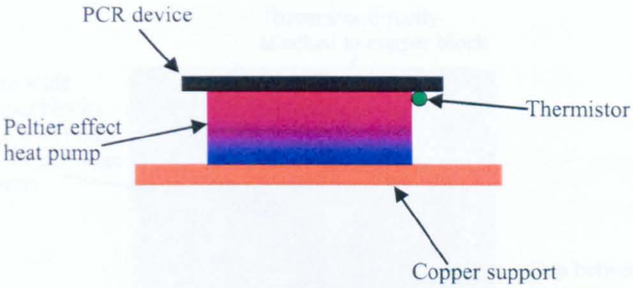

Figure 4.20: Illustration of the positioning of the thermistor in relation to the Peltier effect heat pump and the PCR device.

In using this configuration, it was found that three distinct temperature zones could not be maintained. The temperature of each Peltier could be maintained when operating on its own. When all three Peltier heat pumps were working the system became unstable (the controllers where unable to stabilise the individual Peltiers).

In order to produce a stable temperature profile the Peltier effect heat pumps and controllers were replaced with cartridge heaters and controllers which switched solid state relays to switch the heaters on and off. The cartridge heaters (Hawco, Surrey, UK) were 12V 18W with dimensions of 1" long with a diameter of 0.25". The cartridge heaters were inserted into machined copper blocks which had a hole drilled in to the middle to fit the heaters tightly. The copper blocks were 9mm square and 30mm in length. Each copper block was mounted on a heat sink with thermally conductive epoxy (TBS, Electrolube, Swadlincote, UK). The heat sinks were 9mm across and 30mm in length. To align the three individual copper blocks, each was mounted onto a larger heat sink. A gap of just under 1mm was left between the separate blocks, see Figure 4.21.

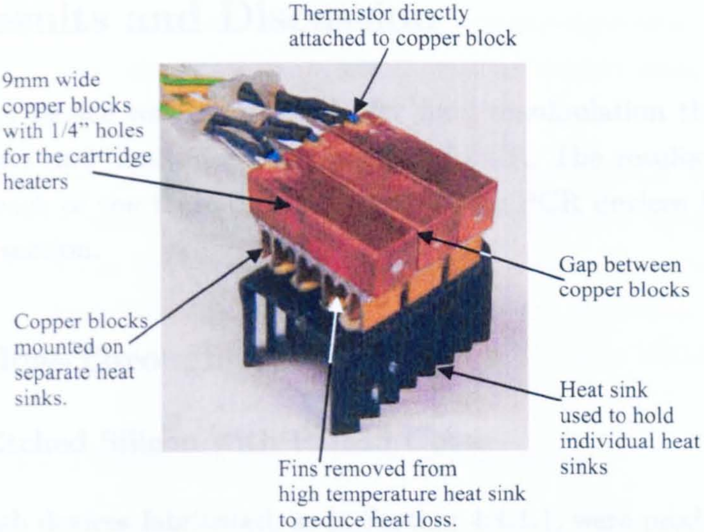
Thermistor directly attached to copper block
9mm wide copper blocks with 1/4" holes for the cartridge heaters
Gap between copper blocks
Copper blocks mounted on separate heat sinks.
Heat sink used to hold individual heat sinks
Fins removed from high temperature heat sink to reduce heat loss.

Figure 4.21: Photograph of the cartridge heaters and heat sink setup.

The temperature of each block was controlled by a separate controller (Cal Controls, Hertfordshire, UK). Each controller controlled the cartridge heaters by using a solid state relay with feedback provided from a 2 x 2.3mm PT100 sensor (RS components Ltd, Corby, Northamptonshire, UK) glued to the blocks. The controllers were calibrated using a digital thermometer placed firstly on the copper block and then on a silicon wafer attached to the blocks with heat sink paste.

In order to maintain each temperature zone at the correct temperature a small fan was used to blow air across the heat sinks. Air was blown from the lower temperature side to the hotter side of the device. Also to assist in the regulation of the temperature, the heat sink for the high temperature block had every other fin removed to reduce the efficiency of the heat loss, thereby reducing the work load for the cartridge heater, see Figure 4.21.

4.5 Results and Discussion

Each type of device was tested fristly for fluid manipulation then thermal characteristics and finally for optimisation of PCR. The results and development of each of the three different microfluidic PCR devices is discussed within this section.

4.5.1 Flow-Through Device

4.5.1.1 Etched Silicon with PDMS Cover

Flow-through devices fabricated, as in Section 4.4.1.1, were produced by using an etched silicon channel and a PDMS "cover" and were used first for PCR experiments. Each temperature zone was confirmed to be held at the correct temperature, achieved using a digital thermometer with a small (1.5mm diameter) thermocouple placed underneath an unbonded layer of PDMS. Each individual temperature zone was held at its separate temperature. The stability of the system was most likely to have come from the differences of the thermal masses of the heaters compared to the device. The copper blocks contain a larger thermal mass than the device, so regulation of the blocks was enough to maintain the device at the correct temperature.

With the correct temperatures established across the device, fluid was flowed (at a flow rate of 0.5μl/min) into the device. When using the device, the channel towards the distant end of the device would clear of water in places. Sections of the channel would appear to be empty, these sections would move through the channel being pushed by the fluid behind. The volume of the sample collected at the outlet was less than the volume pushed into the channel. The difference between the collected and injected volumes varied but was as little as 50% collected. The observations of the empty channel and the difference in injected and collected volumes implies that the fluid was evaporating within the channel. The fluid could have been "out-gassing" although the fluids were degassed under vacuum before the initiation of the experimental run. In addition, it was unlikely that significant "out-gassing" would occur as the device was operated under positive pressure with fluids being pumped through rather than being pulled through using a negative pressure.

The water evaporating was unexpected because the channel was full and under a constant pressure. The evaporation only happened towards the end of the channel when the pressure drop was less compared to the beginning of the device. Also it was possible that room for the expansion of the fluid to form a vapour was made possible by stretching the thin PDMS layer.

4.5.1.2 RTV PDMS Moulded Over Photoresist

In order to reduce the thickness of the top layer of the device, moulding of RTV PDMS over a photoresist mask was attempted, as described in Section 4.4.1.2. By moulding over the photoresist the channel will be closer to the surface even if the RTV PDMS is the same thickness as the PDMS over the rest of the device. Using a thinner layer should improve the thermal characteristics of the device. Due to the large number of turns and the length of channel it proved impossible to completely clear the photoresist from the channel. Photoresist tended to pool together within the device lifting the PDMS off the glass cover slip, see Figure 4.22. This re-solvated photoresist could be forced out of the device but the delicate nature of the fabricated cycles were compromised in the process.

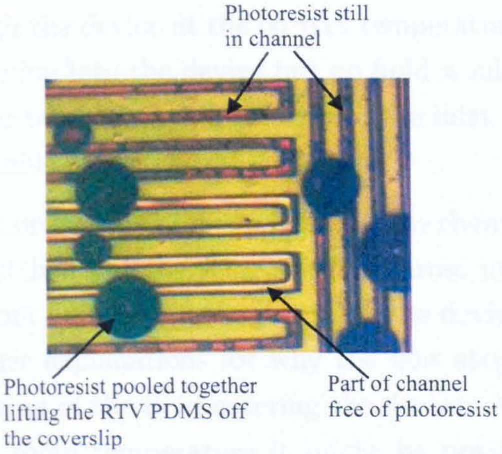
Photoresist still in channel
Photoresist pooled together lifting the RTV PDMS off the coverslip
Part of channel free of photoresist

Figure 4.22: Photograph of a flow through device fabricated by moulding RTV PDMS on a photoresist mould. The channel did not clear of photoresist in some parts, whilst has been cleared in others depending on the amount the photoresist that had pooled together.

4.5.1.3 Etched Silicon with Glass Cover

Changing the top layer of the device from PDMS to glass was used to eliminate the possibility of the PDMS stretching to allow the expansion of water to form a vapour. A further advantage of using a glass cover was the improved heat transfer through the glass to the atmosphere, so helping to maintain the temperature of each zone. The same problem occurred within this device as in the device fabricated with a layer of PDMS. Water towards the distant end of the channel would evaporate within the channel (an observation which demonstrates that the PDMS in the thin layer device may not have been stretching to allow the evaporation). Increasing the flow rate through the device from 0.5μl/min to 0.75μl/min stopped the water evaporating in the latter part of the channel (the pressure within the channel increases as the flow rate increases, and this increase in pressure was enough to stop the liquid evaporating in the channel).

A further problem became apparent, the device quickly heated up and the water remained as a liquid within the channel. At this point, water would stop flowing through the device at the correct temperature. The fluid would be continuously flowing into the device but no fluid would be flowing out of it. Eventually water would escape from around the inlet (as the seal formed by the thermally stable epoxy broke).

A possible explanation for this problem was that the channel could have been blocked or poorly etched but the same situation arose in all devices. As all devices suffered, from fluid not flowing through the device, this explanation was excluded. Other explanations for why the flow stopped are concerned with the rapid heating of the fluid entering the device. As water was flowed into the device at room temperature it might be possible that the rapid heating of the water to 95°C stopped the flow within the device. The quick expansion of the water on heating might have caused the water to stop itself from flowing. In short, as the fluid expanded it might have flowed back up the capillary inlet, as this may of provided an easier route than flowing in to the smaller cross-section area, higher back pressure, of the channel. Water could have tried to flow out at the inlet against the flow which might of been enough to stop the flow into the channel. This might of been the situation until the seal around the inlet failed. This hypothesis would seem unlikely but as the problem only occurred when the device was at the working temperatures, the reason for the problem must be related to the elevated temperatures employed.

The evaporation of fluids within the last part of the channel was solved by increasing the flow rate through the device. When the device was being heated, to form the three distinct temperature zones, the flow through the device would still stop. This problem remained unsolved. Successful PCR was not carried out using the flow-through device due to the flow stopping after the device reached the correct temperatures.

4.5.2 Linear Device

Microfluidic linear PCR devices were fabricated as described in Section 4.4.2. Several problems, were identified, which prevented these devices from being used for PCR. All the different methods of fabricating the linear device encountered the same problem when used. Filling the device to leave a plug of water uniformly within the parallel channels proved to be impossible. In order to form a plug of reaction mixture, the devices were completely filled with light mineral oil first. Water was flowed in to the device displacing the oil to form a plug.

When the water flowed into the devices, it did not flow into all the channels forming a plug across the device. What happened to the water once in the device depended on the method of fabrication, but the overall outcome was the same for all types of device and therefore prevented successful PCR.

4.5.2.1 RTV PDMS Device

The water, when flowed into devices moulded in RTV PDMS, pooled in the triangular shaped area of the device. The water flowed easily into the triangular section but then would not flow into the channel array. As the water pooled, the PDMS stretched. However once stretched the PDMS did not regain its original size or shape. The PDMS stretched until the seal around the inlet broke. Linear devices fabricated by moulding PDMS around a photoresist mould were never used to run PCR experiments.

4.5.2.2 Etched Silicon with PDMS

When water flowed into the devices it did one of two things. It either pooled in the triangular area or, alternatively, the middle channels of the array were filled first and then the water flowed straight through the device. The water always filled the triangular area first, and then it either broke the seal around the inlet or moved into a small number of channels and passed completely through, the device. The water would push in to the middle channels, where the force of the flow was highest and once the water was all the way through the middle channels water could easily pass along the device to the outlet whilst the channels at the edge of the array were not filled. With a path of least resistance in place, the water never filled any more of the channels. Therefore a plug of water across the whole of the channel array was never formed. Unfortunatly, due to the problems in forming the plugs, PCR experiments were not carried out in straight line devices fabricated in this way.

4.5.2.3 Etched Silicon with Glass Cover Device

Devices which were fabricated by etching silicon to form the channels and completed with glass covers, as described in Section 4.4.2.3, suffered from the same problem as the silicon and PDMS devices. The water would displace the mineral oil out of the middle channels. Once the middle channels were filled with water, the outer channels would not be filled and therefore no plug across the whole device was formed.

4.5.2.4 Etched Silicon with Glass Cover and Low Pressure Outlet

Devices with a large outlet which allowed the bulk fluid to exit the device with less resistance also failed to form a plug within the device. The reason why a plug was not formed was the same as for the other etched silicon and glass devices. The difference in performance came with the time taken to fill the middle channels compared to the devices with a capillary in the outlet. Devices with less restrictive outlets allowed the middle channels to fill quicker than the devices with capillary outlets but the overall effect was the same, no plug being formed and therefore cycling of PCR was not possible.

4.5.2.5 Overall Performance of the Straight Line Device

The main flaw with this device appeared to come from the fact that a triangular area with no channels was formed in the design. Had all the channels opened up from a single point source, with the width of the channels varying so the volume remains the same, the variation in pressure across the channel array might have been allowed for. If the force at the opening to all the channels was the same, water would have flowed into all the channels at the same time. Consequently a plug would have been formed and could have been flowed backwards and forwards across the temperature zones.

4.5.3 Cyclic Triangle Device

The cyclic triangle device was fabricated using one method, described in Section 4.4.3. As with the linear device a plug of water was to be formed surrounded by a bulk fluid. The triangle was completely filled with light mineral oil. Water was then pumped into one side of the triangle. The force required to flow the water into the device was large enough to break the seals around the inlets and outlets. Using the 1:1 glycerol:water mixture as the bulk fluid, the pump could pump the fluids through the device and still held the pure water (reaction mixture) as a plug.

Water was introduced into the device through the inlet valve. Opening the correct outlet and pumping the water plug in to the device allowed one side of the triangle to be filled. It also partially filled the other side of the triangle, next to the inlet. Attempting to move the plug around the corner on to the next side caused water to flow into the blocked off outlets as well as the next side along. Every time the water plug was moved around the triangle, more of the water would pass into the wrong channel at the corner junctions. Therefore the plug would break up and water would eventually be in every channel.

There are several possible explanations for the break up of the plug at each intersection. One possible reason is that the system, device and valves, might not have been completely filled with the glycerol water mixture. Air bubbles might have formed within the valves or around the capillaries in the inlets and outlets to the device. To eliminate this problem the system was flushed through with the bulk fluid. Clearing the valves of air by opening the valves at all positions and flushing through with the glycerol water mix cleared any air from the valves that might have been causing the break up of the water plug. After extensive flushing the system with the glycerol water solution, the water plug still would break up when passing a corner intersection.

A second possible reason for the splitting up of the plug was that the valves were not forming a good enough seal. This was difficult to test as a change of valve system was needed to assess this hypothesis.

The last possible reason for the break up of the plug was the possible stretching of the PDMS top layer. When pressure from the syringe pump was applied the silicone rubber cover to the channels, could be stretched under the pressure allowing water from the plug to move into channels that were closed off. This would seem to be the most likely reason for the splitting of the plug as it moved around the cyclic triangle device. To eliminate this problem, the cyclic triangle device should have been fabricated using an anodically bonded sheet of Pyrex.

4.6 Conclusion

Three different microfluidic PCR devices were designed and fabricated. Each of the designs utilised three distinct temperature zones. The possible incorporation of immobilised polymerase enzyme and electrochemical cell was taken in to account when the devices were designed and fabricated, including a flow-through device; a linear device; and cyclic triangle device. PCR was not successfully carried out in any of the three types of device for technical reasons. Each device had insurmountable problems which prevented them from being used to amplifying DNA.

The flow-through device suffered from evaporation within the long serpentine channel, which could be solved with an increased flow rate. Also when the device was heated by the three cartridge heaters, to form the three temperature zones, the flow of the liquid stopped. A number of reasons were considered but no solution to this problem was found.

The straight line device was flawed in design. Overlapping of the channels within the array of channels removed the ability to fill the array of the channels together forming a sample reaction plug. This plug was necessary to allow the cycling of the reaction. As a result of the unresolved features at the inlets and outlets, water entering the device either passed straight through the middle of the device or did not flow into the channels at all, resulting in failure of the device.

The cyclic triangle device was largely unable to successfully produce a fully working PCR device, due to the fabrication method used. A PDMS top layer was used. which might have been stretching under the pressure exerted by the syringe pump as a result of flowing the reaction plug around the triangle. As the PDMS stretched, the plug broke up at each intersection. This plug was needed to be cycled around the device to cycle the PCR. With the plug splitting up around the device the PCR experiments were impractical.

4.7 Future Work

There are several changes that could be made to the devices which would improve the chance of successful amplification of DNA within the devices. The flow-through device could be improved by utilising a different inlet and outlet system. Changing from capillaries, to generate less pressure at the interface, and by dropping most of the pressure drop across the serpentine channel, it maybe possible for the water to remain liquid within the channel. It could also stop the problem of the fluid stopping from flowing. The evaporation problem could also be solved with a change in channel length or cross sectional area. Reducing the number of cycles or length of the channel in the melting and annealing zones could possibly stop the evaporation by having a higher pressure at the end of the channel. Increasing the cross sectional area might stop evaporation as the increase in volume might limit total evaporation of sections of the channel. The opposite effect of a larger volume would be to develop a drop in pressure which could increase the chance of evaporation within the channel. The same pressure could be applied by an equal increase in the flow rate maintaining the same pressure through the device and keeping the time to pass through the device the same.

Future work on the straight line device should focus on delivering the water plug evenly across the device. A possible solution is to subdivide the inlet channel, splitting the flow in to a small number of channels first and then into the array channels. The flow being divided up in steps might spread the main force of the flow across the width of the device. A suggested example is shown in Figure 4.23. Another change in the design to allow for the pressure profile is to have smaller channels in the middle compared to the edges. If the force needed to move water in the centre channels was higher compared to the outer ones, then water might move into all the channels at the same time. This variation in channel dimensions would aid in flowing the plug backwards and forwards across the temperature zones, as the same force profile is exerted when the plug is moved within the channels.

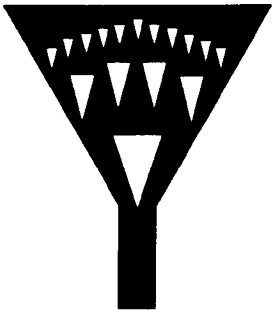

Figure 4.23: Illustration of a possible design to evenly distribute the water plug into all the channels.

The cyclic triangle device should be fabricated out of etched silicon and anodically bonded glass. Inlets and outlets should be compatible with the different top layer. Without a soft polymer layer a reaction plug could be cycled around the device. In order to realise the device, fully automatic valves would need to be added to the system. A control system for the valves would be required either using a computer controlled setup or a stand alone system. Investigation into sample injection is also required for all the three devices but more so with the cyclic triangle due the system already possessing valve control.

Both the straight line and cyclic triangle could be improved by the use of electroosmotic flow (EOF). EOF is the movement of fluids by use of applying high electrical potentials. Using EOF would negate the need to allow for hydrodynamic flow profiles in the straight line device as EOF has a flow profile is flat. Also valving of the cyclic triangle device would not be necessary as the flow can be switched on or off without valves. EOF could be used in conjunction with an electrochemical cell as the EOF potential would not be "on", when the electrochemical sampling was taking place (and therefore no excess background noise would be generated). There problems with using EOF in this system. Using EOF would move fluids around the devices but would also separate the components of the PCR reaction. Also due to the change in the temperature within the device the buffer will have different properties for EOF. Other methods could be used such as pneumatics and electropumping to name a few.

Additional work in to the surface chemistry of the channel surfaces should be undertaken and possibly an investigation into necessary reactant composition changes to allow for the large surface to volume ratio associated with microfluidic devices. Also investigating a range of different materials to allow for faster cheaper fabrication of commercially viable products should be performed.

Chapter 5

DNA Sequence Specific Detection using an Electrochemical Cell Within a Microfluidic Device

5.1 Introduction

In this chapter, a microfluidic device in which an assay for sequence specific detection of DNA using an incorporated electrochemical cell is described and discussed. Electrochemical detection incorporated within microdevices has already been discussed in Chapter 1.

5.1.1 Sequence Specific Detection of DNA Assay

The electrochemical DNA assay works by utilising a biotin-streptavidin coupling, combined with the ability to melt dsDNA but not break the biotin-streptavidin couple. Target DNA labelled with a ferrocene moiety that can be detected electrochemically within a microfluidic device, was hybridised to a complementary biotinylated ssDNA target sequence which enabled the sequence recognition and therefore the detection of specific DNA sequences.

This ferrocene oligonucleotide was provided by Molecular Sensing Ltd (Osmetech).

The assay works by coupling a biotinylated target ssDNA to a streptavidin coated surface, followed by the hybridisation of the ferrocenylated complementary oligonucleotide (probe), see Figure 5.1. Washing the surface allows extraneous material to be removed, producing a clean sample for electrochemical detection. On heating the ferrocenylated probe DNA is released allowing detection of the ferrocene and therefore sequence specific detection.

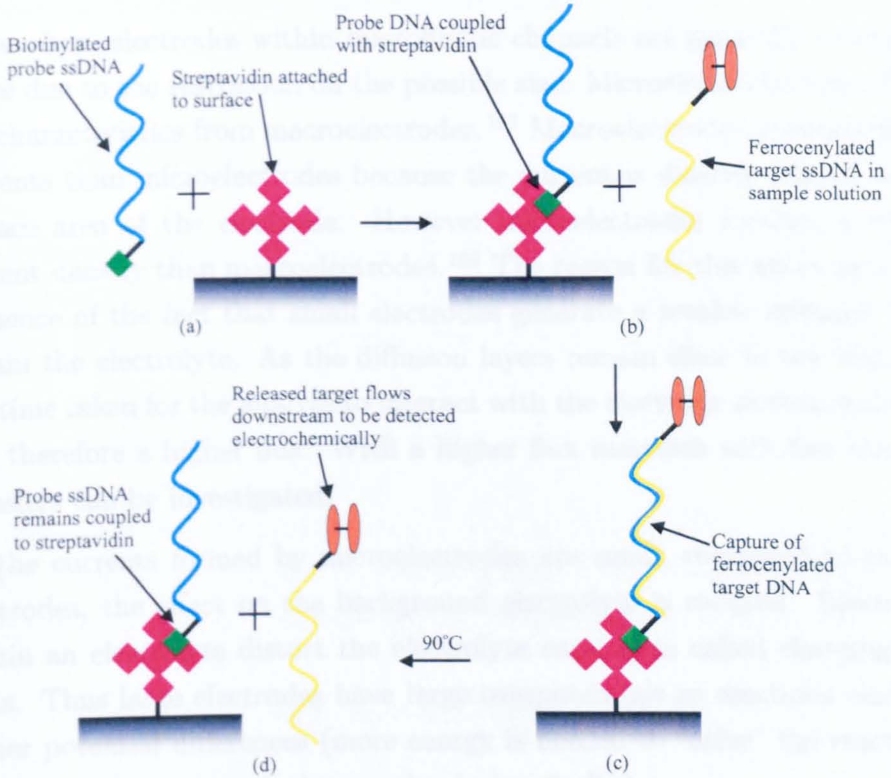
Biotinylated probe ssDNA
Streptavidin attached to surface
Probe DNA coupled with streptavidin
Ferrocenylated target ssDNA in sample solution
(a)
(b)
Released target flows downstream to be detected electrochemically
Probe ssDNA remains coupled to streptavidin
Capture of ferrocenylated target DNA
90°C
(d)
(c)

Figure 5.1: Illustration of the sequence specific detection assay: (a) streptavidin attached to a surface with 4 binding sites available for coupling with biotin; (b) biotinylated probe DNA is coupled to the streptavidin; (c) capture of the ferrocenylated target DNA from the sample solution by hybridisation to the probe DNA also cleaning the sample before the detection; (d) heating of the surface to 90°C releases the target DNA allow downstream detection by an electrochemical cell.

A microfluidic device provides a convenient platform to deliver this assay. Using streptavidin coated microspheres held within the microfluidic channel, rather than an open channel with streptavidin coated walls, produces a higher surface area per unit volume and reducing diffusion distances and therefore enhances the chance of capturing the desired sequence from the sample solution.

5.1.2 Microelectrodes vs Macroelectrodes

More often, electrodes within microfluidic channels are generally microelectrode due to the restriction on the possible size. Microelectrodes have different characteristics from macroelectrodes.[163] Macroelectrodes produce higher currents than microelectrodes because the current is directly related to the surface area of the electrode. However microelectrodes produce a higher current density than macroelectrodes.[163] The reason for this arises as a consequence of the fact that small electrodes generate a smaller diffusion layer within the electrolyte. As the diffusion layers remain close to the electrode the time taken for the analyte to interact with the electrode surface is shorter and therefore a higher flux. With a higher flux reactions with fast electron transfers can be investigated.

As the currents formed by microelectrodes are small, compared to macroelectrodes, the effect on the background electrolyte is reduced. Electrodes within an electrolyte distort the electrolyte causing so called charging currents. Thus large electrodes have large overpotentials so reactions occur at higher potential differences (more energy is needed to "drive" the reaction). These currents can mask the reaction being studied.

A brief discussion on the differences between the investigation of the assay using macro- and micro-electrodes is also included in this chapter.

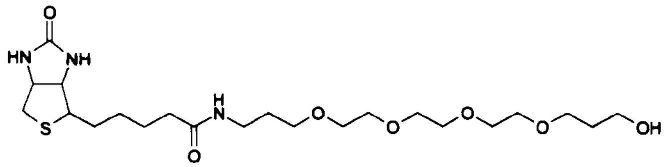

Figure 5.2: The biotin and TEG spacer used to attach the biotin to the ssDNA. The TEG spacer gives a 16 atom spacer to help the binding of the biotin to the streptavidin with limited steric hindrance. An advantage in using TEG as a spacer is that the oxygen atoms within the spacer produce a straighter backbone than other spacers, which can aid in hybridization.

5.2 Materials

The ferrocene labelled oligonucleotide was supplied by Molecular Sensing Ltd (Melksham, Wiltshire, UK). The attachment of the two ferrocene molecules is shown in Figure 4.1. The sequence of the ferrocenylated strand was:

5'-TGC CCT CCC CCA TGC CAT CCT GCG T-3'

The ferrocene was attached at the 5' end with a phosphate group on the 3' end. The sequence of the biotinylated ssDNA was complementary to the ferrocenylated strand. The biotinylated strand had the sequence of:

5'-ACG CAG GAT GGC ATG GGG GAG GGC A-3'

The biotin moiety was attached to the 5' end via a triethyleneglycol (TEG) spacer, see Figure 5.2. Biotinylated DNA was supplied by Eurogentec Ltd (Southampton, Hampshire, UK).

Macro gold working electrodes (BAS, Kenilworth, Warwickshire, UK) had a surface area of $4.7 mm^2$ in a flat circle encased in plastic. Macro reference electrodes (BAS, Kenilworth, Warwickshire, UK) were Ag/AgCl electrodes.

The counter electrodes were wound silver and platinum wire (Goodfellow, Huntingdon, Cambridge, UK).

The microspheres were coated with streptavidin with a diameter of 9.77μm and a density of 1.062g/cm^2, supplied as 1% solids. 0.04μg of biotin could be held on 1mg of beads (Bangs labs, Fishers, IN, USA).

An in-house constructed potentiostat with MS-DOS data collection software was used for measurements. A 2.4W, 9mm by 9mm square Peltier effect heat pump (Melcor, NJ, USA) was controlled by microchip Peltier controller (Hytek microsystems, Las Vegas, NV, USA). A syringe pump (Kloehn, Las Vegas, NV, USA) was used to deliver and control fluid using a Labview environment (Labview 6, National Instruments).

5.3 Design and Fabrication

The design of the microfluidic device used for this electrochemical determination is discussed along with the fabrication of the device.

5.3.1 Device Design

The device had to incorporate two main features. Firstly, a method of retaining the beads within the channel to provide a localised solid phase support to enable the capture of the target. The beads were retained by a microfilter structure fabricated within the microfluidic channel. The second feature was the incorporation of the electrochemical cell. A number of design rules were taken in to account when designing the electrodes.

5.3.1.1 Electrode Design

A three electrode system was required because of the stability of a three electrode cell when compared to a two electrode cell. A gold working electrode, a silver counter electrode and a Ag/AgCl reference electrode was incorporated into the design. A "golden" rule in electrochemistry is the counter electrode has to be at least three times the surface area of the working electrode,[164] in order to ensure that the current is only limited by the chemical reaction occurring at the working electrode and not the reaction at the counter electrode. The placement of the three electrodes relative to each other, was such that the reference electrode was in between the other electrodes. This was to separate the working and counter electrode to increase the field within the solution.

The actual size of the electrodes was 5μm wide for the working electrode which dictates that the counter electrode was 15μm wide. The reference electrode was 10μm wide and being placed in between the two other electrodes. The electrodes were spaced by 10μm. Using only a 15μm wide counter electrode and 10μm reference was beneficial because "lift off" of silver achieved best results with small area features, whereas lift off of other metals was not effected by the size of the electrodes. The length of the electrodes was defined by the width of the channel as the electrodes cross the whole of the channel. The channel width was 122μm, giving a surface area of $610\mu m^2$ for the working electrode. In order to make alignment of the channel onto the electrodes easy the actual length of the electrodes on the mask were 2mm long.

The electrodes were designed to fit on a glass microscope slide, 76 x 26mm. The bonding pads were 4 x 3mm with the connections between the electrodes and the bonding pads being as large as possible. The reason that the connections and bonding pads were large was to ensure good electrical conduction. The electrode is shown in Figure 5.3.

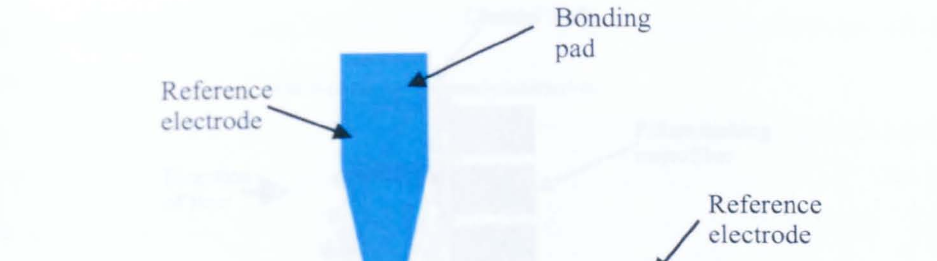
Bonding pad
Reference electrode
Reference electrode
Working electrode
Connecting wire
Counter electrode
Electrode identification and alignment marker
C
W
Electrode identification and alignment marker
Counter electrode
Working electrode

Figure 5.3: The design of electrodes for the electrochemical detection of ferrocene oligonucleotide within a microfluidic channel. The insert shows the electrodes with widths of 15μm, 10μm and 5μm for the counter, reference and working electrode respectively with 10μm spacing between each of the electrodes.

5.3.1.2 Filter Design

In order to retain the beads in place within the device, a microfilter structure was designed. It consisted of three pillars spaced out across the channel, in order to retain the microspheres whilst still allowing fluids to pass unhindered, see Figure 5.4. The pillars were 30μm wide and 100μm long with a gap of 8μm in between the pillars.

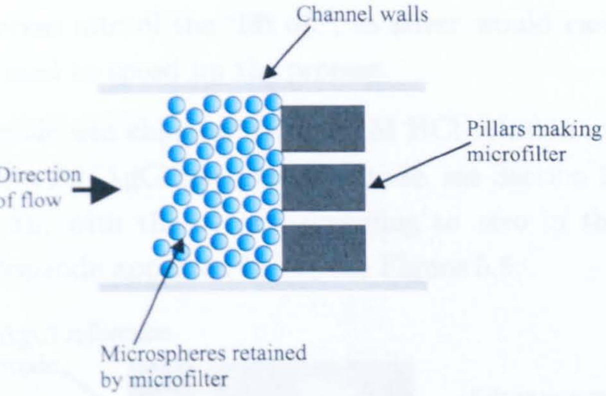
Channel walls
Pillars making microfilter
Direction of flow
Microspheres retained by microfilter

Figure 5.4: Illustration of the microfilter capturing microspheres within a flow channel.

5.3.2 Fabrication of Device

The device was fabricated from glass and PDMS, using techniques discussed in Chapter 2 (electrodes were patterned on to a glass substrate and the microfluidic channel and filter could be moulded with PDMS). Using a glass and PDMS channel enabled the alignment of the electrodes in the channel without the need for a mask alignment stage in the fabrication.

5.3.2.1 Electrode Fabrication

The electrodes were fabricated photolithographically, using S1818 photoresist, see Section 2.3.4, and followed by evaporation and lift off on glass slides as described in Section 2.3. Titanium (10μm), palladium (10μm) and gold (100μm) were evaporated on to the glass to form the electrodes, see Section 2.3.8. Titanium was evaporated first because it adheres well to glass, whereas gold does not. The palladium was used as a barrier to stop the leaching of the titanium into the gold, which would effect the electrochemistry. A second layer of photoresist (S1818) was spun on to the glass and patterned to allow the evaporation of silver (100μm), see Section 2.3.8 on to the counter and reference electrode. The "lift off" of the silver took place overnight, to increase the success rate of the "lift off", as silver would easily tear off the electrode if agitated to speed up the process.

The silver electrode was chlorinated, in 0.1M HCl solution at a potential of 0.2V, to provide a Ag/AgCl reference electrode, see Section 2.3.14. The cell was active for 20s, with the current dropping to zero in this time. After oxidation the electrode appeared black, see Figure 5.5.

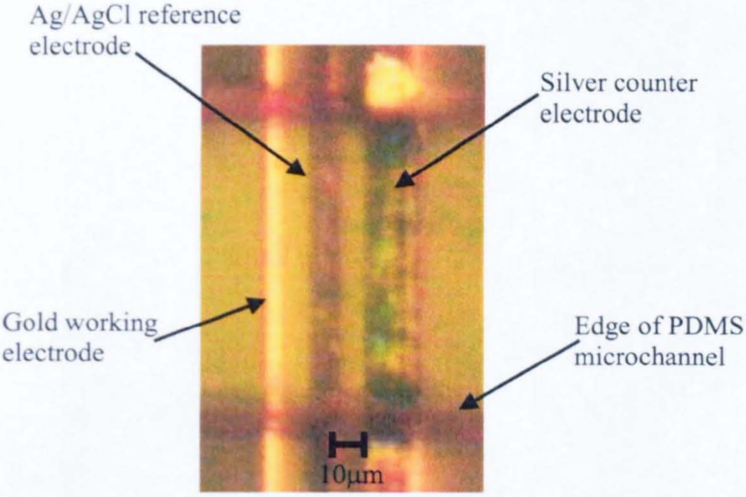

Figure 5.5: Photograph of microelectrodes within microfluidic channel. The channel edge can be seen as it was placed over the 2mm long electrodes to ease the alignment of the channel (the slight out of focus is due to the PDMS substrate and the empty channel above the electrodes). The Ag/AgCl reference electrode is darker and not reflective like the Ag counter electrode due to the addition of chlorine to make the salt surface.

5.3.2.2 Microchannel and Filter Fabrication

The microfluidic channel with microsphere filter was fabricated from PDMS, by moulding the PDMS around a silcon master, see Section 2.3.10.1. In order to mould the PDMS, a silicon master was etched to a depth of 75μm, using a STS ICP, see Section 2.3.7. Etching the inverse of the pillar structures into the silicon mould and then fabricating in PDMS provided a convenient reproducible way of fabricating the filter within the channel. The pillar structures formed in PDMS are shown in Figure 5.6, along with the silicon master.

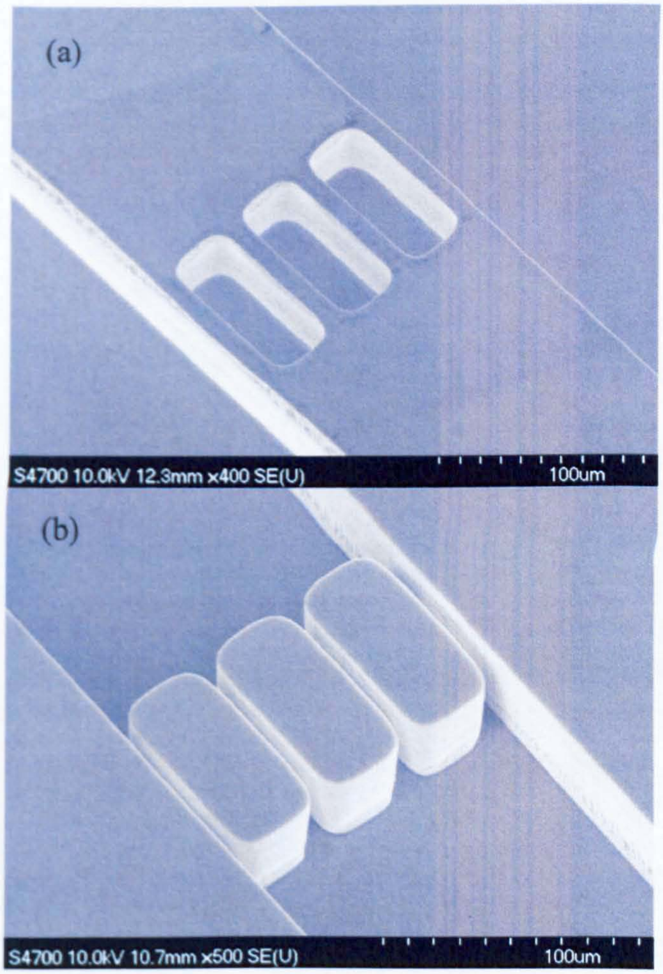
(a)
S4700 10.0kV 12.3mm x400 SE(U)
100um
(b)
S4700 10.0kV 10.7mm x500 SE(U)
100um

Figure 5.6: Scanning electron microscope picture of (a) the etched silicon mould showing the unetched channel with etched holes, which form raised pillars in the moulded PDMS and (b) structured PDMS showing the raised pillars, which make the filter, within the microchannel.

5.3.2.3 Device Integration

The interface between the device and the syringe pump was enabled using modified syringe needles, see Section 2.3.12.2. Therefore holes were introduced prior to bonding of the two parts of the device. Also before bonding the PDMS was cut to uncover the bonding pads of the electrodes. The device was bonded together using plasma oxidation, see Section 2.3.11.2. The channel was aligned against the electrodes by eye (the electrodes being 2mm long allowing for easy alignment). Connecting wires were attached to the bonding pads by silver conductive paint and then covered with RTV PDMS to protect them.

5.4 Experimental Procedure

The experimental procedures employed for the detection of the ferrocene labelled oligonucleotide within a macroelectrode system and in the microsystem are outlined within this section. The procedures used to investigate the oxidation potential and the availability for oxidation of the ferrocene oligonucleotide both within a macro-system and the microsystem are also described. Finally, the experimental procedure used to determine sequence specific detection of ferrocene labelled DNA is discussed.

5.4.1 Macroelectrodes

For these investigations a standard solution of ferrocene oligonucleotide was prepared by adding 100μl of the 10μM ferrocenylated oligonucleotide to 100μl of 100mM sodium acetate (NaAc) solution in deionised water. This produced a sample of suitable volume for the macroelectrode cell. The final sample concentration was 5μM with a final NaAc concentration of 50mM at pH 8.5 (25°C). As stated a three electrode system, consisting of a gold working electrode, with a 4.7mm^2 working area, a silver counter electrode and a Ag/AgCl reference electrode was used.

The oxidation potential of the ferrocene attached to the oligonucleotide was investigated using cyclic voltammetry, using the above sample solution. The voltage was swept between -0.15V to 0.75V starting at 0V and scanning upwards first with a scan rate of 20mV/s. The experiment was run within a Faraday cage to reduce electromagnetic noise.

5.4.2 Microelectrodes

In order to select a suitable voltage for the oxidisation of the ferrocene, attached to the ssDNA, the oxidisation potential of the ferrocenylated oligonucleotide was investigated by cyclic voltammetry within the microfluidic device. The oxidation potential for this system was required as it would be different to the macrosystem due to different sized electrodes. Once the oxidation potential was determined, the sequence specific detection of DNA was performed. The procedures are outlined below.

5.4.2.1 Cyclic Voltammetry of Single Stranded Ferrocenylated DNA

To investigate the oxidation potential of the ferrocenylated ssDNA within the microfluidic electrochemical detection, the device was filled with 10μM ferrocenylated oligonucleotide in 50mM NaAc solution, pH 8.5 at 25°C. The potentiostat cycled the potential between 0.02V and 0.4V, against the internal Ag/AgCl. A scan rate of 20mV/s was used starting at the lowest voltage and scanning upwards. The whole experiment was carried out within a Faraday cage.

5.4.2.2 Detection of Sequence Specific Ferrocenylated Oligonucleotide

To detect a specific sequence of DNA within the electrochemical device the device was filled with streptavidin coated beads. 28.75μl of 0.1% w/v streptavidin coated beads in 50mM NaAc solution, pH 8.5. This equates to ~6500 beads within the channel, such that the beads stack up ~4mm behind the pillars. ~0.4ng of biotin could be captured by this number of beads held by the filter. The beads where then washed with 30μl of 50mM NaAc solution.

100μl of 10μM ferrocenylated ssDNA was hybridised with 50μl of the complementary biotinylated ssDNA at a concentration of 20μM in 50mM NaAc solution at pH 8.5. This DNA solution was heated to 90°C for 5min in a thermocycler (MJ 100PTC, MJ research inc., Bio-rad, Hemel Hempsted, Hertfordshire, UK). The DNA was then allowed to hybridise as it cooled to room temperature. This maximized the hybridisation by ensuring that all the DNA was melted and then allowing it to cool down and hybridise with the complementary strand. It was assumed that all the DNA had been hybridised. For loading the DNA into the device, 20μl of the hybridised complex, at 10μM, was diluted to 50μl with 50mM NaAc solution, pH 8.5. This was then flowed into the device at a flow rate of 2.5μl/min, using a syringe pump (Kloehn M6, Kloehn, Las Vegas, NV, USA). As the biotinylated DNA flowed across the streptavidin coated beads the biotin coupled to the streptavidin. The beads within the channel could capture 2pmol (0.4ng) of biotin. A total of 0.2nmol of biotinylated dsDNA was allowed to flow into the channel, therefore ensuring that DNA was captured on the beads. After the DNA had been loaded into the device, it was washed with 40μl of 50mM NaAc solution to remove any unwanted components of the sample solution.

The device was then placed on the Peltier effect heat pump within a Faraday cage. The Peltier covered most of the device not just the area where the beads were retained. The electrochemical cell was held at 0.3V, the oxidation potential of the ferrocene in this system, for 2.5min to stabilise the signal and allow it to reach a steady-state value. After the electrochemical cell had stabilised, the Peltier was switched on with the temperature set at 90°C. The device was heated for 3min, after which the syringe pump flowed 50mM NaAc solution, pH 8.5, through the device, to displace the released ferrocene labelled oligonucleotide from the beads. From the beginning of the heating phase, the current produced by the electrochemical cell at 0.3V was recorded against time. A sampling rate of 10Hz was used. NaAc solution was flowed through the device for 3.5min with the Peltier still heating the device.

Background measurements were taken with the beads in place within the device and the same heating and flow profiles were preformed but without any

DNA present. This background reading was used to investigate the interference from the heating system and how the electrodes reacted under heating.

5.5 Results and Discussion

The voltammograms from the three different experiments and a discussion of the results are given below.

5.5.1 Macroelectrodes

To investigate the oxidation potential for ferrocenylated ssDNA a sample was investigated using cyclic voltammetry. A typical voltammogram is shown in Figure 5.7.

From the shoulder on the voltammogram, point A, the oxidation of the ferrocene within the macroelectrode system was at 0.5V. The reaction was quasi-reversible[163] as there was some reduction of the oxidised ferrocene on the reduction sweep of the voltage, point D. Quasi-reversible means that the amount of reduction is related to the scan rate and the rate of mass transport. Point B shows the electrolysis of the buffer on the working electrode. Point C is indicative of a irreversible reaction, showing that no electrochemistry took place on the reduction sweep of the cycle. As there was a small reduction reaction, point D, it shows it was quasi-reversible.

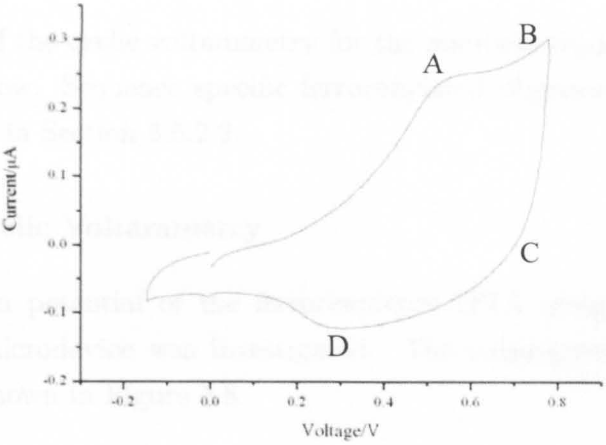

Figure 5.7: The voltammogram of the cyclic voltammetry investigation of ferrocenylated ssDNA within a macrosystem: (A) indicates the oxidation of the ferrocene; (B) shows the electrolysis of the background electrolyte; (C) indicates that the reaction was non-reversible as no reduction reaction is taking place; (D) shows the system has a small reduciton reaction so was quasi-reversible.[163]

The quasi-reversible nature of this voltammogram maybe due to the electrolysis of the electrolyte, this would give an irreversible reaction but as the reaction is actually reversible the voltammogram looks quasi-reversible. The voltage would not normally be cycled high enough to electrolyse the buffer but as only the oxidation potential of the system was required rather than any mechanistic information it is not significant.

The oxidation potential, 0.5V vs Ag/AgCl, measured using the macroelectrode system showed that ferrocene attached to ssDNA is still available to interact with the surface of the electrodes and as such can be used for detection. There was the possibility that the ferrocene might be sterically hindered by the DNA strand, but the addition of a spacer retained the ferrocene activity.

5.5.2 Microelectrodes

The results of the cyclic voltammetry for the microelectrodes are shown and discussed below. Sequence specific ferrocenylated oligonucleotide detection are discussed in *Section 5.5.2.2*.

5.5.2.1 Cyclic Voltammetry

The oxidation potential of the ferrocenylated DNA using microelectrodes within the microdevice was investigated. The subsequent voltammogram obtained is shown in Figure 5.8.

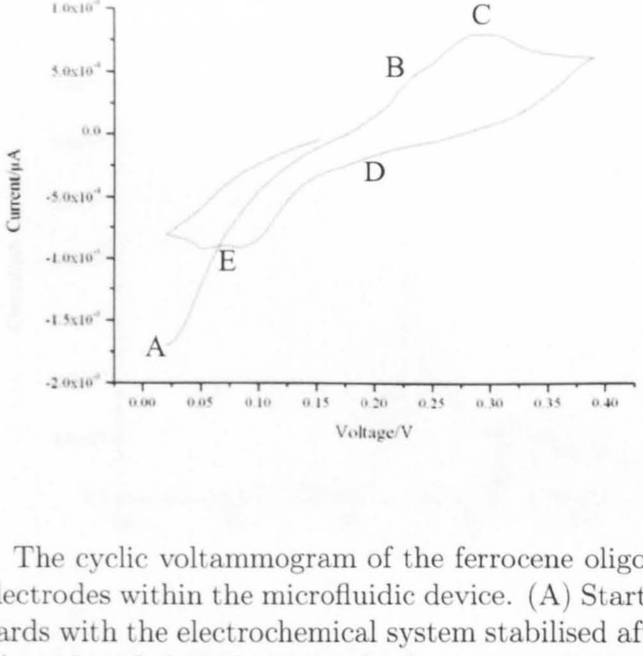

Figure 5.8: The cyclic voltammogram of the ferrocene oligonucleotide using the microelectrodes within the microfluidic device. (A) Start of the oxidation sweep upwards with the electrochemical system stabilised after connection of the cell; (B) unidentified oxidation peak of unknown within the electrochemical cell; (C) the oxidation of the ferrocenylated oligonucleotide. (D) lack of a peak here shows the irreversible nature of the reaction within this system; (E) is a small reduction peak of the ferrocene making for a quasi-irreversible reaction.

Within the microfluidic device, the oxidation potential had changed to 0.3V from 0.5V in the macroelectrode system. This difference in the oxidation potential originates because of different overpotentials of the systems. The macroelectrodes "charge" the electrolyte so the oxidation potential has to be increased to overcome this, whereas the microelectrodes have a reduced effect on the electrolyte so the oxidation potential was reduced.

5.5.2.2 Sequence Specific Ferrocenylated Oligonucleotide

The hybridisation of the ferrocenylated ssDNA to the biotinylated ssDNA and subsequent capture of the biotin was used as the mechanism for performing sequence specific oligonucleotide detection. When the electrolyte flowed through the microfluidic channel after the device had been heated to 90°C for 3min, a peak current was produced, see Figure 5.9.

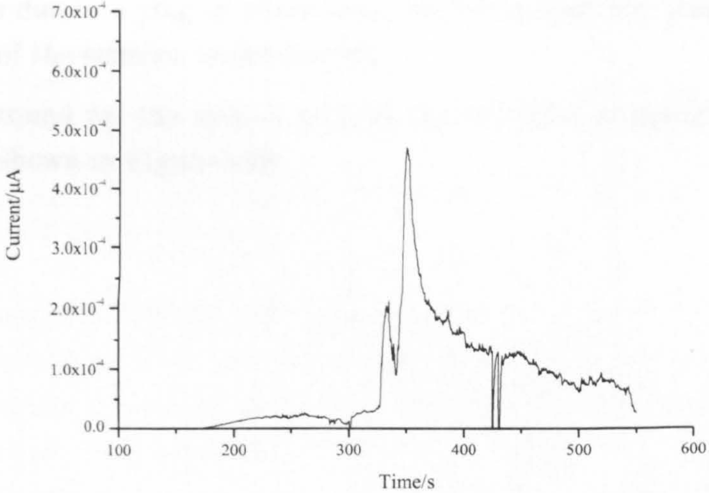

Figure 5.9: Baseline corrected voltammogram of the detection of a specific DNA sequence using the biotinylated oligonucleotide assay. The device was heated from 150s and the flow through the device was started at 350s. The peak current is observed at 350s. Data starts at 150s due to the first 150s allowing the stabilisation of the electrochemical cell.

Figure 5.9 shows that when the flow was started through the device a signal was obtained. The start of the peak occurs before the flow was started at 350s this was because of two reasons. Firstly due to there being no direct link between the pump, the heating system and the current recording software exact times were difficult to coordinate. Secondly the channel would dry out under heating. Within the channel downstream of the beads and filter the electrolyte would flow out of the channel when the device was heated. This explains why the peak would start before the syringe flow was applied.

The ferrocenylated ssDNA was melted into solution and detected when the solution flowed through the channel even without any external pressure. Once the pump starts the peak reaches its maximum. The peak tails off due to the hydrodynamic flow profile spreading out the plug of DNA, which was generated by capturing and concentrating the DNA at the beads. Another feature of Figure 5.9 is the peak before the main peak. This is most likely to be due to a plug of water being forced through the channel by the expansion of the solution under heating.

The background for the system used in the detection of specific DNA sequences is shown in Figure 5.10.

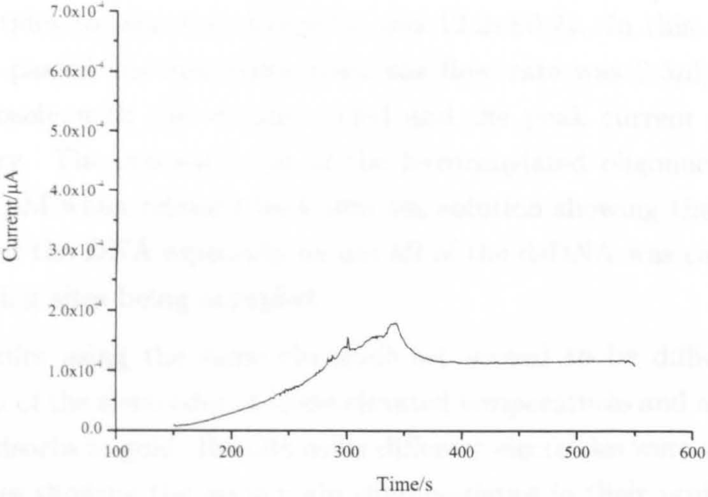

Figure 5.10: Background current generated by the heating of the device by the Peltier effect heat pump in the electrochemical cell within the microfluidic channel. The current rises as the electrodes were heated and after the flow starts, at 350s, the electrodes are again in solution and the temperature stops increasing. The first 150s are not displayed as these were to allow the electrochemical cell to stabilize.

The background current measured increased as the temperature rises. This could be due to both the channel drying out as water evaporates and to the temperature of the electrochemical cell increasing. When the electrolyte flowed through the channel after 350s the current reduces and levels out. This was because the electrodes are continuously in solution which produces a stable background and the temperature is held constant as the water cools the electrodes to a certain extent.

From the baseline corrected voltammogram, Figure 5.9, it can be seen that ferrocenylated oligonucleotide is being detected. Integration (Origin 6.1, Originlab corporation, Northampton, MA, USA) of the ferrocenylated peak gives the total amount of charge as ~10x10^{-9}C±4x10^{-10}C, which relates to 6x10^{10}e^{-}. The number of oligonucleotides detected was ~3x10^{10}±1x10^{10}. From the width of the peak, the volume of electrolyte which contained the oligonucleotides can be defined. The time taken for the ferrocenylated oligonucleotides to pass the electrodes was 12.2s±0.2s. In this time 30.5μl of solution passed the electrodes since the flow rate was 2.5μl/min. This matches closely with the volume added and the peak current from cyclic voltammetry. The concentration of the ferrocenylated oligonucleotide was ~10μM ±1μM when released back into the solution showing that the assay concentrated the DNA especially as not all of the dsDNA was captured due to the binding sites being occupied.

Repeat results using the same electrode set proved to be difficult due to degradation of the electrodes at these elevated temperatures and also because ferrocene adsorbs to gold. Results using different electrodes were similar with all electrodes showing the same main characteristics in their profile.

5.6 Conclusion

This method of detection could potentially be used for routine analysis of specific sequences of DNA. As a result of the capture of the target sequence on the beads, non-complementary sequences and other material and debris that might interfere with the measurements were washed away to allow the determination of the desired sequence. Due to the solid phase extraction of the specific sequence the sample is "cleaned" and concentrated within the device prior to detection. This simple analysis method has a number of benefits for many applications. The addition of a ferrocenylated or biotinylated primer during PCR followed by this assay would prove to be an excellent analysis protocol for real samples. Also raw DNA samples can be resolved to determine if a specific sequence is present with minimal pre-detection cleaning producing a fast analysis. Also the approach can be used to probe an opaque sample that can not be investigated with microscopy.

To call the system turly sequence specfic another ferrocenylated oligo should of been tested through the device. The specfic nature of the assay and the device would depend on the exact number of mismatches of bases within the sample DNA. Single mismatches would most likely give a postive result but the princple remains that specfic sequences can be detected using this assay and device system.

5.7 Future Work

This system has been shown to work, however further work into certain areas is still required. Pressurizing the device to stop the channel around the electrodes from becoming empty under heating, would be the first improvement. This would help in prolonging the lifetime of the electrodes by keeping them in solution whilst reducing background peaks. To achieve this, a valve placed at the outlet could prevent this from happening but the mechanism for interfacing the device would need to be changed in order to seal the outlet fully. Addition of integrated heaters to the device would be an improvement to the device by possibly reducing the time to heat the device and therefore the time taken for the assay. Calibration of the electrode system to enable quantitative detection rather than just qualitative is also required. Ultimately, this would make the whole system more applicable for real samples on a small footprint as there is no need for optical components.

Chapter 6

Conclusion and Future Work

There are a number of outcomes which can be drawn from the research presented in this thesis. These are summarized in this chapter. Also included in this chapter is a summary of the possible future work.

6.1 Conclusions Drawn From Research

6.1.1 Immobilisation of Polymerase Enzymes

Immobilised *Taq* polymerase and T7 DNA polymerase showed a lack of activity. This lack of activity can be explained in two ways. The first being that the active site is not available for polymerisation due to being sterically hindered. Secondly, the enzyme is physically restrained so is unable to change conformation, which means it can not align the active site for polymerisation.

From these two explanations of immobilisation inhibiting the activity of polymerase enzymes the same general conclusion can be drawn. Polymerase enzymes, and in case specifically *Taq* polymerase and to a lesser extent T7 DNA polymerase, does not remain active when close to or attached to a substrate. The enzymes were shown to be able to regain activity once they had been removed from the substrate, demonstrating that the polymerase enzyme was not permanently altered by being adsorbed onto a surface, just hindered.

6.1.2 Microfluidic PCR Devices

Fabrication of the designed microfluidic PCR devices was achieved although the performance varied both between the different devices and the different fabrication methods used. All three devices fulfilled the basic requirements of the system in the design, however not in total performance. In the case of the cyclic triangle device, the alternative methods of fabrication should have been investigated and in the case of the linear device, the design was flawed but the principle remains robust. The flow-through device suffered from more fundamental problems due to the length of the device and size of the device and the elevated temperatures required with PCR.

6.1.3 Sequence Specific Detection of DNA

The sequence specific detection of DNA, using the ferrocenylated oligonucleotide assay from Molecular Sensing Ltd, was shown to work for the first time within a microdevice using an integrated electrochemical cell. Using a filter and microspheres in conjunction with the ferrocenylated oligonucleotide as the probe, a biotinylated target ssDNA was trapped and separated and cleaned from other DNA molecules in the sample, and detected electrochemically. The detection was not quantitive but was shown to detect a large percentage of the probe DNA present.

6.2 Future Work

6.2.1 Immobilisation of Polymerase Enzymes

Although this research concluded that the immobilisation of polymerase enzymes inhibits their activity, it might still be possible to achieve this aim. As polymerase enzymes are not permanently damaged after immobilisation, a method of attachment could be possible. Firstly, different polymerase enzymes could be chosen. The same basic structure is likely to exist in all polymerases but the variation could be great enough to allow activity after immobilisation. Secondly, by identifying an amino acid that is accessible and not involved in the conformational changes within the enzyme during addition of bases, an alternative method of immobilisation maybe developed. If this particular amino acid could be individually attached to the enzyme, it might remain active and therefore PCR could be performed.

6.2.2 Microfluidic PCR Devices

Initially, future work on the microfluidic PCR devices should be addressed in two ways. Firstly, a more robust fabrication and valving of the cyclic triangle device should be undertaken. This idea is the most practical for a complete PCR system. The second way of improving the device is to redesign the flow-through and linear device. Adjusting the length and channel cross section of the flow-through device might solve the problem of evaporation within the channel. Changing the width of the channels or splitting the incoming flow more evenly across the array of channels, in the linear device, would improve the usability of the device.

An overall improvement to the linear and cyclic triangle device would be to change the method of fluid control to a electrokinetic system. Using an electrokinetic flow system would allow greater flow control due to control on direction and better precision on volumes moved. Integration of an electrochemical detection cell would be possible by timing the sampling to be over the electrodes when the electrokinetic voltage is off.

6.2.3 Sequence Specific Detection of DNA

The calibration of the system, so that quantitive data on the amount of the target DNA in the sample is recorded, needs to be undertaken. This would enable the system to be integrated into a number of different devices with relative ease with the view to probing "real" samples.

For a more complete system, the integration of heaters below the filter section of the device would enable faster heating and greater temperature control. Also, with the addition of the cooling fluid channel or a heater under the electrochemical cell, therein the possibility of achieving a greater stability of the current, by having a regulated temperature.

Bibliography

1. Saiki, R.; Scharf, S.; Faloona, F.; Mullis, K.; Horn, G.; Erlich, H.; Arnheim, N. *Science* **1985,** *230,* 1350-1354.
2. Klenow, H.; Overgaard-Hansen, K.; Patkar, S. *Eur. J. Biochem.* **1971,** *22,* 371-381.
3. Brock, T.; Freeze, H. *J. Bacteriology* **1969,** *98,* 289-297.
4. Terry, S.; Jerman, J.; Angell, J. *IEEE transactions on electron devices* **1979,** *26,* 1880-1886.
5. Manz, A.; Miyahara, Y.; Miura, J.; Watanabe, Y.; Miyagi, H.; Sato, K. *Sensors and Actuators B Chemical* **1990,** *1,* 249-255 TY - JOUR.
6. Manz, A.; Graber, N.; Widmer, H. M. *Sensors and Actuators B Chemical* **1990,** *1,* 244-248.
7. Manz, A.; Harrison, D. J.; Verpoorte, E. M. J.; Fettinger, J. C.; Paulus, A.; Ludi, H.; Widmer, H. M. *Journal of Chromatography A* **1992,** *593,* 253-258 TY - JOUR.
8. Harrison, D. J.; Manz, A.; Fan, Z.; Ludi, H.; Widmer, H. M. *Analytical Chemistry* **1992,** *64,* 1926-1932.
9. Harrison, D. J.; Fluri, K.; Seiler, K.; Fan, Z.; Effenhauser, C. S.; Manz, A. *Science* **1993,** *261,* 895-897.

10. Schmalzing, D.; Koutny, L.; Taylor, T.; Nashabeh, W.; Fuchs, M. *Journal of Chromatography B* **1997,** *697,* 175-180.

11. Chiem, N.; Harrison, D. J. *Analytical Chemistry* **1997,** *69,* 373-378.

12. Woolley, A. T.; Sensabaugh, G.; Mathies, R. A. *Analytical Chemistry* **1997,** *69,* 2181-2186.

13. Jacobson, S.; Hergenroder, R.; Koutny, L.; Ramsey, J. *Analytical Chemistry* **1994,** *66,* 2369-2373.

14. Effenhauser, C. S.; Paulus, A.; Manz, A.; Widmer, H. M. *Analytical Chemistry* **1994,** *66,* 2949-2953 Article PG636 ANAL CHEM.

15. Woolley, A. T.; Mathies, R. A. *Proceedings of the National Academy of Sciences of the United States of America* **1994,** *91,* 11348-11352 Article PU285 PROC NAT ACAD SCI USA.

16. Wilding, P.; Pfahler, J.; Bau, H.; Zemel, J.; Kricka, L. *Clinical Chemistry* **1994,** *40,* 43-47.

17. Brody, J.; Han, Y.; Austin, R.; Bitensky, M. *Biophyiscal Journal* **1995,** *68,* 2224-2232.

18. Li, P.; Harrison, D. J. *Analytical Chemistry* **1997,** *69,* 1564-1568.

19. Gale, B.; Caldwell, K.; Frazier, A. *IEEE Transactions on Biomedical Engineering* **1998,** *45,* 1459-1469.

20. Nakayama, Y.; Boucher, R. *Introduction to fluid mechanics;* John Wiley and Sons Inc.: New York, USA, 1999.

21. Atkins, P. *Physical Chemistry;* OUP: Oxford, 5th ed.; 1995.

22. Bessoth, F.; deMello, A. J.; Manz, A. *Analytical Commuication* **1999,** *36,* 213-215.

23. Jacobson, S.; Ramsey, J. *Analytical Chemistry* **1996,** *68,* 720-723.

24. Hadd, A.; Raymond, D.; Halliwell, J.; Jacobson, S.; Ramsey, J. *Analytical Chemistry* **1997,** *69,* 3407-3412.

25. Yakovleva, J.; Davidsson, R.; Lobanova, A.; Bengtsson, M.; Eremin, S.; Laurell, T.; Emneus, J. *Analytical Chemistry* **2002,** *74,* 2994-3004.

26. Srinivasan, A.; Wu, X.; Lee, M.-Y.; Dordick, J. *Biotechnology and Bioengineering* **2003,** *81,* 563-569.

27. Schilling, E.; Kamholz, A.; Yager, P. *Analytical Chemistry* **2002,** *74,* 1798-1804.

28. Burke, B.; Regnier, F. *Analytical Chemistry* **2003,** *75,* 1786-1791.

29. Hayashi, K.; Iwasaki, Y.; Kurita, R.; Sunagawa, K.; Niwa, O. *Electrochemistry Communications* **2003,** *5,* 1037-1042.

30. Pease, A.; Solas, D.; Sullivan, E.; Cronin, M.; Holmes, C.; Fodor, S. *Proc. Natl. Acad. Sci. USA* **1994,** *91,* 5022-5026.

31. Sosnowski, R.; Tu, E.; Butler, W.; O'Connell, J.; Heller, M. *Proc. Natl. ACad. Sci. USA* **1997,** *94,* 1119-1123.

32. Wilding, P.; Shoffner, M.; Kricka, L. *Clinical Chemistry* **1994,** *40,* 1815-1818.

33. Shoffner, M.; Cheng, J.; Hvichia, G.; Kricka, L.; Wilding, P. *Nucleic acids research* **1996,** *24,* 375-379.

34. Nagai, H.; Murakami, Y.; Morita, Y.; Yokoyama, K.; Tamiya, E. *Analytical Chemistry.* **2001,** *73,* 1043-1047.

35. Daniel, J.; Iqbal, S.; Millington, R.; Moore, D.; Lowe, C.; Lesile, D.; Lee, M.; Pearce, M. *Sensors and Actuators A Physical* **1998,** *71,* 81-88.

36. Taylor, T.; Winn-Deen, E.; Picozza, E.; Woudenberg, T.; Albin, M. *Nucleic acids research* **1997,** *25,* 3164-3168.

37. Lin, Y.; Huang, M.; Young, K.; Chang, T.; Wu, C. *Sensors and Actuators B Chemical* **2000,** *71,* 2-8.

38. Lin, Y.; Yang, C.; Huang, M. *Sensors and Actuators B Chemical* **2000,** *71,* 127-133.

39. Gulliksen, A.; Solli, L.; Karlsen, F.; Rogne, H.; Hovig, E.; Nordstrom, T.; Sirevag, R. *Analytical Chemistry* **2004,** *76,* 9-14 760HT ANAL CHEM.

40. Yu, X.; Zhang, D.; Li, T.; Hao, L.; Li, X. *Sensors and Actuators A Physical* **2003,** *108,* 103-107.

41. Shin, Y. S.; Cho, K.; Lim, S. H.; Chung, S.; Park, S. J.; Chung, C.; Han, D. C.; Chang, J. K. *Journal of Micromechanics and Microengineering* **2003,** *13,* 768-774 727JZ J MICROMECHANIC MICROENGINEER.

42. El-Ali, J.; Perch-Nielsen, I. R.; Poulsen, C. R.; Bang, D. D.; Telleman, P.; Wolff, A. *Sensors and Actuators A Physical* **2004,** *110,* 3-10 770AK SENSOR ACTUATOR A-PHYS.

43. Liu, Y. J.; Rauch, C. B.; Stevens, R. L.; Lenigk, R.; Yang, J. N.; Rhine, D. B.; Grodzinski, P. *Analytical Chemistry* **2002,** *74,* 3063-3070 Article 569FH ANAL CHEM.

44. Koh, C. G.; Tan, W.; Zhao, M. Q.; Ricco, A. J.; Fan, Z. H. *Analytical Chemistry* **2003,** *75,* 4591-4598 719FE ANAL CHEM.

45. Woolley, A.; Hadley, D.; Landre, P.; de Mello, A. J.; Mathies, R.; Northrup, M. *Analytical Chemistry* **1996,** *68,* 4081-4086.

46. Waters, L.; Jacobson, S.; Kroutchinina, N.; Khandria, J.; Foote, R. S.; Ramsey, J. *Analytical Chemistry.* **1998,** *70,* 5172-5176.

47. Dunn, W.; Jacobson, S.; Waters, L.; Kroutchinina, N.; Khandurina, J.; Foote, R.; Justice, M.; Stubbs, L.; Ramsey, J. *Analytical Biochemistry* **2000,** *277,* 157-160.

48. Khandurina, J.; McKinght, T.; Jacobson, S.; Waters, L.; Foote, R.; Ramsey, J. *Analytical Chemistry* **2000,** *72,* 2995-3000.

49. Lagally, E.; Medintz, I.; Mathies, R. *Analytical Chemistry* **2001,** *73,* 565-570.

50. Lagally, E. T.; Emrich, C. A.; Mathies, R. A. *Lab on a Chip* **2001,** *1,* 102-107 Article 616UN LAB CHIP.

51. Schabmueller, C.; Pollard, J.; Evans, A.; Wilkinson, J.; Ensell, G.; Brunnschweiler, A. *Journal of Mircomechanics and Microengnnering* **2001,** *11,* 329-333.

52. Belgrader, P.; Bennett, W.; Hadley, D.; Richards, J.; Stratton, P.; Mariella, J. R.; Milanovich, F. *Science* **1999,** *284,* 449-450.

53. Ibrahim, M.; Lofts, R.; Jahrling, P.; Henchal, E.; Weedn, V.; Northrup, M.; Belgrader, P. *Anal.Chem.* **1998,** *70,* 2013-2017.

54. Lee, T. M. H.; Carles, M. C.; Hsing, I. M. *Lab on a Chip* **2003,** *3,* 100-105 680QC LAB CHIP.

55. Liu, R. H.; Yang, J. N.; Lenigk, R.; Bonanno, J.; Grodzinski, P. *Analytical Chemistry* **2004,** *76,* 1824-1831 809DW ANAL CHEM.

56. Nakano, H.; Matsuda, K.; Yohda, M.; Nagamune, T.; Endo, I.; Yamane, T. *Bioscience Biotechnology and Biochemistry* **1994,** *58,* 349-352 MY649 BIOSCI BIOTECHNOL BIOCHEM.

57. Kopp, M.; de Mello, A.; Manz, A. *Science* **1998,** *280,* 1046-1048.

58. Chou, C. F.; Changrani, R.; Roberts, P.; Sadler, D.; Burdon, J.; Zenhausern, F.; Lin, S.; Mulholland, A.; Swami, N.; Terbrueggen, R. *Microelectronic Engineering* **2002,** *61-2,* 921-925 Article 569HB MICROELECTRON ENG.

59. Obeid, P. J.; Christopoulos, T. K.; Crabtree, H. J.; Backhouse, C. J. *Analytical Chemistry* **2003,** *75,* 288-295 Article 635ZM ANAL CHEM.

60. Fukuba, T.; Yamamoto, T.; Naganuma, T.; Fujii, T. *Chemical Engineering Journal* **2004,** *101,* 151-156.

61. Bu, M. Q.; Tracy, M.; Ensell, G.; Wilkinson, J. S.; Evans, A. G. R. *Journal of Micromechanics and Microengineering* **2003,** *13,* S125-S130 704WV J MICROMECHANIC MICROENGINEER.

62. Liu, J.; Enzelberger, M.; Quake, S. *Electrophoresis* **2002,** *23,* 1531-1536 Article 558XK ELECTROPHORESIS.

63. Pal, D.; Venkataraman, V. *Sensors and Actuators A Physical* **2002,** *102,* 151-156 Article 619LZ SENSOR ACTUATOR A-PHYS.

64. Oda, R.; Strausbauch, M.; Hubmer, A.; Borson, N.; Jurrens, S.; Craighead, J.; Wettstein, P.; Eckloff, B.; Kline, B.; Landers, J. *Analytical Chemistry* **1998,** *70,* 4361-4368.

65. Giordano, B.; Ferrance, J.; Swedberg, S.; Hubmer, A.; Landers, J. *Analytical Biochemistry* **2001,** *291,* 124-132.

66. Kopf-Sill, A.; Miick, C.; Burd Mehta, T.; Brooks, C.; Fisher, M.; Gleich, L. DNA amplification by joule heating on a labchip. In *smallTalk'99*; San Diego, CA, 1999.

67. Sorensen, O.; Drese, K.; Hardt, S. Liquid Slug Transport, Synchronziation and Mixing Driven by Ferrofluids. In *7th International conference on Miniaturized Chemical and Biochemical Analysis Systems*; Squaw Valley, CA, USA, 2003.

68. Auroux, P. A.; Koc, Y.; de Mello, A. J.; Manz, A.; Day, P. *Lab on a chip* **2004,** *4,* 534-546.

69. Haugland, R. *Handbook of fluorscent probes and research products;* Molecular Probes, Inc.: 9th ed.; 2002.

70. Umist., C. d. *www.cp.umist.ac.uk/lecturenotes/Echem/Document2.htm* .

71. Palecek, E. *Nature* **1960,** *188,* 656-657.

72. Kafil, J.; Cheng, H.-Y.; Last, T. *Analytical Chemistry* **1986,** *58,* 285-289.

73. Wang, J.; Rivas, G.; Fernandes, J.; Paz, J.; Jiang, M.; Waymire, R. *Anal. Chim. Acta* **1998,** *375,* 197-203.

74. Ozkan, D.; Erdem, A.; Kara, P.; Kerman, K.; Meric, B.; Hassmann, J.; Ozsoz, M. *Analytical Chemistry* **2002,** *74,* 2.

75. Singhal, P.; Kuhr, W. *Anal. Chem.* **1997,** *69,* 4828-4832.

76. Wang, J.; Cai, X.; Rivas, G.; Shiraish, H.; Dontha, N. *Biosensors and Bioelectronics* **1997,** *12,* 587-599.

77. Wang, J.; Bollo, S.; Paz, J.; Sahlin, E.; Mukherjee, B. *Anal. Chem.* **1999,** *71,* 1910-1913.

78. Authier, L.; Grossiord, C.; Brossier, P. *Anal. Chem.* **2001,** *73,* 4450-4456.

79. Dequaire, M.; Degrand, C.; Limoges, B. *Analytical Chemistry* **2000,** *72,* 5521-5528.

80. Wang, J.; Liu, G.; Merkoci, A. *Analytica Chimica Acta* **2003,** *482,* 149-155.

81. Wang, M.; Sun, C.; Wang, L.; Ji, X.; Bai, Y.; Li, T.; Li, J. *Journal of Pharmaceutical and Biomedical Analysis* **2003,** *33,* 1117-1125.

82. Aslanoglu, M.; Houlton, A.; Horrocks, B. *Analyst* **1998,** *123,* 753-757.

83. Zhu, N.; Zhang, A.; Wang, Q.; He, P.; Fang, Y. *Analytica Chimica Acta* **2004,** *510,* 163-168.

84. Xu, Y.; Jiang, Y.; Cai, H.; He, P.-G.; Fang, Y.-Z. *Analytica Chimica Acta* **2004,** *516,* 19-27.

85. Sun, X.; He, P.; Liu, S.; Ye, J.; Fang, Y. *Talanta* **1998,** *47,* 487-495.

86. Pividori, M.; Merkoci, A.; Alegret, S. *Biosensors and Bioelectronics* **2001,** *16,* 1133-1142.

87. Hurley, D.; Tor, Y. *Journal of the American Chemical Society* **1998,** *120,* 2194-2195.

88. Greenwood, N.; Earnshaw, A. *Chemistry of elements;* Pergamon: Oxford, 1984.

89. Takenaka, S.; Uto, Y.; Kondo, H.; Ihara, T.; Takagi, M. *Anal. Biotech.* **1994,** *218,* 436-443.

90. Ihara, T.; Maruo, Y.; Takenaka, S.; Takagi, M. *Nucl. Acids. Res.* **1996,** *24,* 4273-4280.

91. Uto, Y.; Kondo, H.; Abe, M.; Suzuki, T.; Takenaka, S. *Anal. Biochem.* **1997,** *250,* 122-124.

92. Xu, C.; Cai, H.; He, P.; Fang, Y. *Analyst* **2001,** *126,* 62-65.

93. Yu, C.; Wang, H.; Wan, Y.; Yowanto, H.; Kim, J.; Donilon, L.; Tao, C.; Strong, M.; Chong, Y. *Journal of Organic Chemistry* **2001,** *66,* 2937-2942.

94. Wlassoff, W. A.; King, G. C. *Nucleic Acids Research* **2002,** *30,* art. no.-e58 565ZG NUCL ACID RES.

95. Takenaka, S.; Uto, Y.; Saita, H.; Yokoyama, M.; Kondo, H.; Wilson, W. *Chemical Communications* **1998,** 1111-1112.

96. Takenaka, S.; Yamashita, K.; Takagi, M.; Uto, Y.; Kondo, H. *Analytical Chemistry* **2000,** *72,* 1334-1341.

97. Cai, H.; Xu, C.; He, P.; Fang, Y. *J. Electroanal. Chem.* **2001,** *510,* 78-85.

98. Nakayama, M.; Ihara, T.; Nakano, K.; Maeda, M. *Talanta* **2002,** *56,* 857-866.

99. Gavin, P.; Ewing, A. *Journal of the American Chemical Society* **1996,** *118,* 8932-8936.

100. Woolley, A.; Lao, K.; Glazer, A.; Mathies, R. *Anal. Chem.* **1998,** *70,* 684-688.

101. Martin, R.; Gawron, A.; Lunte, S.; Henry, C. *Anal. Chem.* **2000,** *72,* 3196-3202.

102. Balwin, R.; Roussel, T.; Crain, M.; Bathlagunda, V.; Jackson, D.; Gullapalli, J.; Conklin, J.; Pai, R.; Naber, J.; Walsh, K.; Keynton, R. *Anal. Chem.* **2002,** *74,* 3690-3697.

103. Ertl, P.; Emrich, C.; Singhal, P.; Mathies, R. *Analytical Chemistry* **2004,** *76,* 3749-3755.

104. Bratten, C.; Cobbold, P.; Cooper, J. *Anal. Chem* **1997,** *69,* 253-258.

105. Clark, R.; Hietpas, P.; Ewing, A. *Anal. Chem.* **1997,** *69,* 259-263.

106. Bratten, C.; Cobbold, P.; Cooper, J. M. *Chemical Communications* **1998,** 471-472.

107. Nagy, G.; Xu, C. X.; Buck, R. P.; Lindner, E.; Neuman, M. R. *Analytical Chemistry* **1998,** *70,* 2156-2162 ZN641 ANAL CHEM.

108. Kaya, T.; Nagamine, K.; Matsui, N.; Yasukawa, T.; Shiku, H.; Matsue, T. *Chemical Communications* **2004,** 248-249 769FZ CHEM COMMUN.

109. Rossier, J.; Girault, H. *Lab on a Chip* **2001,** *1,* 153-157 616UN LAB CHIP.

110. Cai, X. X.; Klauke, N.; Glidle, A.; Cobbold, P.; Smith, G. L.; Cooper, J. M. *Analytical Chemistry* **2002,** *74,* 908-914 522UL ANAL CHEM.

111. Liu, D.; Perdue, R.; Sun, L.; Crooks, R. *Langmuir* **2004,** *20,* 5905-5910 834RU LANGMUIR.

112. Umek, R.; Lin, S.; Vielmetter, J.; Terbrueggen, R.; Irvine, B.; Yu, C.; Kayyem, J.; Yowanto, H.; Blackburn, G.; Farkas, D.; Chen, Y. *J. Mol. Diag.* **2001,** *3,* 74-84.

113. Shaw, G.; Stone, D.; A.D., J.; Ellis, A.; Crone, W. *Applied Physics Letters* **2003,** *83,* 257-259.

114. Wabuyele, M. B.; Ford, S. M.; Stryjewski, W.; Barrow, J.; Soper, S. A. *Electrophoresis* **2001,** *22,* 3939-3948 487FX ELECTROPHORESIS.

115. Duong, T. T.; Kim, G.; Ros, R.; Streek, M.; Schmid, F.; Brugger, J.; Anselmetti, D.; Ros, A. *Microelectronic Engineering* **2003,** *67-8,* 905-912 695QQ MICROELECTRON ENG.

116. Madou, M. *Fundamentals of microfabrication, The science of miniaturization;* CRC press: Boca Raton, Florida, 2nd ed.; 2002.

117. Pacansky, J.; Lyeria, J. *IBM Journal Research Development* **1979,** *23,* 42-55.

118. Xia, Y.; Whitesides, G. *Annual Review of Material Science* **1998,** *28,* 153-184.

119. Duffy, D.; McDonald, J.; Schueller, O.; Whitesides, G. *Analytical Chemistry* **1998,** *70,* 4974-4984.

120. Colas, A. "Silicone chemistry overview", www.dowcorning.com 1997.

121. Mimura, Y. *Journal of Vacuum Science Technology B* **1986,** *4,* 15-21.

122. Peterman, M.; Huie, P.; Bloom, D.; Fishman, H. *Journal of Micromechanics and Microengineering* **2003,** *13,* 380-382.

123. Shalish, I.; Shapira, Y. *Journal of Vacuum Science Technology B* **1999,** *17,* 166-173.

124. Schmidt, B.; Nitzsche, P.; Lange, K.; Grigull, S.; Kreissig, U.; Thomas, B.; Herzog, K. *Sensors and Actuators a-Physical* **1998,** *67,* 191-198.

125. Monaghan, P. *Microfluidic devices for cell growth and assays,* Ph.D thesis, Imperial college, London, 2002.

126. Simonis, A.; Luth, H.; Wang, L.; Schoning, M. *Sensors* **2003,** *3,* 330-339.

127. Rybricki, E. *www.mcb.uct.ac.za/manual/pcroptim.htm* **2001,** .

128. Yap, E.; McGee, J. *Nucleic acids research* **1991,** *19,* 1713-1717.

129. Levene, M. J.; Korlach, J.; Turner, S. W.; Foquet, M.; Craighead, H. G.; Webb, W. W. *Science* **2003,** *299,* 682-686 640KH SCIENCE.

130. Saiki, R.; Gelfand, D.; Stoffel, S.; Scharf, S.; Higuchi, R.; Horn, G.; Mullis, K.; Erlich, H. *Science* **1988,** *239,* 487-491.

131. Kim, Y.; Eom, S. H.; Wang, J. M.; Lee, D. S.; Suh, S. W.; Steitz, T. A. *Nature* **1995,** *376,* 612-616 Article RP756 NATURE.

132. Li, Y.; Korolev, S.; Waksman, G. *The EMBO journal* **1998,** *17,* 7514-7525.

133. Ho, D.; Byrnes, W.; Ma, W.; Shi, Y.; Callaway, D. *Journal of Biological Chemistry* **2004,** *279,* 39146-39154.

134. Eom, S. H.; Wang, J. M.; Steitz, T. A. *Nature* **1996,** *382,* 278-281 Article UX790 NATURE.

135. Patel, P.; Jacobo-Molina, A.; Ding, J.; Tantillo, C.; Clark, A.; Raag, R.; Nanni, R.; Hughes, S.; Arnold, E. *Biochemistry* **1995,** *34,* 5351-5363.

136. Wlassoff, W. A.; Dymshits, G.; Lavrik, O. *FEBS letters* **1996,** *390,* 6-9.

137. Wilchek, M.; Bayer, E. *Avidin-Biotin Technology;* volume 184 of *Methods of Enzymology* Academic press, inc.: San Diego, California, 1990.

138. Gast, F.-U.; Franke, I.; Meiss, G.; Pingoud, A. *Journal of Biotechnology* **2001,** *87,* 131-141.

139. Steinkuhler, C.; Biasiol, G.; Cerretani, M.; Di Renzo, L.; Brunetti, M.; Ingallinella, P.; De Francesco, R.; Altamura, S. *Analytical Biochemistry* **2002,** *307,* 99-104.

140. Yao, D.; Vlessidis, A.; Evmiridis, N. *Analytical Chimica Acta* **2003,** *478,* 23-30.

141. Situmorang, M.; Gooding, J.; Hibbert, D. *Analytical Chimica Acta* **1999,** *394,* 211-223.

142. Badea, M.; Curulli, A.; Palleschi, G. *Biosensors and Bioelectronics* **2003,** *18,* 689-698.

143. Quan, D.; Shin, W. *Materials Science and Engineering C* **2004,** *24,* 113-115.

144. "Bangs laboratories technote 205", www.bangslabs.com 2002.

145. Nakajima, N.; Ikada, Y. *Bioconjugate Chemistry* **1995,** *6,* 123-130.

146. Wong, S. *Chemistry of protein conjugation and cross-linking;* CRC press: Boco Raton, Florida, 1st ed.; 1993.

147. Ukeda, H.; Ohira, M.; Sawamura, M. *Analytical Sciences* **1999,** *15,* 447-450.

148. Kim, S.; Yun, S.-E.; Kang, C. *Bullitin of Korean Chemistry Society* **2001,** *22,* 1192-1196.

149. Wu, C.-W.; Lee, J.-G.; Lee, W.-C. *Biotechology and Applied Biochemistry* **1998,** *27,* 225-230.

150. Hardy, P.; Nicholls, A.; Rydon, H. *Chemical Communications* **1969,** 565-566.

151. Richards, F.; Knowles, J. *Journal of Molecular Biology* **1968,** *37,* 231-233.

152. "Bangs laboratories technote 204", www.bangslabs.com 1999.

153. Rojas-Melgarejo, F.; Rodriguez-Lopez, J.; Garcia-Canovas, F.; Garcia-Ruiz, P. *Process Biochemistry* **2004,** *39,* 1455-1464.

154. Takhinstov, P. *Biosensors and Bioelectronics* **2004,** *19,* 1445-1456.

155. Kumar, A.; Malhotra, R.; Malhotra, B.; Grover, S. *Analytica Chimica Acta* **2000,** *414,* 43-50.

156. Cuatrecasas, P.; Parikh, I. *Biochemistry* **1972,** *11,* 2291-2299.

157. Nilsson, J.; Bosnes, M.; Larsen, F.; Nygren, P. A.; Uhlen, M.; Lundeberg, J. *Biotechniques* **1997,** *22,* 744-751 WT815 BIOTECHNIQUES.

158. Cook, P. R.; Gove, F. *Nucleic Acids Research* **1992,** *20,* 3591-3598 Article JG812 NUCL ACID RES.

159. Cook, P. R. *Science* **1999,** *284,* 1790-1795 Review 205EU SCIENCE.

160. Innis, M.; Myambo, K.; Gelfand, D.; Brow, M. *Proc Natl Acad Sci U S A.* **1988,** *85,* 9436-9440.

161. Wittwer, C.; Garling, D. *Biotechniques* **1991,** *10,* 76-83.

162. *CRC Handbook of Chemistry and Physics;* CRC Press: 74th ed.; 1993-1994.

163. Fisher, A. *Electrode dynamics;* volume 34 of *Oxford chemistry primers* Oxford University Press: Oxford, 1996.

164. Lambrechts, M.; Sansen, W. *Biosensors: Microelectrochemical devices;* Sensors series Institute of Physics: London, 1st ed.; 1992.

GLASGOW
[illegible]